SSI-DT46195035

Doctoral Dissertation

Vibration Control for Nonlinear Mechanical Systems with Relative Information

Sheng Hao

HOKKAIDO
UNIVERSITY

February, 2022

Course of Systems Science and Informatics
Graduate School of Information Science and Technology
Hokkaido University

Doctoral Dissertation
submitted to Graduate School of Information Science and Technology,
Hokkaido University
in partial fulfillment of the requirements for the degree of
Doctor of Philosophy.

Sheng Hao

Dissertation Committee: Professor Yuh Yamashita (Chief examinar)
Professor Masahiko Onosato
Professor Satoshi Kanai
Associate Professor Koichi Kobayashi

Vibration Control for Nonlinear Mechanical Systems with Relative Information*

Sheng Hao

Abstract

In this dissertation, vibration controllers based on relative information for nonlinear mechanical systems are proposed. Vibration suppression is a core concern in mechanical system design. With the advancement of society's informatization, the demand for vibration control for information technology has grown in recent years. For decades, active vibration reduction technologies have been employed in mechanical systems. Unfortunately, most active vibration control approaches are based on the premise that all states are precisely understood. It will be simple for sensors to observe the state if it is relative information with a reference plane. If the reference plane, on the other hand, vibrates, it is impossible to determine the absolute location and velocity using affordable sensors.

The key idea of the proposed controllers is to use the passivity properties of the mechanical systems and skyhook strategies. Interconnection and damping assignment passivity-based control (IDA-PBC) method is applied in most of our results due to its theoretical advantages on energy shaping and stabilization of nonlinear systems. The content of this dissertation is as follows.

In Chapter 1, we illustrate this study's background and the motivation.

Chapter 2 considers the vibration control problem for the system with an external control force. Any floating nonlinear mechanical structure with spring and damper can be used to represent the system under consideration. The matching condition between the controllable and desired systems is derived. We derive a control law with some limitations and some free parameters. Only relative information, which is easily measured, is used by the controller. In comparison to earlier work, we offer a novel parameter design technique for more generalized nonlinear controlled devices. The inertia matrix of the intended closed-loop system is determined using differential equations. The IDA-PBC approach theoretically guarantees the stability of the nonlinear closed-loop system. We have presented a parameter selection strategy that is both efficient and effective in providing a decent vibration suppression effect. The suggested control law achieved a virtual skyhook damper utilizing just relative information under the specified parameter selection. The suggested controller's vibration impact is confirmed by simulation results for an example.

Chapter 3 considers the vibration control problem for the system with an internal control force. We present a new nonlinear active dynamic vibration absorber control system in which the information of the controller is not based on the world-coordinate information. The proposed method can simultaneously control the vibrations that are excited by a force disturbance and velocity disturbance. The control law uses only the relative displacement and velocity of the vibration system, which can be easily measured by

*Doctoral Dissertation, Course of Systems Science and Informatics, Graduate School of Information Science and Technology, Hokkaido University, SSI-DT46195035, February 14, 2022.

sensors. We revealed the equality and inequality constraints for matching the plant system with the desired system. The numerical solutions of the partial differential equations are not required with our proposed method. The main idea of the controller design is to convert a nonlinear DVA system into a desired system with multiple virtual springs and dampers. We also derived selection guidelines for the parameters of the desired system. The global asymptotical stability is guaranteed automatically through passivity-based control theory, although the parameter design is based on linearization.

In Chapter 4, the input-to-state stability (ISS) analysis for nonlinear systems with multiple disturbances is proposed. For a class of nonlinear mechanical Hamilton systems with a force noise and a velocity noise, we build an ISS Lyapunov function. The system is divided into two types: one with a force disturbance and the other with a feedback input and a velocity disturbance. Then, for each of those two systems, we built the ISS Lyapunov function. The construction is based on a number of assumptions regarding the system parameters, all of which are easily met in practice.

Chapter 5 proposes a novel IDA-PBC design for a quarter car nonlinear active suspension system. We develop a feedback rule based solely on the relative displacement and velocity of the suspension system, whereas most previous research has relied on absolute data. It is calculated by obtaining the suspension system's port-Hamiltonian form from the dynamics of the suspension system and rewriting it using relative coordinates. A low-cost sensor may be employed in practice with our unique controller. There is a proposal for an IDA-PBC-based controller design for an active suspension system with a nonlinear spring, a nonlinear damper, and mass uncertainty. Unlike other IDA-PBC implementations, our approaches focus on changing the nonlinear suspension system into a desired linear system with perfect aseismatic features, which tend to regulate the position or velocity. We design a virtual vehicle body, an unsprung mass, and damper coefficients in addition to a standard controller utilizing the skyhook control approach. We establish the requirements that guarantee the suspension system's global asymptotic stability in the absence of model errors or disturbances, as well as parameter selection suggestions that can assure robust stability in the face of parameter uncertainties in the mass, springs, and dampers. Variations in passenger numbers and vehicle body loads, as well as aging suspension parts and measurement mistakes, can all contribute to these inaccuracies.

Chapter 6 describes the conclusion of this dissertation.

Keywords: Vibration control, nonlinear system, port-Hamiltonian, passivity-based control, IDA-PBC

Contents

List of Figures

List of Tables

Chapter 1

Introduction

1.1 Background

Vibration suppression is a core concern in mechanical system design. With the advancement of society's informatization, the demand for vibration control for information technology has grown in recent years. Many projects may fail if resonance effects are not considered, resulting in economic losses and casualties. Power machinery such as steam turbines, water turbines and motors, transportation vehicles such as automobiles, trains, ships and airplanes, as well as work machines, mining machinery and construction machinery, all develop in the direction of high-speed and heavy-load, and their vibrations are also increasingly strong, and many studies are proposed in [1, 2, 3, 4, 5]. With the development of precision machine tools and precision machining technology, if one leaves a calm environment with strict vibration isolation, the work will break, and the expected accuracy goals cannot be achieved. With the development of the material industry and the construction industry, high-strength building materials are widely used. The building's height is constantly rising. As a result, the buildings have a significant amplitude of several meters after being excited by wind loads, challenging to meet the comfort and safety requirements [6, 7, 8].

For decades, active vibration reduction technologies have been employed in mechanical systems. From the standpoint of vibration suppression, active vibration reduction can provide much better results than passive approaches, according to survey [9]. Unfortunately, most active vibration control approaches [10, 11, 12, 13, 14] are based on the premise that all states are precisely understood. It will be simple for sensors to observe the state if it is relative information with a reference plane. If the reference plane, on the other hand, vibrates, it is impossible to determine the absolute location and velocity using affordable sensors.

Although the advancement of sensor technology allows for the observation of entire information, there are certain drawbacks, such as pricey equipment and restricted frequency characteristics. We may currently employ low-cost micro-electro-mechanical systems (MEMS) accelerometers, and ways for obtaining comprehensive information using an accelerometer have been developed [15]. They will, on the other hand, generate an algebraic loop, and such approaches are difficult to use in nonlinear scenarios. The absolute information can be estimated utilizing observer approaches [16]. Still, in the nonlinear scenario, such strategies are tough to implement, and it's important to note that they usually worsen performance.

The automobile industry has developed many works on suspension design using robust control methods against unmeasured external vibration during the last two decades. The robust controller can be designed by Linear-Quadratic-Gaussian (LQG) methodology[17, 18, 19, 20, 21], H_∞ technique[22, 23], saturated adaptive robust control (ARC) strategy [24] and so on. Significantly, the works based on H_∞ technique show good performance on the robustness concerning the uncertainties due to sensors. Even so, to apply these methods to nonlinear systems, we often need to solve Hamilton-Jacobi equations.

During the last two decades, the vehicle industry has produced several works on suspension design that include strong control mechanisms against unmeasured external vibration. Linear-QuaThe robust controller can be designed by Linear-Quadratic-Gaussian (LQG) methodology[17], H_∞ technique[22, 23], saturated adaptive robust control (ARC) strategy[24] and so on may all be used to create a robust controller. Significantly, the studies based on the H_∞ approach demonstrate high resilience in the face of sensor uncertainties. Even yet, we frequently need to solve Hamilton-Jacobi equations in order to apply these approaches to nonlinear systems.

To avoid the Hamilton-Jacobi equations while designing the controllers for nonlinear systems, interconnection and damping assignment passivity-based control (IDA-PBC) design approach [25], as a powerful energy shaping control method for nonlinear systems, is widely used in nonlinear mechanical systems. The global asymptotic stability of the system under IDA-PBC without a disturbance is guaranteed because one can naturally design a desired Hamiltonian function as a Lyapunov function [26, 27]. Although the classical PBC approach [28, 29, 30] can handle a wide variety of control issues, it is difficult to tackle vibration control problems using the classical PBC technique due to a lack of freedom in controller design. One of the advantages of IDA-PBC over other PBC techniques is that we can vary the kinetic energy, which provides us a lot of flexibility when constructing the controller. The virtual changes in inertia, elasticity coefficients or gravity terms, and viscous resistance coefficients are represented by changes in the kinetic energy, potential energy, and damping matrix, respectively. These variables have a direct impact on vibration suppression. The most difficult component of the IDA-PBC design approach is ensuring the solution of a set of partial differential equations induced by matching dynamics.

Recently, Aoki et.al[31] developed a solution that uses IDA-PBC and a device comparable to a tuned mass damper (TMD)[32] on the target system. They employ the added device as an accelerometer in the study [31], but they examine its dynamics to prevent the algebraic loop. To convert the controlled system to the system with skyhook damper[13], they employ IDA-PBC. Despite the fact that Aoki et al. [31] were successful in suppressing vibrations using only local information and without an accelerometer data, the approach only works in the linear and basic nonlinear-spring cases. Since they only consider a constant inertia matrix, the solution of partial differential equations induced by matching dynamics are simplified. But if we consider a system with a nonlinear inertia matrix, we must deal with the partial differential equations.

To summarize, the following problems are considered in this dissertation.

1. A new vibration controller only using relative information is expected.

2. Proposed vibration controller should guarantee the closed-loop system asymptotic stability even for nonlinear cases.

3. The general solutions of the partial differential equations induced by matching dynamics should be derived.

4. The effectiveness of the proposed approaches should be verified by a practical example, like suspension design.

1.2 Preview of Chapters

In this dissertation, we propose several vibration suppression controllers for nonlinear mechanical systems. The Figure 1.1 at the end of this chapter shows the relationship between each chapter.

In Chapter 1, we illustrate the background and motivation of this dissertation.

In Chapter 2, we firstly consider the vibration control problem for the system with an external control force. Any floating nonlinear mechanical structure with spring and damper can be used to represent the system under consideration. The matching condition between the controllable and desired systems is derived. We derive a control law with some limitations and some free parameters. Only relative information, which is easily measured, is used by the controller. In comparison to earlier work, we offer a novel parameter design technique for more generalized nonlinear controlled devices. The inertia matrix of the intended closed-loop system is determined using differential equations. The IDA-PBC approach theoretically guarantees the stability of the nonlinear closed-loop system. We have presented a parameter selection strategy that is both efficient and effective in providing a decent vibration suppression effect. The suggested control law achieved a virtual skyhook damper utilizing just relative information under the specified parameter selection. The suggested controller's vibration impact is confirmed by simulation results for an example.

Chapter 3 considers the vibration control problem for the system with an internal control force. We present a new nonlinear active dynamic vibration absorber control system in which the information of the controller is not based on the world-coordinate information. The proposed method can simultaneously control the vibrations that are excited by a force disturbance and velocity disturbance. The control law uses only the relative displacement and velocity of the vibration system, which can be easily measured by sensors. We revealed the equality and inequality constraints for matching the plant system with the desired system. The numerical solutions of the partial differential equations are not required with our proposed method. The main idea of the controller design is to convert a nonlinear DVA system into a desired system with multiple virtual springs and dampers. We also derived selection guidelines for the parameters of the desired system. The global asymptotical stability is guaranteed automatically through passivity-based control theory, although the parameter design is based on linearization.

In Chapter 4, the input-to-state stability (ISS) analysis for nonlinear systems with multiple disturbances is proposed. For a class of nonlinear mechanical Hamilton systems with a force noise and a velocity noise, we build an ISS Lyapunov function. The system is divided into two types: one with a force disturbance and the other with a feedback input and a velocity disturbance. Then, for each of those two systems, we built the ISS Lyapunov function. The construction is based on a number of assumptions regarding the system parameters, all of which are easily met in practice.

Chapter 5 proposes a novel IDA-PBC design for a quarter car nonlinear active sus-

pension system. We develop a feedback rule based solely on the relative displacement and velocity of the suspension system, whereas most previous research has relied on absolute data. It is calculated by obtaining the suspension system's port-Hamiltonian form from the dynamics of the suspension system and rewriting it using relative coordinates. A low-cost sensor may be employed in practice with our unique controller. There is a proposal for an IDA-PBC-based controller design for an active suspension system with a nonlinear spring, a nonlinear damper, and mass uncertainty. Unlike other IDA-PBC implementations, our approaches focus on changing the nonlinear suspension system into a desired linear system with perfect aseismatic features, which tend to regulate the position or velocity. We design a virtual vehicle body, an unsprung mass, and damper coefficients in addition to a standard controller utilizing the skyhook control approach. We establish the requirements that guarantee the suspension system's global asymptotic stability in the absence of model errors or disturbances, as well as parameter selection suggestions that can assure robust stability in the face of parameter uncertainties in the mass, springs, and dampers. Variations in passenger numbers and vehicle body loads, as well as aging suspension parts and measurement mistakes, can all contribute to these inaccuracies.

Chapter 6 describes the conclusion of this dissertation.

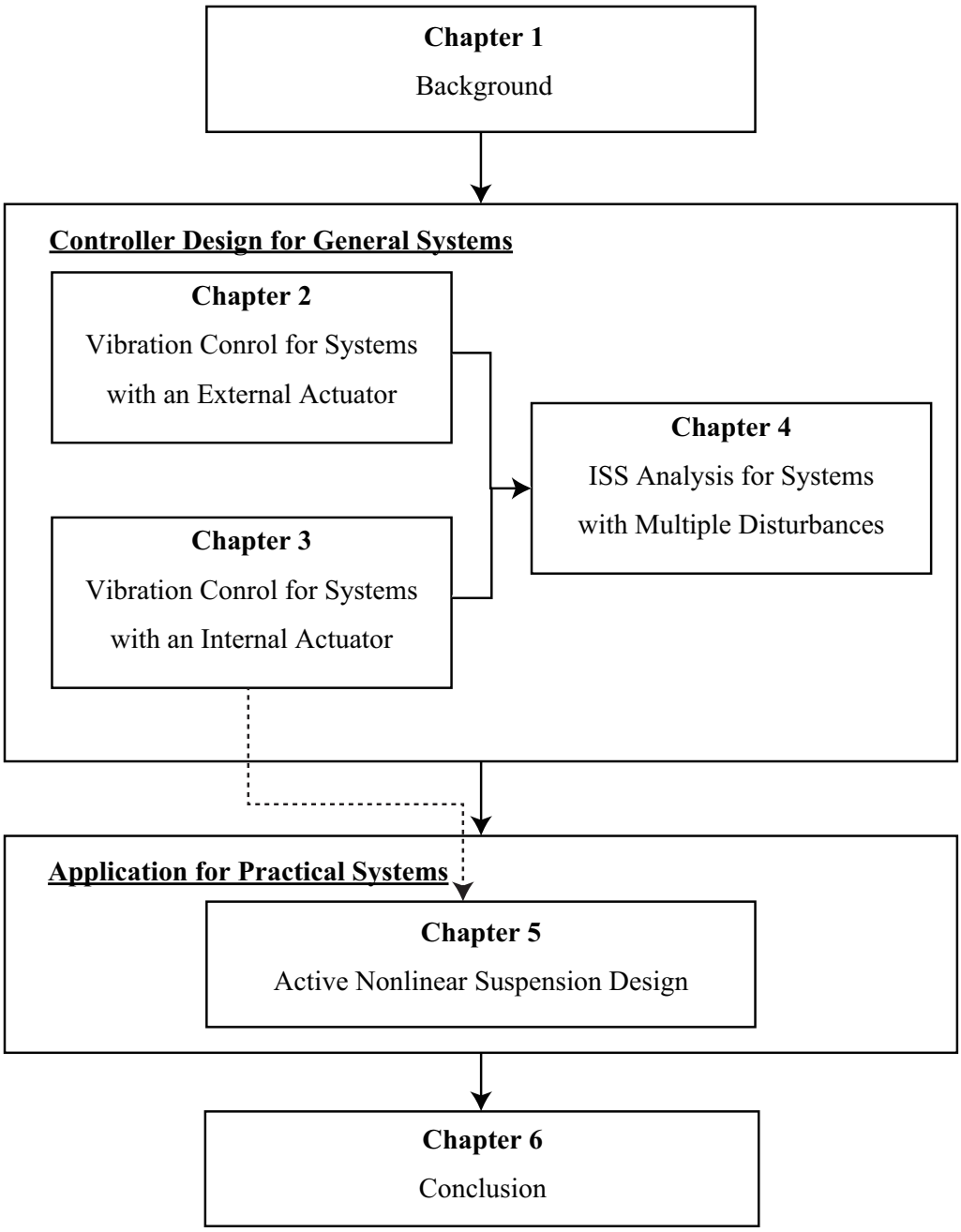

Figure 1.1: Overview of this dissertation

Chapter 2

Vibration Control for Systems with an External Actuator

2.1 Introduction

Consider the following basic linear structure like Fig. 2.1(a), where u, F, k, c, and z represent feedback input, force disturbance, spring elastic coefficient, damping coefficient, and floor displacement, respectively. It's simple to suppress vibrations using active vibration control methods if we know the primary body's absolute displacement. The skyhook damper mechanism, as depicted in Fig. 2.1(b), functions as a virtual damper between the main body and a fixed ceiling. We can get good control performance using this strategy. However, owing to floor vibrations, the absolute position reference point is lost, making obtaining the whole information of the main body, which is necessary for the skyhook damper technique, difficult.

With the help of an accelerometer, we can get all the information we need. A static loop is created via direct feedback of the acceleration signal, and a drift issue is generated by integrating the acceleration signal to acquire the velocity. Although filtering techniques can alleviate the static-loop problem, the frequency-domain design is frequently necessary due to the filter's undesirable phase lag.

As a result, this chapter presents a novel vibration-suppression control based solely on relative data. We suppose that the controlled item has an extra mechanical degree-

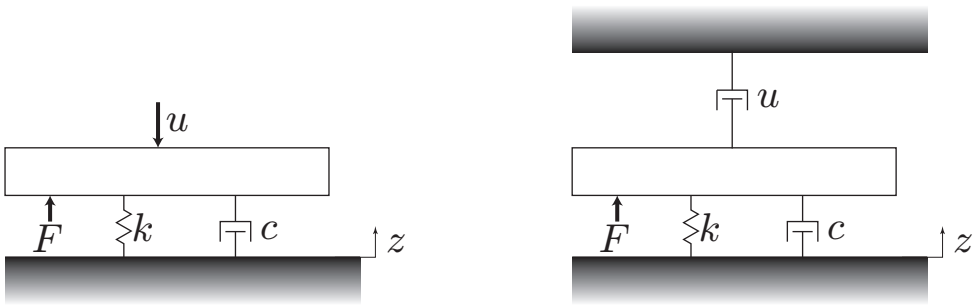

(a) Basic structure (b) Skyhook system

Figure 2.1: Conventional vibration suppression method

of-freedom (DOF) to collect more rich information from the relative movement measurements. This method is nearly identical to carefully studying the internal dynamics of an accelerometer. Our technique may be used in systems where the extra (nonlinear) dynamic structure is naturally contained, in addition to examples using accelerometers. In some circumstances, the extra structure may have a mass that cannot be disregarded, and its motion, even in the low-frequency range, has a phase lag.

2.2 Notation and Preliminaries

2.2.1 Notation

Notation	Description
$\mathbb{R}$	the set of real numbers
$\mathbb{R}^n$	the set of n-dimensional vectors
$\mathbb{R}^{m\times n}$	the set of $m \times n$ real matrices
$0_{m\times n}$	the $m \times n$ matrix whose elements are all zero
$\lvert\cdot\rvert$	a 2-norm
λ_{min}	the minimum eigenvalue

For matrix $A(x)$, $A(x) > 0$ means that $A(x)$ is a positive definite matrix, $A(x) \geq 0$ means that $M(x)$ is a semi-positive definite matrix. $A^{\perp}$ denotes the full row rank left annihilator of A, i.e., $A^{\perp} \cdot A = 0$.

2.2.2 Port-Hamiltonian systems

The presence of a storage function fulfilling the dissipation inequality with respect to the supply rate is well-known, and passive systems are characterized by the existence of a storage function satisfying the dissipation inequality with respect to the supply rate. Port-Hamiltonian (pH) systems, on the other hand, are endowed with the attribute of passivity as a result of their system formulation. pH systems are, in reality, the result of first-principles physical modeling. They are described in terms of a Hamiltonian function and two geometric structures (corresponding to power-conserving connectivity and energy dissipation, respectively), with the Hamiltonian function satisfying the dissipation criteria theoretically. pH system is a more general physical system expression formulation which including Euler-Lagrange systems. It is suitable for modeling and analyzing large-scale and complex systems, including complex physical areas such as electrical, mechanical, and thermal fluids, and has been actively researched in recent years.

A general form of pH systems is defined as follows.

Definition 1. A port-Hamiltonian system with n-dimensional state space manifold $\mathcal{X}$, input and output spaces $U = Y = \mathbb{R}^m$, and Hamiltonian $H : \mathcal{X} \to \mathbb{R}$, is given as

$$\begin{aligned} \dot{x} &= [J(x) - R(x)] \frac{\partial H}{\partial x}(x) + g(x)u \\ y &= g^{\top}(x) \frac{\partial H}{\partial x}(x) \end{aligned} \tag{2.1}$$

where the $n \times n$ matrices $J(x)$, $R(x)$ satisfy $J(x) = -J^{\top}(x)$ and $R(x) = R^{\top}(x)$

By the properties of $J(x)$, $R(x)$, it immediately follows that

$$\frac{dH}{dt}(x(t)) = \frac{\partial H}{\partial x}(x(t))\dot{x}(t) = -\frac{\partial H}{\partial x}(x(t))R(x(t))\frac{\partial H}{\partial x}(x(t)) + y^\top(t)u(t) \leq u^\top(t)y(t), \tag{2.2}$$

implying passivity if $H \geq 0$.

The Hamiltonian H represents the system's total stored energy, whereas $u^\top y$ represents the externally provided power. Geometric structures on the state space $\mathcal{X}$ play important roles in the definition of a pH system: the internal interconnection structure given by $J(x)$, which is power-conserving due to skew-symmetry, and a resistive structure given by $R(x)$, which is responsible for internal energy dissipation due to nonnegativity.

The pH formulation of standard mechanical systems directly follows from classical mechanics. The Hamiltonian representation of fully actuated Euler-Lagrange equations in n configuration coordinates $q = (q_1, ..., q_n)$ given by the $2n$ -dimensional system

$$\begin{aligned} \dot{q} &= \frac{\partial H}{\partial p}(q,p), \\ \dot{p} &= -\frac{\partial H}{\partial q}(q,p) + u, \\ y &= \frac{\partial H}{\partial p}(q,p) \ (\dot{q}), \end{aligned} \tag{2.3}$$

where the generalized forces vector and generalized velocities vector are represented by u and y, respectively. Herein (q, p) is the state space, also known as the phase space. The Hamiltonian function $H(q, p)$ is the sum of a kinetic energy and a potential energy in most mechanical systems.

$$H(q,p) = \frac{1}{2}p^\top M^{-1}(q)p + V(q). \tag{2.4}$$

2.2.3 IDA-PBC Method

IDA-PBC shapes both the kinetic energy and potential energy of the system while preserving the structure of the pH system and finally achieves stabilization by utilizing passive energy. Here we use an example of a simple pendulum to illustrate the mechanism, as shown in Figure 2.2. It is assumed that the support part of the pendulum is connected to the external environment by a frictionless joint, and torque can be input to the pendulum from the joint. Consider controlling the simple pendulum to an inverted state from the viewpoint of energy. The simple pendulum vibrates vertically and downward when there is no control input. This can be explained by the fact that the vertically downward direction is the minimum energy state of the simple pendulum system. IDA-PBC initially controls the minimum energy state of the system to be an inverted state by Energy Shaping. As a result, it becomes a natural state in the sense that the simple pendulum makes a simple vibration around the vertically upward direction. On top of that, a damping effect called Damping Injection is added, and the system converges to the minimum energy state. In other words, the simple pendulum is controlled to the inverted state. In this case, the damping effect is the negative feedback of the angular velocity of the pendulum, which physically corresponds to the damper and friction. In addition, the pendulum's angular

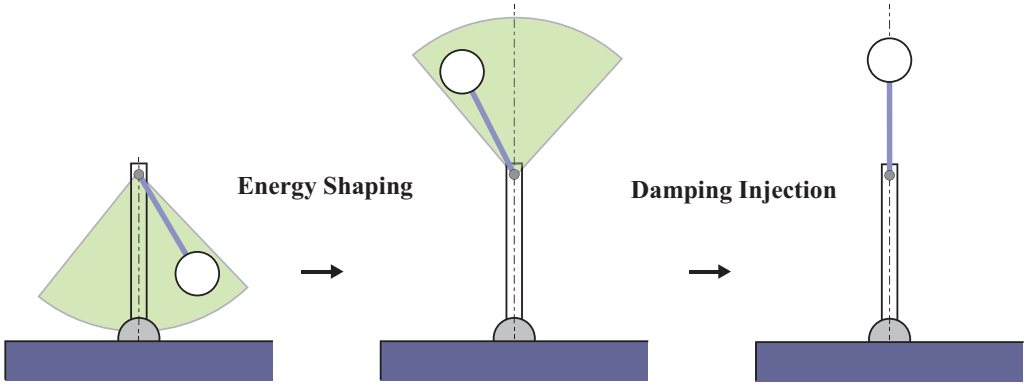

Figure 2.2: Illustration of IDA-PBC with an example of single pendulum

velocity corresponds to this system's passive output, and since stabilization is achieved by negative feedback, it is called passivity-based control (PBC).

The IDA-PBC approach is a strong controller design methodology for solving the stabilization problem, and the dynamics with a pH form are frequently described as follows:

$$\dot{x} = \begin{bmatrix} \dot{q} \\ \dot{p} \end{bmatrix} = \begin{bmatrix} 0_{n\times n} & I_n \\ -I_n & 0_{n\times n} \end{bmatrix} \frac{\partial H}{\partial x}^\top + \begin{bmatrix} 0_{n\times m} \\ G(q) \end{bmatrix} u, \tag{2.5}$$

where $q, p \in \mathbb{R}^n$ are the generalized displacement and momentum, respectively, $u \in \mathbb{R}^m$ represents the input force, and $G(q) \in \mathbb{R}^{n\times m}$, with rank$(G)= m$. When $m < n$, we say that the controlled system is underactuated. The Hamiltonian function H is defined as follows:

$$H(q,p) = \frac{1}{2} p^\top M^{-1}(q) p + V(q),$$

where $M \in \mathbb{R}^{n\times n}$ is the positive definite inertia matrix, and $V \in \mathbb{R}$ is the potential energy. Designing a static state feedback that stabilizes the target system is the control goal. In IDA-PBC, this is accomplished by matching the pH target dynamics.

$$\dot{x} = \begin{bmatrix} 0_{n\times n} & M^{-1}(q) M_d(q) \\ -M_d(q) M^{-1}(q) & J_2(q,p) - C_d(q) \end{bmatrix} \frac{\partial H_d}{\partial x}^\top, \tag{2.6}$$

with the new Hamiltonian function

$$H_d(q,p) = \frac{1}{2} p^\top M_d^{-1}(q) p + V_d(q),$$

where the desired mass matrix $M_d \in \mathbb{R}^{n\times n}$ is positive definite, the desired potential energy $V_d \in \mathbb{R}$ verifies

$$q^\star = \text{argmin} H_d(q) = \text{argmin} V_d(q), \tag{2.7}$$

and the desired damping matrix is defined by

$$C_d(q) = G(q) C_{dp} G^\top(q) \geq 0, \tag{2.8}$$

with C_{dp} a positive-definite matrix. The matrix $J_2 \in \mathbb{R}^{n\times n}$ is free to the designer and fulfills the skew-symmetry condition $J_2(q,p) = -J_2^\top(q,p)$. For holding (2.7), two conditions need to be satisfied.

1. Necessary extremum assignment: $\nabla_q H_d(q^\star) = 0$.
2. Sufficient minimum assignment: $\nabla_q^2 H_d(q^\star) > 0$, which indicates that the Hessian of the function at the equilibrium point is positive.

By equating the right-hand sides of (2.5) and (2.6), we obtain the matching equation

$$G^\perp(x)\left[\nabla_q H - M_d M^{-1}\nabla_q H_d + J_2 M_d^{-1} p\right] = 0, \tag{2.9}$$

and explicit expression of the control input

$$u = \left(G^\top G\right)^{-1} G^\top \left(\nabla_q H - M_d M^{-1}\nabla_q H_d + J_2 M_d^{-1} p\right) - R_d G^\top \nabla_p H_d, \tag{2.10}$$

The structural matrix is unaltered in the original PBC technique; that is, $J = J_d$. We may also adjust the kinetic energy by considering the new artificial structure matrix, giving us a lot of flexibility in selecting the desired Hamiltonian H_d. The requirement to solve nonlinear partial differential equations (2.9) is the fundamental disadvantage of IDA-PBC. Because a closed-form solution of the matching equation is seldom found, it is required to assess whether the desired goal dynamics can be achieved. The IDA-PBC approach is used to build an active DVA controller in the next section, with extra matching requirements for the disturbance terms taken into account.

Remark 2. For the general position control problem, like controlling crane, we usually only need to ensure the passivity and the equilibrium point, which can be achieved by classical PBC method. However, in vibration control problem, we have to consider the frequency response from disturbances, which varies by the setting of mass, springs, and dampers. If we can shape the kinetic energy, that means we can change the mass parameter of plant system, this will help us while suppressing the vibration. For instance, skyhook damper control, as a famous vibration control strategy, can be realized by classical PBC technique. The designed dissipation matrix represents the designed skyhook damper, which can suppress the vibration in limited frequency domain. However, if we can design the desired kinetic energy, which determined by mass parameter, the vibration suppression effect in frequency domain will be extended.

2.3 Controlled Objectives and Problem Setting

We define a class of port Hamiltonian systems with force and velocity disturbances in this section, which are typically encountered in vibration suppression problems. In our study, we added a nonlinear extra mass to the main body, as shown in Fig. 2.3(a), where q_1 represents the additional mass's relative displacement and $\tilde{q}_2$ denotes the main body's displacement in world coordinate. The system is a component of a managed object, but it is not the actual target system.

We can receive the absolute information of the primary body indirectly because the extra mass is aroused by the absolute movement of the main body. The main purpose of an accelerometer is to obtain absolute information from another device; consequently, this added mass serves the same purpose as an accelerometer. We investigate the dynamics of the added mass to prevent the algebraic loop caused by the direct feedback of the acceleration signal. In addition to examples using accelerometers, our technique may be used in systems with naturally occurring extra dynamic structure.

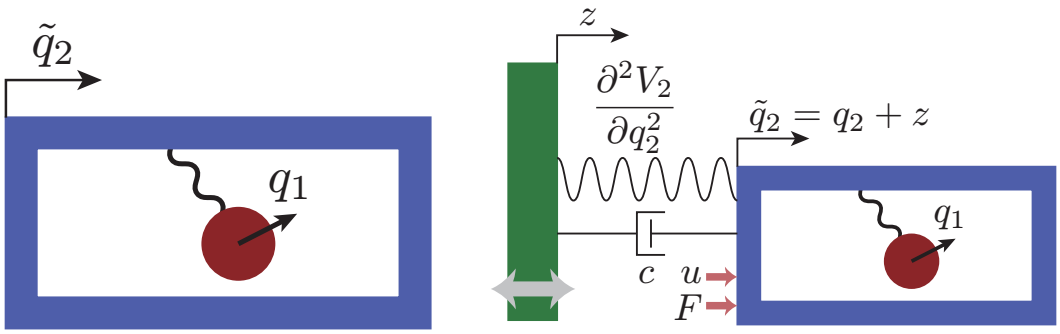

(a) Floating system (b) Controlled object

Figure 2.3: Structure of controlled object

We suppose that there is a symmetry on the change of $\tilde{q}_2$, from which Noether's theorem [33, 34, 35, 36] derives a law of conservation of momentum with regard to the movement of the whole mass in the $\tilde{q}_2$ direction. According to the symmetry, the Hamiltonian of this system is not the function of $\tilde{q}_2$, i.e. the inertia matrix and the potential energy only depend on q_1. Consequently, the Hamiltonian of the system of Fig. 2.3(a) can be written as

$$\begin{aligned} \tilde{H}(q_1, p) &= \frac{1}{2} p^\top M(q_1)^{-1} p + V_1(q_1) \\ M(q_1) &= \begin{bmatrix} m_1(q_1) & m_2(q_1) \\ m_2(q_1) & m_3(q_1) \end{bmatrix} \end{aligned} \tag{2.11}$$

$$p = M(q_1) \begin{pmatrix} \dot{q}_1 \\ \dot{\tilde{q}}_2 \end{pmatrix}, \tag{2.12}$$

and the friction coefficient matrix becomes $\tilde{C} = \mathrm{diag}(\mu, 0)$, where $\mu > 0$ is the friction coefficient of the additional movement. The positive-definite matrix $M(q_1)$ is the inertia matrix, $V_1(q_1)$ is the potential energy of the internal structure, and p is the generalized momentum. We assume that $V_1(q_1)$ is positive definite with respect to q_1. The law of conservation of momentum of the basic structure is $p_2 = m_2(q_1)\dot{q}_1 + m_3(q_1)\dot{\tilde{q}}_2 = \text{const.}$ We assume that there exists an interconnection between the motion of q_1 and $\tilde{q}_2$, and thus $m_2(q_1) \neq 0$.

By adding a potential force $V_2(q_2)$ and a damping term $c\dot{q}_2$ with respect to the relative movement between the main body and a vibrating object, a force disturbance F, and a control input u, we obtain the controlled object like Fig. 2.3(b). We assume that the control force and the force disturbance act on the main body. The Hamiltonian of the controlled system is

$$\begin{aligned} H(p, q) &= \tilde{H}(q_1, p) + V_2(q_2) \\ q &= (q_1, q_2)^\top, \quad q_2 = \tilde{q}_2 - z(t), \end{aligned} \tag{2.13}$$

where z and q_2 denote the displacement of the vibrating object and the relative displacement of main body from the object, respectively. We let the additional potential $V_2(q_2)$ be positive definite with respect to q_2 as well. The definition (2.12) of p can be rewritten as

$$p = M(q_1)\left(\dot{q} - a\omega\right), \tag{2.14}$$

where $\omega = \dot{z}$ is a velocity disturbance, and $a = (0, -1)^\top$. Notice that p is defined in the world coordinate, while q is a relative displacement vector.

Thus, the controlled object can be expressed by a port-Hamiltonian (pH) system

$$\dot{x} = (J - R)\frac{\partial H}{\partial x}^\top + D\omega + B(u + F), \tag{2.15}$$

where $x = (q^\top, p^\top)^\top$ is the state, and

$$J = \begin{bmatrix} O & I \\ -I & O \end{bmatrix}, \; R = \begin{bmatrix} O & O \\ O & C \end{bmatrix}, \; C = \tilde{C} + \tilde{C}_a = \begin{bmatrix} \mu & 0 \\ 0 & c \end{bmatrix},$$
$$B = (0\ 0\ 0\ 1)^\top,$$
$$D = (a^\top \ -(Ca)^\top)^\top = (0\ -1\ 0\ c)^\top.$$

Our main purpose is the vibration suppression of $\tilde{q}_2$ against the velocity disturbance $\omega(t)$ and the force disturbance $F(t)$. Note that $\tilde{q}_2 \approx 0$ means $q_2 \approx -z(t)$. Since the second element of D is -1, a feedforward term of ω exists in the dynamics of q_2, and therefore suppression of p will achieve the control objective. In this study, we construct an IDA passivity-based controller using only the relative displacements q and velocities $\dot{q}$, which can be easily measured by sensors. Note that our control law is not a function of q and p but q and $\dot{q}$, because p is defined in the world coordinate and (2.14) includes ω.

2.4 Modified IDA-PBC Method

2.4.1 Overview

The solution to the control problem indicated in the preceding part is given in this section, which involves building an IDA-PBC-based controller. The control variables of the IDA-PBC basic controller are relative displacement q, absolute momenta p, and disturbance signal ω. A feedback rule that only requires the relative displacement, q, and the relative velocity, $\dot{q}$, is produced by rewriting momenta p into the form of $M(\dot{q}+\omega)$ and canceling the coefficient of ω. The following is a summary of our suggested controller's design scheme:

Step 1: The plant system's pH form is calculated, and it is rebuilt using relative coordinates.

Step 2: IDA-PBC is used to develop the feedback law.

Step 3: The feedback law is split into two parts: relative information and disturbance. The criteria for making the disturbance component zero have been discovered.

Step 4: To ensure suspension performance and strong stability, criteria for parameter selection for the controller are established.

Step 5: The feedback law's precise form is achieved.

In this section, we define the dynamics of desired system at first, and then obtain a matching condition between the controlled system and the desired system. The matching condition clarifies the degree of freedom in the controller design and the expression of feedback law with free parameters as well as equality and inequality constraints.

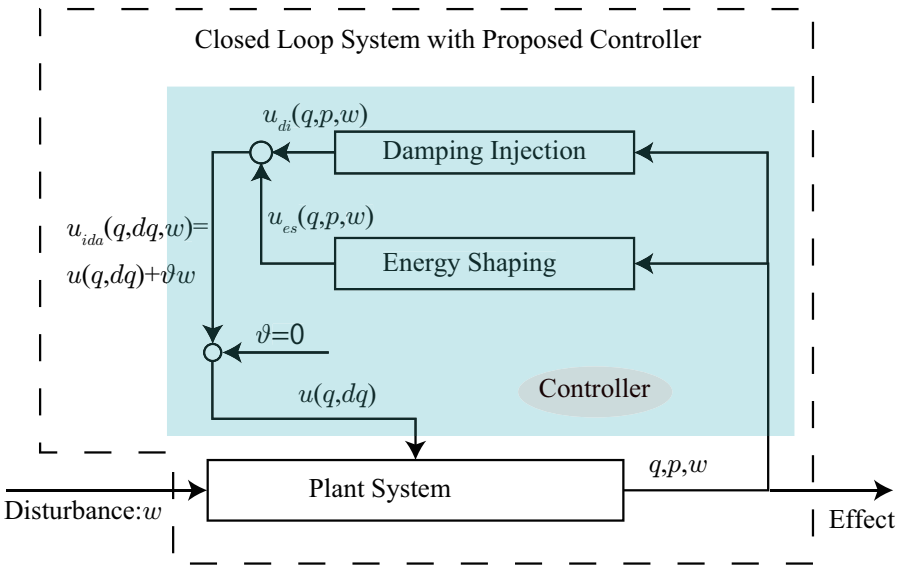

Figure 2.4: Control diagram of proposed method

2.4.2 Desired System

We construct the desired system with artificial structure matrix as follows:

$$\begin{aligned}\dot{x} = (J_d(q_1) - R_d(q_1))\frac{\partial H_d}{\partial x}^\top + D_d(q_1)\omega \\ + D_{dp}(q_1)p\cdot\omega + D_{d\omega}(q_1)\omega^2 + BF,\end{aligned} \tag{2.16}$$

where

$$H_d(x) = \frac{1}{2}p^\top M_d(q_1)^{-1}p + V_d(q_1,q_2) \tag{2.17}$$

denotes the Hamiltonian of desired system, and

$$\begin{aligned}
M_d(q_1) &= \begin{bmatrix} m_{d1}(q_1) & m_{d2}(q_1) \\ m_{d2}(q_1) & m_{d3}(q_1)\end{bmatrix}, \\
J_d(q_1) &= \begin{bmatrix} O & M(q_1)^{-1}M_d(q_1) \\ -M_d(q_1)M(q_1)^{-1} & J_2(q_1)\end{bmatrix}, \\
J_2(q_1) &= \begin{bmatrix} 0 & j_e(q_1) \\ -j_e(q_1) & 0\end{bmatrix}, \\
R_d(q_1) &= \begin{bmatrix} O & O \\ O & C_d(q_1)\end{bmatrix},\ C_d(q_1) = \begin{bmatrix} c_{d1}(q_1) & c_{d2}(q_1) \\ c_{d2}(q_1) & c_{d3}(q_1)\end{bmatrix}, \\
D_d(q_1) &= (0\ -1\ 0\ d_1(q_1))^\top, \\
D_{dp}(q_1) &= \begin{bmatrix} 0 & 0 & 0 & d_2(q_1) \\ 0 & 0 & 0 & d_3(q_1)\end{bmatrix}^\top, \\
D_{d\omega}(q_1) &= (0\ 0\ 0\ d_4(q_1))^\top.
\end{aligned}$$

$J_d(q_1)$, $R_d(q_1)$, $V_d(q)$, and $M_d(q_1)$ denote an artificial skew-symmetric structure matrix, a semi-positive definite damping matrix, a potential energy, and the inertia matrix in the desired Hamiltonian, respectively.

2.4.3 Application of IDA-PBC Method

We can derive the expression of feedback law with equality and inequality constraints on the parameters of the desired system by matching the dynamics of desired system with that of controlled system as follows:

$$(J_d - R_d)\frac{\partial H_d}{\partial x}^\top = (J - R)\frac{\partial H}{\partial x}^\top + Bu + (D - D_d)\omega - D_{dp}(q_1)p \cdot \omega - D_{d\omega}(q_1)\omega^2. \tag{2.18}$$

For convenience of calculations, we set

$$\begin{aligned} S(q_1) = M^{-1}(q_1) &= \begin{bmatrix} s_1(q_1) & s_2(q_1) \\ s_2(q_1) & s_3(q_1) \end{bmatrix} \\ S_d(q_1) = M_d^{-1}(q_1) &= \begin{bmatrix} s_{d1}(q_1) & s_{d2}(q_1) \\ s_{d2}(q_1) & s_{d3}(q_1) \end{bmatrix}. \end{aligned} \tag{2.19}$$

Hereafter, by omitting '(q_1)', we simply express them as S, S_d, s_i and s_{di}. Each side of (2.18) is four dimensions vector. The first two components of (2.18) are already satisfied for all x and ω. We can easily derive the equality constraints of parameters by extracting the coefficients of p, q and their higher-order terms. By focusing on the coefficients of p_1^2, p_1p_2 and p_2^2 in the third component of (2.18), we obtain

$$\begin{aligned} {s_{d1}}' &= \frac{|S_d|{s_1}'}{s_1s_{d3} - s_2s_{d2}} \\ {s_{d2}}' &= \frac{|S_d|{s_2}'}{s_1s_{d3} - s_2s_{d2}} \\ {s_{d3}}' &= \frac{|S_d|{s_3}'}{s_1s_{d3} - s_2s_{d2}}, \end{aligned} \tag{2.20}$$

where $*'$ means the derivative with respect to q_1.

The coefficients of p_1 and p_2 in the third component of (5.25) derive the following relations:

$$c_{d1}(q_1) = \frac{\mu}{|S_d|}(s_1s_{d3} - s_2s_{d2}) \tag{2.21}$$

$$j_e(q_1) = c_{d2}(q_1) + \frac{\mu}{|S_d|}(s_1s_{d2} - s_2s_{d1}). \tag{2.22}$$

The rest of the third component of (5.25) leads an equation for the potential energy

$$\frac{s_2s_{d2} - s_1s_{d3}}{|S_d|} \cdot \frac{\partial V_d}{\partial q_1} + \frac{s_3s_{d2} - s_2s_{d3}}{|S_d|} \cdot \frac{\partial V_d}{\partial q_2} + V_1' = 0.$$

The general solution of the above equation is

$$\begin{aligned} V_d(q) = P\left[q_2 + \int_0^{q_1} \frac{s_3s_{d2} - s_2s_{d3}}{s_1s_{d3} - s_2s_{d2}}\bigg|_{q_1=\tau} d\tau\right] \\ + \int_0^{q_1} \frac{V_1'|S_d|}{s_1s_{d3} - s_2s_{d2}}\bigg|_{q_1=\tau} d\tau, \end{aligned} \tag{2.23}$$

where P will be an arbitrary positive-definite function.

By solving the forth equation of (5.25) with respect to u, we can obtain a feedback law $u = \alpha_{\text{raw}}(q, p, \omega)$. Notice that the feedback should be a function of q and $\dot{q}$ only. Hence, we decompose α_{raw} as

$$\alpha_{\text{raw}}\left(q, M(q_1)(\dot{q} - a\omega), \omega\right) = \alpha(q, \dot{q}) + \alpha_{\text{rest}}(q, \dot{q}, \omega)\omega.$$

The coefficient $\alpha_{\text{rest}}(\cdot)$ should be identically zero, and thus we decompose it again as

$$\begin{aligned}&\alpha_{\text{rest}}(q, S(q_1)p + a\omega, \omega) = \\ &\quad \alpha_1(q_1) + \alpha_2(q_1)p_1 + \alpha_3(q_1)p_2 + \alpha_4(q_1)\omega.\end{aligned}$$

By solving $\alpha_i(q_1) = 0$ $(i = 1, \ldots, 4)$with respect to $d_1(q_1), \ldots, d_4(q_1)$ and applying (2.20), we obtain additional equality constraints

$$\begin{aligned}d_1(q_1) = \frac{1}{|S|}\{&(s_1 s_{d3} - s_2 s_{d2})c_{d3}(q_1) \\ &+ (s_1 s_{d2} - s_2 s_{d1})(j_e(q_1) + c_{d2}(q_1))\}\end{aligned} \tag{2.24}$$

$$(d_2(q_1)\ d_3(q_1)) = g(q_1) \cdot (0\ 1)M'S \tag{2.25}$$

$$d_4(q_1) = \frac{g(q_1)}{2} \cdot (0\ 1)M'(0\ 1)^\top, \tag{2.26}$$

where $M' = \partial M / \partial q_1$ and

$$g(q_1) = \frac{s_2 s_{d1} - s_1 s_{d2}}{s_1 s_{d3} - s_2 s_{d2}}.$$

The control input can be written as

$$\begin{aligned}u &= \alpha(q, \dot{q}) \\ &= \frac{(s_2 s_{d3} - s_3 s_{d2})c_{d3} - (s_3 s_{d1} - s_2 s_{d2})(c_{d2} + j_e)}{|S|}\dot{q}_1 \\ &+ (c - d_1(q_1))\dot{q}_2 + \frac{g(q_1)}{2} \cdot \dot{q}^\top M' \dot{q} + \frac{\partial V_2(q_2)}{\partial q_2} \\ &+ \frac{s_1 s_{d2} - s_2 s_{d1}}{|S_d|} \cdot \frac{\partial V_d}{\partial q_1} - \frac{s_3 s_{d1} - s_2 s_{d2}}{|S_d|} \cdot \frac{\partial V_d}{\partial q_2}.\end{aligned} \tag{2.27}$$

Because of the feature of IDA-PBC, the closed-loop system is identical to the desired system. Therefore, the asymptotic stability of zero-disturbance case can be guaranteed by the nature of pH system. Thus, we need to ensure the positive definiteness of M_d, V_d and C_d, and the following inequality constraints can be derived:

$$s_{d3}(q_1) > 0, \quad |S_d(q_1)| > 0, \tag{2.28}$$

$$s_1 s_{d3} - s_2 s_{d2} > 0, \quad {}^\forall q_1, \tag{2.29}$$

$$|C_d(q_1)| > 0, \tag{2.30}$$

$$P[\sigma] > 0, \quad \sigma \neq 0. \tag{2.31}$$

Inequalities (2.28) show the positive definiteness of the inertia matrix of the desired system. We can show $c_{d1}(q_1) > 0$ from (2.29) and (2.21), and therefore (2.29) and (2.30) means that the damping matrix of the desired system is positive definite. Because of (2.29), the positivity of the second term of (2.23) will be automatically satisfied if $q_1 V_1' \geq 0$. Hence, under the constraint (2.31), the potential energy function $V_d(q)$ is positive definite.

We can gain $s_{di}(q_1)$ by solving (2.20), while the initial value $S_d(0) = S_{d0}$ is a degree of freedom. The inequality constraints of parameters are (2.28), (2.29), (2.30), and (2.31). The equality constraints of parameters are (2.21), (2.22), (2.23), (2.24), (2.25), (2.26), and (2.27).

Note that the asymptotic stability is guaranteed by the positive definiteness of M_d, V_d and C_d. Therefore, stability of the numerical solution process of differential equation (2.20) is not required when designing the control law.

In next section, we derive the guideline of parameter selection in order that we can obtain an aseismic desired system.

2.5 Parameter Selection Guideline

2.5.1 Linear Approximation

We need to know what function all factors play in vibration dynamics in order to develop the parameters of the desired system. The actual significance of parameters in an inertia matrix, however, is uncertain due to the nonlinear term. As a result, we will first develop the parameter selection guideline based on the linearly approximated systems of (2.15) and (2.16), which define the free parameters' low-order terms. Then we'll use it in a nonlinear situation. By the quadratic approximation of H, the Hamiltonian of the linearized plant is

$$H_L(p,q) = \frac{1}{2}p^\top S_0 p + \frac{1}{2}(K_1 q_1^2 + K_2 q_2^2),$$

where

$$S_0 = \begin{bmatrix} s_{10} & s_{20} \\ s_{20} & s_{30} \end{bmatrix} = S(0)$$
$$K_1 = \frac{\partial^2 V_1}{\partial q_1^2}(0), \quad K_2 = \frac{\partial^2 V_2}{\partial q_2^2}(0).$$

The linearized controlled object can be described as

$$\dot{x} = \begin{bmatrix} 0 & I \\ -I & -C \end{bmatrix} \begin{pmatrix} \mathrm{diag}(K_1, K_2)q \\ S_0 p \end{pmatrix} + \begin{pmatrix} a \\ -Ca \end{pmatrix} \omega. \tag{2.32}$$

The quadratic approximation of H_d can be also obtained as

$$H_{dL}(p,q) = \frac{1}{2}\{p^\top S_{d0} p + K_{d1} q_1^2 + K_{d2}(q_2 + h q_1)^2\},$$

where

$$S_{d0} = \begin{bmatrix} s_{d10} & s_{d20} \\ s_{d20} & s_{d30} \end{bmatrix} = S_d(0),$$
$$h = \frac{s_{30}s_{d20} - s_{20}s_{d30}}{s_{10}s_{d30} - s_{20}s_{d20}} \tag{2.33}$$
$$K_{d1} = \frac{K_1 |S_{d0}|}{s_{10}s_{d30} - s_{20}s_{d20}}, \quad K_{d2} = \left.\frac{\partial^2 P(y')}{\partial y'^2}\right|_{y'=0}. \tag{2.34}$$

The linearized desired system is

$$\dot{x} = (J_{d0} - R_{d0}) \begin{pmatrix} K_{d0}q \\ S_{d0}p \end{pmatrix} + D_{w0}\omega + BF, \tag{2.35}$$

where

$$J_{d0} = \begin{bmatrix} O & M_0^{-1}M_{d0} \\ -M_{d0}M_0^{-1} & J_{20} \end{bmatrix}, \; J_{20} = \begin{bmatrix} 0 & j_{e0} \\ -j_{e0} & 0 \end{bmatrix}$$
$$M_{d0} = S_{d0}^{-1} = \begin{bmatrix} m_{d1} & m_{d2} \\ m_{d2} & m_{d3} \end{bmatrix}, K_{d0} = \mathrm{diag}(K_{d1}, K_{d2})$$
$$R_{d0} = \begin{bmatrix} O & O \\ O & C_{d0} \end{bmatrix}, \; C_{d0} = \begin{bmatrix} c_{d10} & c_{d20} \\ c_{d20} & c_{d30} \end{bmatrix}$$
$$D_{w0} = (0 \;\; -1 \;\; 0 \;\; d_{10})^\top$$

2.5.2 Coordinate Transformation

The diagonalized inertia matrix can help us clarify the structure of linearized system, thus we consider new transformed variables

$$\hat{q} = L^{-1}q, \quad \hat{p} = L^\top p, \tag{2.36}$$

where

$$L = \begin{bmatrix} r_0 & -r_0 \\ 0 & 1 \end{bmatrix}, \tag{2.37}$$
$$r_0 = \frac{m_{20}}{m_{10}} = -\frac{s_{20}}{s_{30}}. \tag{2.38}$$

To simplify the problem, we choose S_{d0} such that h defined by (2.33) becomes zero, i.e.

$$\frac{s_{20}}{s_{30}} = \frac{s_{d20}}{s_{d30}}. \tag{2.39}$$

Under the new constraint (2.39),

$$r_0 = \frac{m_{d20}}{m_{d10}} = -\frac{s_{d20}}{s_{d30}}$$

is also satisfied as well as (2.38).

The coordinate of main mass q_2 is maintained with this coordinate transformation, i.e. $\hat{q}_2 = q_2$. Please recall that the control objective is the vibration suppression of the main body. Then, the linear approximation of (3.2) can be transformed to

$$\hat{p} = L^\top M_0 L(\dot{\hat{q}} - L^{-1}L^\top a\omega) = \hat{M}(\dot{\hat{q}} - \hat{a}\omega),$$

where

$$\hat{M} = L^\top M_0 L = \mathrm{diag.}(\hat{m}_1, \hat{m}_2)$$
$$\hat{m}_1 = m_{10}r_0^2, \quad \hat{m}_2 = m_{30} - m_{10}r_0^2$$
$$\hat{a} = L^{-1}L^\top a = (-1 \;\; -1)^\top.$$

Consequently, the linearized controlled object (2.32) can be transformed to

$$\begin{pmatrix}\dot{\hat{q}}\\ \dot{\hat{p}}\end{pmatrix} = \begin{bmatrix}0 & I\\ -I & -\hat{C}\end{bmatrix}\begin{pmatrix}\hat{K}\hat{q}\\ \hat{S}\hat{p}\end{pmatrix} + \begin{pmatrix}\hat{a}\\ -\hat{C}\hat{a}\end{pmatrix}\omega, \tag{2.40}$$

where

$$\begin{aligned}
&\hat{S} = \hat{M}^{-1} = \mathrm{diag}(\hat{m}_1^{-1}, \hat{m}_2^{-1})\\
&\hat{K} = L^T \mathrm{diag}(K_1, K_2) L = \begin{bmatrix}\hat{K}_1 & -\hat{K}_1\\ -\hat{K}_1 & \hat{K}_1 + \hat{K}_2\end{bmatrix}\\
&\hat{C} = L^T C L = \begin{bmatrix}\hat{C}_1 & -\hat{C}_1\\ -\hat{C}_1 & \hat{C}_1 + \hat{C}_2\end{bmatrix}\\
&\hat{K}_1 = K_1 r_0^2, \quad \hat{K}_2 = K_2, \quad \hat{C}_1 = \mu r_0^2, \quad \hat{C}_2 = c.
\end{aligned}$$

Under the assumption (2.39), the inertia matrix of the linearized desired system (2.35) in the new coordinate is

$$\begin{aligned}
\hat{M}_d &= L^\top M_{d0} L = \mathrm{diag}(\hat{m}_{d1}, \hat{m}_{d2})\\
&= \mathrm{diag}(m_{d10} r_0^2, m_{d30} - m_{d10} r_0^2),
\end{aligned}$$

which is also a diagonal matrix under the constraint of (2.39). The linearized desired system is also converted into

$$\begin{pmatrix}\dot{\hat{q}}\\ \dot{\hat{p}}\end{pmatrix} = (\hat{J}_d - \hat{R}_d)\begin{pmatrix}\hat{K}_d\hat{q}\\ \hat{S}_d\hat{p}\end{pmatrix} + \hat{D}_d\omega + \hat{B}F, \tag{2.41}$$

where

$$\begin{aligned}
&\hat{J}_d = \begin{bmatrix}O & \hat{M}^{-1}\hat{M}_d\\ -\hat{M}_d\hat{M}^{-1} & \hat{J}_2\end{bmatrix}, \quad \hat{J}_2 = L^T J_{20} L,\\
&\hat{S}_d = \hat{M}_d^{-1} = \mathrm{diag}(\hat{m}_{d1}^{-1}, \hat{m}_{d2}^{-1}),\\
&\hat{K}_d = L^T \begin{bmatrix}K_{d1} & 0\\ 0 & K_{d2}\end{bmatrix} L = \begin{bmatrix}\hat{K}_{d1} & -\hat{K}_{d1}\\ -\hat{K}_{d1} & \hat{K}_{d1} + \hat{K}_{d2}\end{bmatrix},\\
&\hat{K}_{d1} = K_{d1} r_0^2, \quad \hat{K}_{d2} = K_{d2},\\
&\hat{R}_d = \mathrm{diag}\,(O, \hat{C}_d),\\
&\hat{C}_d = L^T C_{d0} L = \begin{bmatrix}\hat{C}_{d1} + \hat{C}_{d2} & -\hat{C}_{d2}\\ -\hat{C}_{d2} & \hat{C}_{d2} + \hat{C}_{d3} + \hat{C}_{d4}\end{bmatrix},\\
&\hat{C}_{d1} = r_0 c_{d2}, \quad \hat{C}_{d2} = r_0^2 c_{d10} - r_0 c_{d2},\\
&\hat{C}_{d3} = c_{d30} - r_0 c_{d20} - d_{10}, \quad \hat{C}_{d4} = d_{10},\\
&\hat{D}_d = \mathrm{diag}(L^{-1}, L^T) D_{w0} = (-1 \;\; -1 \;\; 0 \;\; d_{10})^\top,\\
&\hat{B} = \mathrm{diag}(L^{-1}, L^T) B = B.
\end{aligned}$$

The linearized controlled object (2.40) can be considered as a mass-spring-damper (MSD) system with a device similar to tuned mass damper (TMD) in Fig. 2.5(a). When we ignore the difference between J and $\hat{J}_d$, the linearized desired system (2.41) is regarded as an MSD system with a TMD-like device and multiple skyhook dampers in Fig. 2.5(b). Thus, in linearized case, the feedback law in this research realizes the virtual skyhook dampers by only relative displacements and velocities.

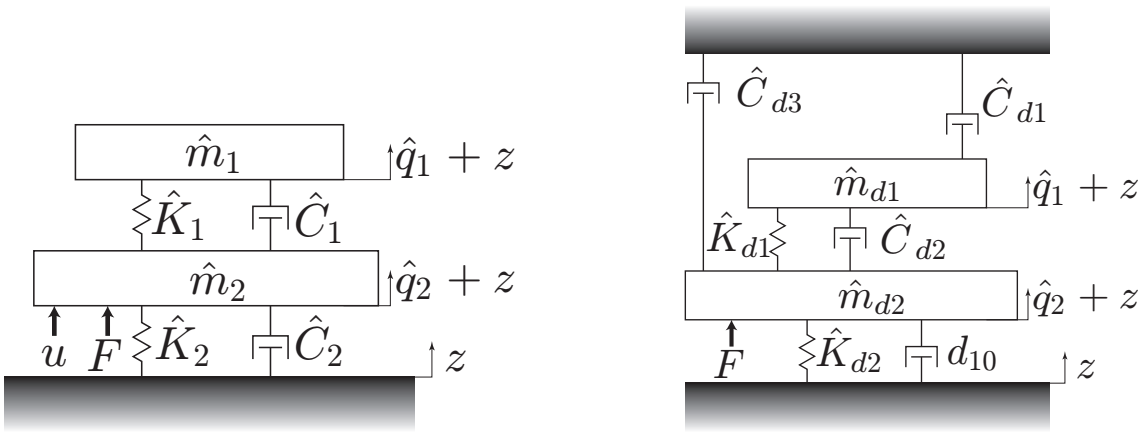

(a) Controlled object (b) Desired system

Figure 2.5: Linearized system

2.5.3 Parameter Design

We define mass ratios

$$r_1 = \frac{\hat{m}_{d1}}{\hat{m}_1} = \frac{m_{d10}}{m_{10}}, \quad r_2 = \frac{\hat{m}_{d2}}{\hat{m}_2}. \tag{2.42}$$

The values r_1 and r_2 are positive, if and only if $S_{d0} > 0$.

From the definition (2.42), the inequality constraint (2.30) can be rewritten as

$$|C_{d0}| = \mu d_{10} r_1 r_2 - [c_{d20} - \mu r_0 (r_1 - r_2)]^2 > 0. \tag{2.43}$$

From the view point of energy, the small dissipation matrix is unsuitable for the control objective. Thus, we set c_{d20} as

$$c_{d20} = \mu r_0 (r_1 - r_2), \tag{2.44}$$

which maximizes $|C_{d0}|$ for fixed r_1 and r_2. Hence, positive r_1, r_2, and d_{10} make C_{d0} and M_{d0} positive definite, and the asymptotical stability of the linearized desired system is guaranteed. We will design d_{10}, r_1, and r_2 such that $|C_{d0}|$ is sufficiently large, under the new constraint (2.44).

Under the assumptions (2.39) and (2.44), we obtain

$$c_{d30} = r_2 d_{10} + \frac{\mu r_0^2 (r_2 - r_1)^2}{r_1}. \tag{2.45}$$

The value of skyhook-damper coefficient of the main body becomes

$$\hat{C}_{d3} = d_{10}(r_2 - 1) + \frac{\mu r_0^2 r_2 (r_2 - r_1)}{r_1}. \tag{2.46}$$

Obviously, large d_{10}, r_2 and small r_1 can make skyhook damper coefficient (2.46) be large. However, large d_{10} will lead to an increase in high frequency gain from z to q_2, because d_{10} indicates the damping coefficient between the vibrating object and the main body, as seen in Fig. 2.5(b).

Hence, we choose small d_{10} first, and design small r_1 and large r_2 so that skyhook damper term coefficient $\hat{C}_{d3}$ is sufficiently large, because of (2.46). From the empirical knowledge, small d_{10} and large $\hat{C}_{d3}$ in Fig. 2.5(b) make a good vibration suppression effect.

The selection (2.44) makes $\hat{C}_{d1}$, which is the coefficient of the skyhook damper of the additional mass in Fig. 2.5(b), negative, but $|C_{d0}| > 0$ is guaranteed by a large c_{d30}. A large r_2 also decreases the low-frequency gain from F as

$$G_{F\tilde{q}_2}(0) = \frac{K_{d2}}{r_2}. \tag{2.47}$$

The above parameter selection guideline is more sophisticated than that in Aoki, et al[31]. The parameter selection procedure is summarized as follows.

1. Choose sufficiently small $d_{10} > 0$, sufficiently small $r_1 > 0$, and sufficiently large $r_2 > 0$. Select a small low-frequency gain with r_2 and K_{d2} in (2.47). Then design a positive-definite function $P[\cdot]$ by (2.34). From (2.39) and (5.19), S_{d0} (> 0) is determined.

2. Calculate $S_d(q_1)$ by solving the differential equations (2.20) with the initial condition $S_d(0) = S_{d0}$.

3. Check the conditions (2.28) and (2.29). If these inequalities are not satisfied for all q_1, return to the first step and choose the parameters again.

4. Set $c_{d1}(q_1)$ as (2.21). The values of $c_{d2}(0) = c_{d20}$ and $c_{d3}(0) = c_{d30}$ are determined by (2.44) and (2.45), respectively, and then $C_{d0} = C_d(0) > 0$ is guaranteed. Choose the high-order terms of $c_{d2}(q_1)$ and $c_{d3}(q_1)$ adequately so that $C_d(q_1) > 0$.

5. Calculate $j_e(q_1)$, $V_d(q)$, and $d_1(q_1)$ by (3.10), (2.23), and (2.24), respectively.

6. Obtain the control law (2.27).

Despite the constructive nature of the design approach, the high-order terms of c_{d2} and c_{d3} should be selected to fulfill $C_d(q_1) > 0$. The practical meaning of the inertia matrix in the desired system will be considerably different from that of the linear approximation case as q_1 increases. As a result, changes in the inertia matrix must be accompanied by changes in $C_d(q_1)$ distant from the origin. Large $|q_1|$, on the other hand, frequently indicates that the present vibration is severe, therefore it is reasonable to increase the feedback gain when $|q_1|$ hits a threshold. The concept of a control barrier function might be used for this, however this is a matter for future research. The parameter selection guideline in this chapter focuses on increasing the size of the skyhook damper term, whereas the free parameter selection in this suggested technique can regulate not only the skyhook damper term but also the mass and spring term. The sensitivity of the free-parameter selection to control performance will determine how to alter those terms to suppress vibration in a larger frequency domain, and that will be the focus of our future study.

2.6 Parameter Selection under Uncertainties

Although with the parameter selection for the case mentioned above we can obtain a perfect aseismatic desired system, the robustness against parameter uncertainties should

be considered. Especially in vibration suppression industry, the attenuation of damper property and the uncertainty of damper property often worsen the vibration suppression effect. Thus, in this section, we clarify the parameter selection for the robust controller. We redefine the damping coefficients μ and c as

$$\mu = \tilde{\mu} + \Delta\mu, \tag{2.48}$$
$$c = \tilde{c} + \Delta c, \tag{2.49}$$

where $\tilde{\mu}$, $\tilde{c}$ are the nominal values, and $\Delta\mu, \Delta c$ represent the uncertainties. The control input u can be decomposed as

$$u = u_c + u_\mu + u_{rest}, \tag{2.50}$$

where

$$u_c = (c - d_1(q_1)) \cdot \dot{q}_2, \tag{2.51}$$
$$u_\mu = \frac{(s_2 s_{d3} - s_3 s_{d2}) c_{d3} - (s_3 s_{d1} - s_2 s_{d2})(c_{d2} + j_e)}{|S|} \dot{q}_1. \tag{2.52}$$

The ideal robust control input u should satisfy

$$e_c = \frac{u_c(c) - u_c(\tilde{c})}{u_c(c)} = \frac{\Delta c}{c - d_1(q_1)} \approx 0, \tag{2.53}$$
$$e_\mu = \frac{u_\mu(\mu) - u_\mu(\tilde{\mu})}{u_\mu(\mu)} \approx 0. \tag{2.54}$$

The first condition (2.53) can be easily satisfied by setting $d_1(q_1)$ sufficiently large. Although the second condition (2.54) is difficult to satisfied directly, we can find that the vibration suppression effect highly depends on the value of skyhook-damper coefficient (2.46) in linear approximated systems. Therefore, we focus on the cancelling the uncertainty of μ in linear approximated systems. The uncertainty of μ in the value of skyhook-damper coefficient (2.46) can be described as

$$e_{s\mu} = \frac{\Delta\mu r_0^2 r_2 (r_2 - r_1)}{r_1}, \tag{2.55}$$

which can be ignored by setting $r_1 = r_2$. Thus, with $r_1 = r_2$ and large value of $d_1(q_1)$, the controller will be robust against the uncertainty of damping term μ and c.

Besides the robustness against uncertainty, we also must ensure the vibration suppression effect of the controller. Especially, a large $d_1(q_1)$ is needed for the robustness to Δc, but large d_{10} also increases the high frequency gain from z to q_2. Although it seems like a trade-off problem, we can recall the effect of d_{10} in detail, which can be expressed as

$$\ddot{x} = -\frac{G_d}{\hat{m}_2}(\dot{x} - \omega) = -\frac{d_{10}}{\hat{m}_2 r_2}(\dot{x} - \omega). \tag{2.56}$$

As long as we guarantee the small value of G_d, the high frequency gain from z to q_2 will be safe. In addition, the effect of skyhook damper G will be ensured by setting large d_{10} and small G_d.

The parameter selection procedure is summarized as follows.

1. Choose appropriate values of d_{10}, r_1, and r_2. If there is no uncertainty, choose large r_2 and small r_1, d_{10}. If there are uncertainties of c and μ, choose large d_{10} and r_2, and set $r_1 = r_2$. A positive definite function $P[\cdot]$ is also determined by a desired $G_{F\tilde{q}_2}(0)$ with (2.47). From (2.39) and (5.19), S_{d0} (> 0) is determined.

2. Calculate $S_d(q_1)$ by solving the differential equations (2.20) with the initial condition $S_d(0) = S_{d0}$.

3. Check the conditions (2.28) and (2.29). If these inequalities are not satisfied for all q_1, return to the first step and choose the parameters again.

4. Set $c_{d1}(q_1)$ as (2.21). The values of $c_{d2}(0) = c_{d20}$ and $c_{d3}(0) = c_{d30}$ are determined by (2.44) and (2.45), respectively, and then $C_{d0} = C_d(0) > 0$ is guaranteed. Choose the high-order terms of $c_{d2}(q_1)$ and $c_{d3}(q_1)$ adequately so that $C_d(q_1) > 0$.

5. Calculate $j_e(q_1)$, $V_d(q)$, and $d_1(q_1)$ by (3.10), (2.23), and (2.24), respectively.

6. Obtain the control law (2.27).

Although the design procedure is constructive, the high-order terms of c_{d2} and c_{d3} should be chosen to satisfy $C_d(q_1) > 0$. As well as increasing q_1, the practical meaning of the inertia matrix of the desired system will differ significantly from that of the linear approximated case. Therefore, $C_d(q_1)$ far from the origin must be varied, as well as changes in the inertia matrix. On the other hand, a large $|q_1|$ often implies that the current vibration is violent, and therefore it is natural to use a high feedback gain when $|q_1|$ reaches a threshold. The concept of the control barrier function may be utilized for this purpose, but this topic is outside the scope of the present study and will be addressed in the future.

2.7 An Example and Simulation

In this section, we illustrate the vibration suppression effect of the proposed feedback law by providing a numerical example. We consider a cart-pendulum system, which is one

Table 2.1: Parameters of the cart pendulum system

Parameters	Symbol	Unit	Value
pendulum mass	m_p	Kg	0.2
cart mass	m_c	Kg	10
length of mass less bar	l	m	5
viscosity dumper coefficient	c	N/(m/s)	2
rotational friction coefficient	μ	N/(m^2/s)	10
elastic coefficient	k_2	N/m	3

of the benchmark models of a 2DOF system. The model is shown in Fig. 2.6, where q_1, $\tilde{q}_2$, z, F, and u denote the swing angle of a pendulum, displacement of a cart in world coordinates, a disturbance from the basement, a force disturbance on a cart, and an input force, respectively. The system is tested by the disturbances $z = \sin(bt)$ and $F = 100\cos(bt)$ for $b = 1$ and $b = 10$.

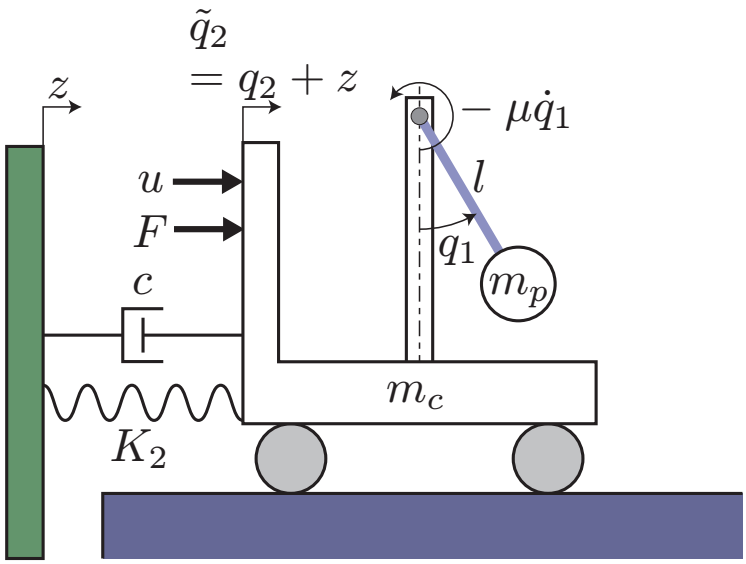

Figure 2.6: Cart and pendulum system.

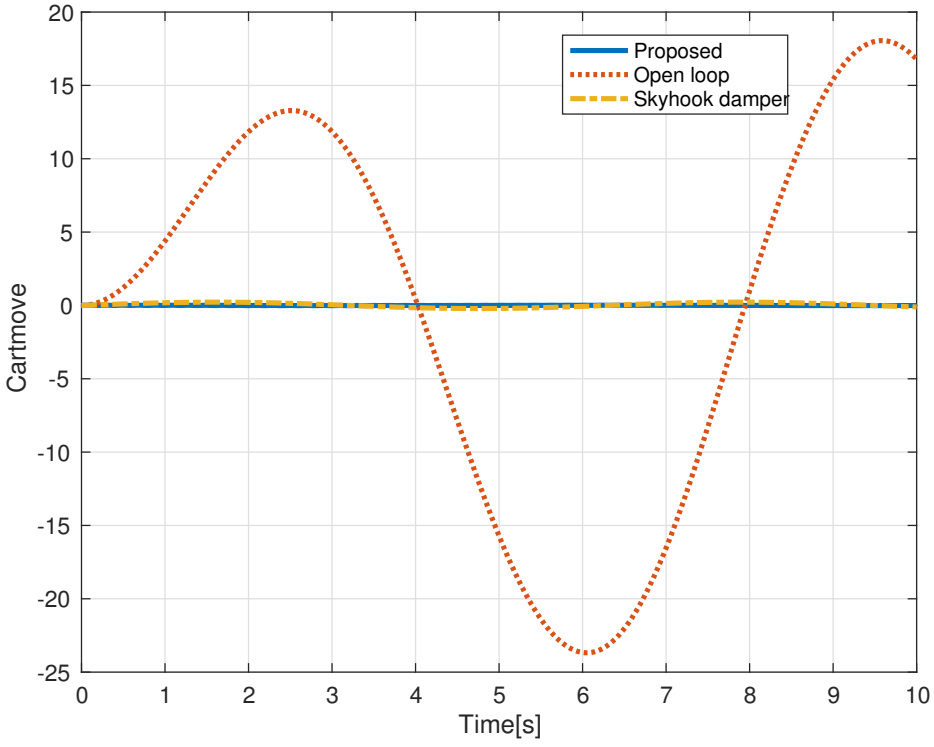

Figure 2.7: Time responses of the cart displacement ($b = 1$).

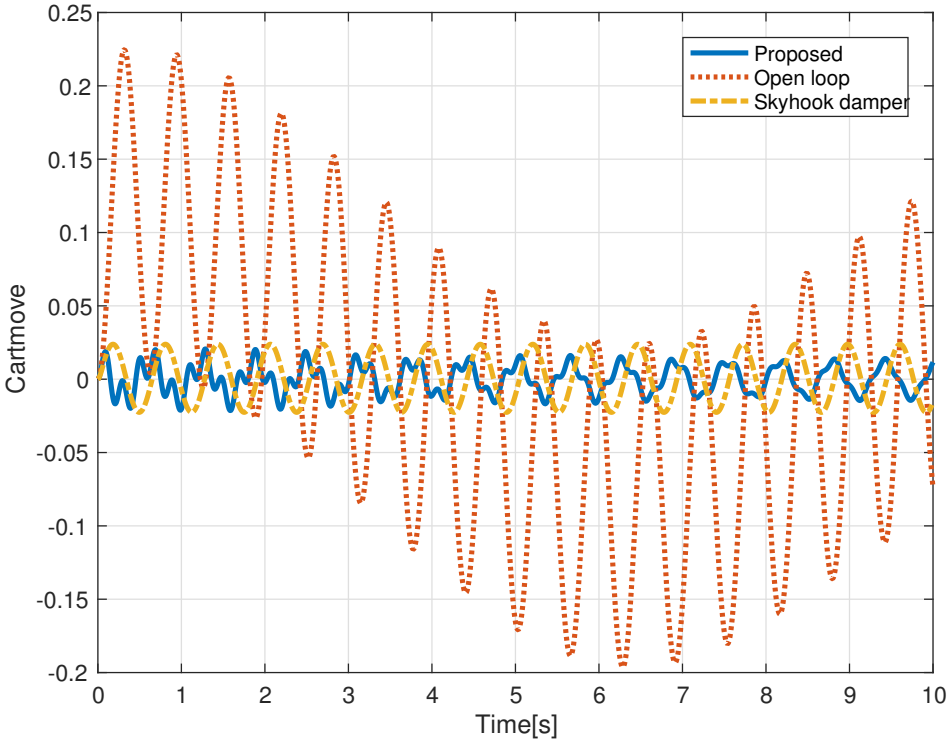

Figure 2.8: Time responses of the cart displacement ($b = 10$).

Author run simulations for the open loop system, the closed-loop system using the suggested feedback law, and the closed-loop system using the traditional skyhook damper approach to verify the proposed method's effectiveness. The feedback law of skyhook damper controller is given as

$$u = -\hat{C}_{d3}\dot{\tilde{q}}_2,$$

where the skyhook damper value $\hat{C}_{d3}$ is set as the same value as the one of our proposed method. The skyhook damper approach, on the other hand, is used with the premise that the cart's absolute displacement and velocity are observable, but our suggested solution simply employs relative displacement and velocity information.

According to the proposed guideline of parameter selection in section 5, we firstly set small d_{10}, small r_1 and large r_2 as $d_{10} = 2$, $r_1 = 15$ and $r_2 = 1000$. Since a small low-frequency gain $G_{F\tilde{q}_2}(0)$ is preferred, we design the part of the desired potential energy function $P[\cdot]$ as $P[\gamma] = 5\gamma^2$, so that $G_{F\tilde{q}_2}(0) = 0.005$. By setting $c_{d2}(q_1) = c_{d20}$ and $c_{d3}(q_1) = c_{d30}$, we can ensure that the inequality constraints (2.28), (2.29) and (2.30) are satisfied.

We analyze the displacements of the main body $\tilde{q}_2$, whose vibration should be dampened, using simulations. Figures 2.7 and 2.8 depict the temporal responses of the cart displacement in open-loop system and closed-loop system, respectively, when $b = 1$ and 10. One can observe that in the closed-loop system with the suggested controller, the main structure vibration is well controlled, whereas the open-loop approach has only a little vibration suppression impact. Nevertheless, there is no discernible difference in performance between the skyhook damper approach and the suggested method. As a result, we were able to demonstrate that the suggested approach can accomplish the same successful vibration reduction performance as the skyhook damper method without the need for world-coordinate measurements.

To verify the parameter selection guideline, considering parameter uncertainties, proposed in Section 2.6, we use the suggested controller to simulate the open-loop and closed-loop systems, with disturbances of $z = \sin(bt)$ and $F = 100\cos(bt)$ for $b = 1$ and $b = 10$, respectively, with initial state of $q(0) = 0$ and $p(0) = 0$. We analyze the displacements of the main body $\tilde{q}_2$, whose oscillation should be reduced, using simulations.

We first verify the vibration suppression effect without parameter uncertainties. Thus, we set $\Delta\mu = \Delta c = 0$. We choose free parameters of the controller as $r_1 = 100$, $r_2 = 1000$, $d_{10} = 2$, $P[\gamma] = 5\gamma^2$, $c_{d2}(q_1) = c_{d20}$, and $c_{d3}(q_1) = c_{d30}$. The temporal responses of the cart movement in the open-loop system and closed-loop system, respectively, are shown in 2.9 and 2.10. One can observe that in the closed-loop system with the suggested controller, the main structure vibration is well controlled, whereas the open-loop approach has only a little vibration suppression impact.

Author chose free parameters like $r_1 = r_2 = 1000000$ and $d_10 = 2000$, and standard parameters like $r_1 = r_2 = 1000000$ and $d_10 = 2000$. Author set $\Delta\mu = -9$ and $\Delta c = -1$, implying that the true values of damper parameters are $mu = 1$ and $c = 1$, respectively, to test robustness against μ and c uncertainty. The actual parameters μ, c are used in the dynamics of experiment model, whereas the nominal values $\tilde{\mu}, \tilde{c}$ are used in the feedback law. Figures 2.11 and 2.13 depict the temporal response of cart displacement in an open and closed loop system, respectively, using a conventional controller that disregards uncertainties. Figures 2.12 and 2.14 depict the temporal response of cart displacement in an open loop and closed loop system with a robust controller that takes uncertainties

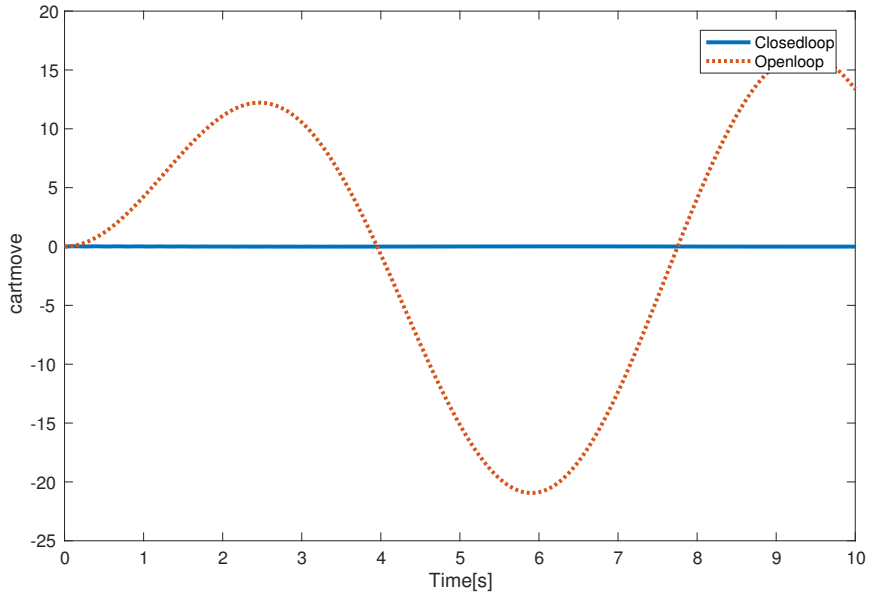

Figure 2.9: Time responses of the cart displacement without parameter uncertainties ($b = 1$).

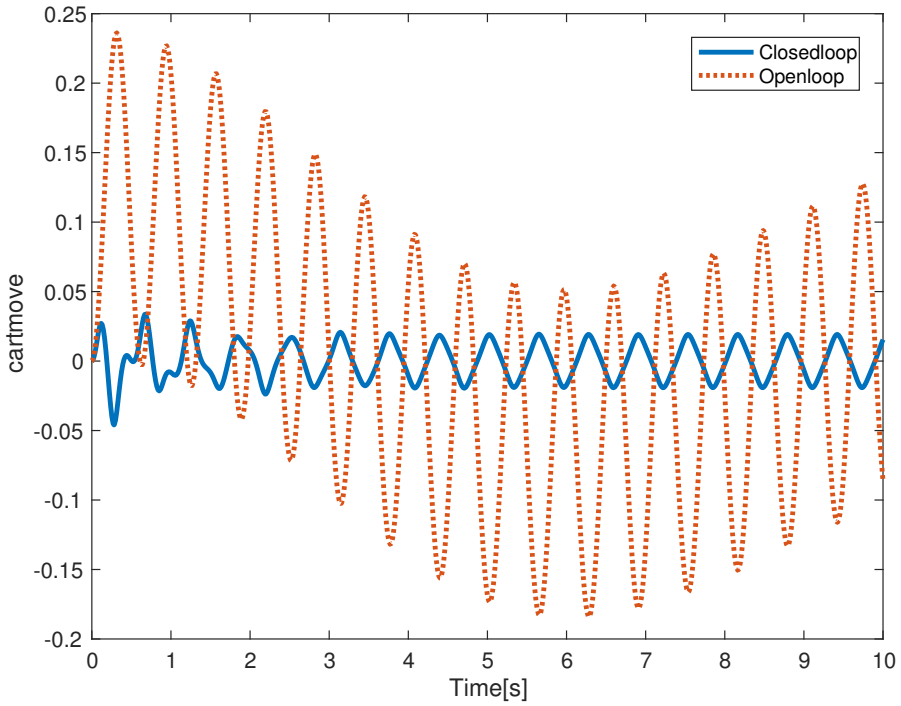

Figure 2.10: Time responses of the cart displacement without parameter uncertainties ($b = 10$).

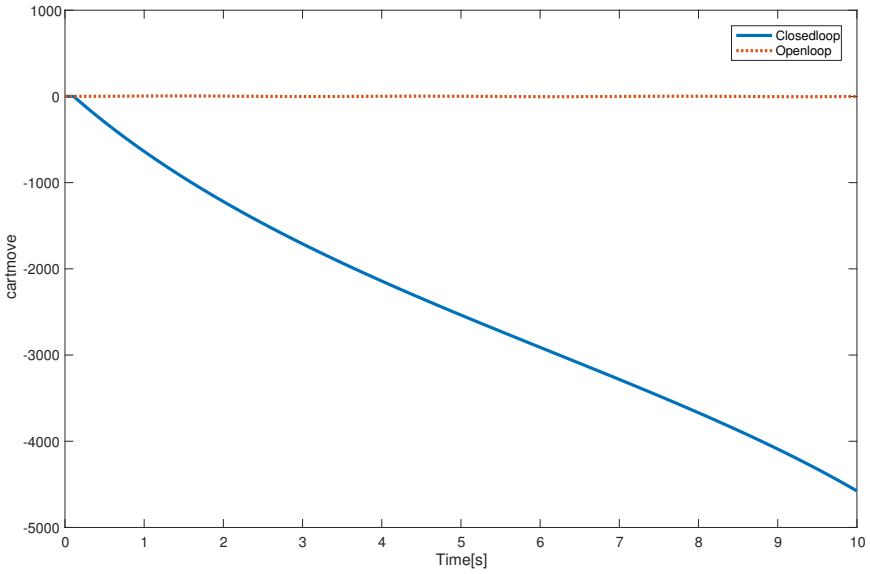

Figure 2.11: Time responses of the cart displacement with standard controller ($b = 2$)

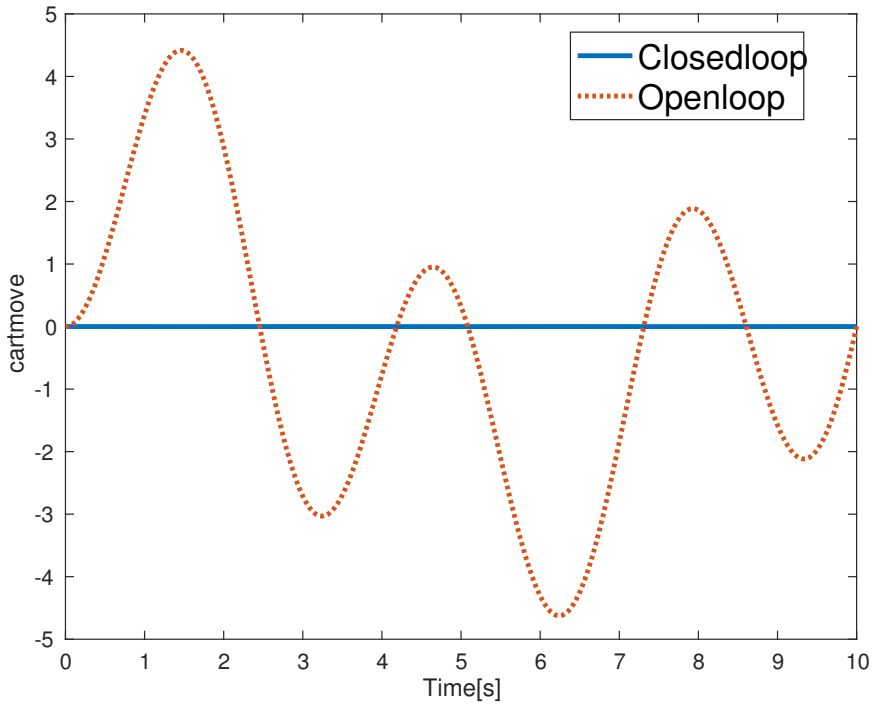

Figure 2.12: Time responses of the cart displacement with robust controller ($b = 2$)

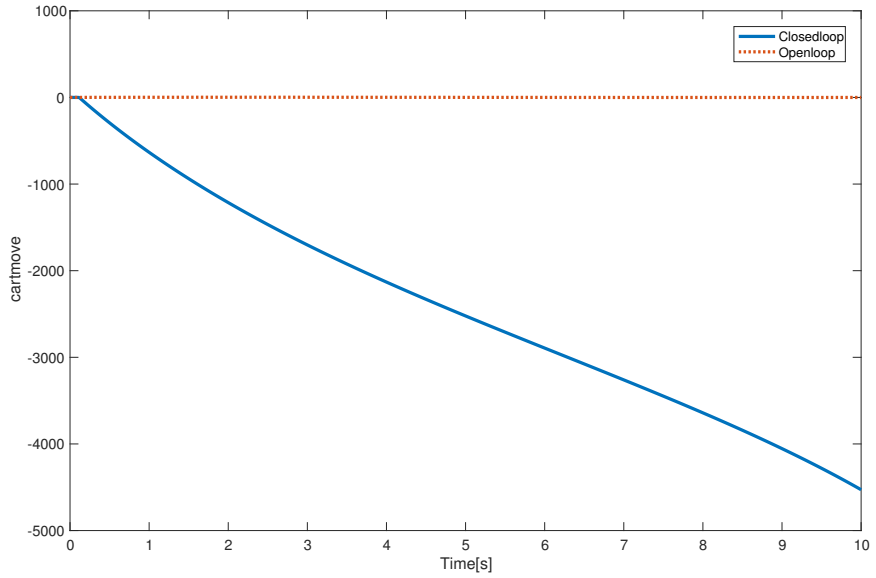

Figure 2.13: Time responses of the cart displacement with standard controller ($b = 10$)

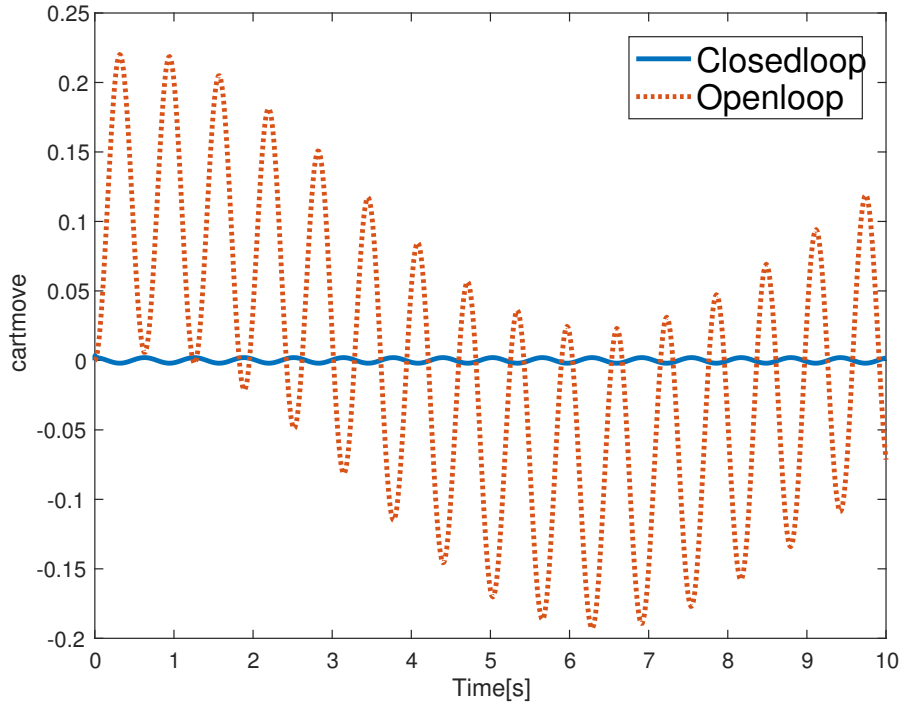

Figure 2.14: Time responses of the cart displacement with robust controller ($b = 10$)

into account. As shown by these figures, the controller created by ignoring uncertainties is unable to suppress vibration, but the controller created by using a robust design effectively suppresses vibration as predicted by the proposed hypothesis.

2.8 Conclusion

We solved the vibration suppression problem of the general pH system in this chapter by inventing the IDA-PBC controller. Any floating nonlinear mechanical structure with spring and damper can be used to represent the system under discussion. The matching condition between the controlled system and the desired system has been demonstrated. We demonstrate a control law with various free parameters and limitations. Only relative information, which is easily measured, is used by the controller. In comparison to earlier work [31], we offer a novel parameter design technique for more generalized nonlinear controlled devices.

The inertia matrix of the intended closed-loop system is determined using differential equations. The IDA-PBC approach theoretically guarantees the stability of the nonlinear closed-loop system. We have proposed an efficient parameter selection scheme achieving a good vibration suppression effect. Under the proposed parameter selection, the proposed control law realized a virtual skyhook damper using only relative information. Simulation results for an example verify the good vibration effect of the proposed controller.

Chapter 3

Vibration Control for Systems with an Internal Actuator

3.1 Introduction

Since the concept of a dynamic vibration absorber (DVA), otherwise known as a tuned mass damper (TMD), was introduced in [37], it has been widely utilized in vibrating mechanical systems during the past few decades. Theories and applications with respect to the use of DVAs have been developed in buildings, bridges, suspension systems applied in automobiles, space robot arms, and many other engineering systems [38, 39, 40].

Roughly speaking, a basic passive DVA is an additional /inertia structure linked to a vibrating system with a spring and viscous damper. A DVA generates a force equal and opposite to the exciting force, and the excited vibration can then be absorbed/suppressed by the DVA. Owing to their simplicity and efficacy, passive DVAs are widely used in many applications, where a balance of certain factors occurs, e.g., mass, spring, and damper, of the DVA. However, the vibrations may become more violent if the factors are out of balance. In particular, the deterioration of the vibration absorption performance will be significant when the ratio of the DVA mass to the system mass is small. In addition to the aforementioned problem, a passive DVA is ineffective when the vibrating system is excited by multiple frequencies, which is a common occurrence, e.g., tall buildings under seismic forces and wind. Accordingly, several solutions have been developed by researchers, including the use of multiple DVAs [41, 42, 43, 44], to reinforce the effect of perturbation cancellation and robustness, although it is still challenging to solve such cases that include varying excitation frequencies. Nonlinear elements are considered in [45] and [46] for solving multiple frequencies, although the analysis of nonlinear phenomena and dynamic behaviors is not straightforward. Consequently, the application of passive DVAs is simple and effective; in practice, however, the effect of vibration suppression remains insufficiently explored.

By utilizing actuators, sensors, controller, and additional energy sources, active DVAs can achieve a better vibration suppression performance and resolve the aforementioned problems. The active DVA's difference from the passive DVA is that we can change the imposed force between the DVA and the primary system according to the different control strategy. Active DVA controllers using frequency domain approaches ([47]), optimal control theory ([48, 49, 50]), H_∞ control theory ([51]), and Fuzzy theory ([52]) have been reported in previous studies. Moreover, methods considering the robustness with respect

to modeling and sensing were reported in [53]. However, few studies have focused on the cost of the sensors. When the exogenous displacement vibration affects the system, the controllers of previous studies utilize world-coordinate information, but have ignored the fact that the information obtained from low-cost sensors is often based on relative coordinates. Requiring the absolute displacement and velocity of a vibration may lead to expensive sensors or high cost calculations such as with a disturbance observer technique.

By contrast, although nonlinear DVAs, e.g., a pendulum TMD ([54]), bidirectional TMD ([55]), and tuned liquid column damper (TLCD) ([56]), can offer a more powerful vibration suppression effect than linear DVAs, the controller should consider the nonlinearity of the DVAs as well. During the past decades, many active nonlinear DVAs designed by [57, 58, 59] have been proposed. A limitation with respect to the cost of the sensors still exists; meanwhile, solving the Hamilton-Jacobi partial differential equations becomes another difficulty(e.g., the existence of analysis solution) when we try to apply some of these theories.

As a powerful energy shaping control method for nonlinear systems, IDA-PBC[25] is widely used in mechanical nonlinear systems. The global asymptotic stability of the system under IDA-PBC without a disturbance is theoretically guaranteed because a desired Hamiltonian function can be naturally designed as a Lyapunov function. Although the classical PBC technique can solve wide range of control problem, as a result of lacking freedom for designing controller, it is difficult to solve vibration control problem by using the classical PBC technique. Different from other PBC technique, one of the advantages of IDA-PBC is that we can change the kinetic energy, which gives a big degree of freedom for designing controller. The changes in the kinetic energy, potential energy, and damping matrix represent the virtual changes in the inertia, the elasticity coefficients or gravity terms, and the viscous resistance coefficients, respectively. These parameters directly influence the vibration suppression effect. The crux in the design procedure of IDA-PBC is how to ensure the solution for a set of partial differential equations caused by matching dynamics. A vibration control method for a general nonlinear two degree-of-freedom (DOF) system based on IDA-PBC was recently proposed by [31, 60]. However, the feedback law proposed by [31, 60] is not suited to an active DVA because it assumes that the actuator is attached to the targeted vibrating object and is not set between the vibrating object and DVA-like structure. Though their study utilize the dynamics of additional structure like other DVA studies, their main objective is to use it as a sensor, not to use it as DVA. Consequently, their additional structure do not have any functions that can absorb the vibration. The vibration energy is totally suppressed by the control force, which does not influence the dynamics between the control object and the additional structure. Furthermore, the previously proposed technique requires numerical solutions of partial differential equations to obtain a new inertia matrix.

In this study, our objective is to design a novel active DVA using IDA-PBC. In particular, we focus on the following:

1. We suppress the vibration excited by multiple disturbances.

2. We suppress the vibration by using only the relative displacement and velocity of the vibration system.

3. The partial differential equations generated by the nonlinearity of controlled object should be easily calculated, or the existence of the solution should be ensured.

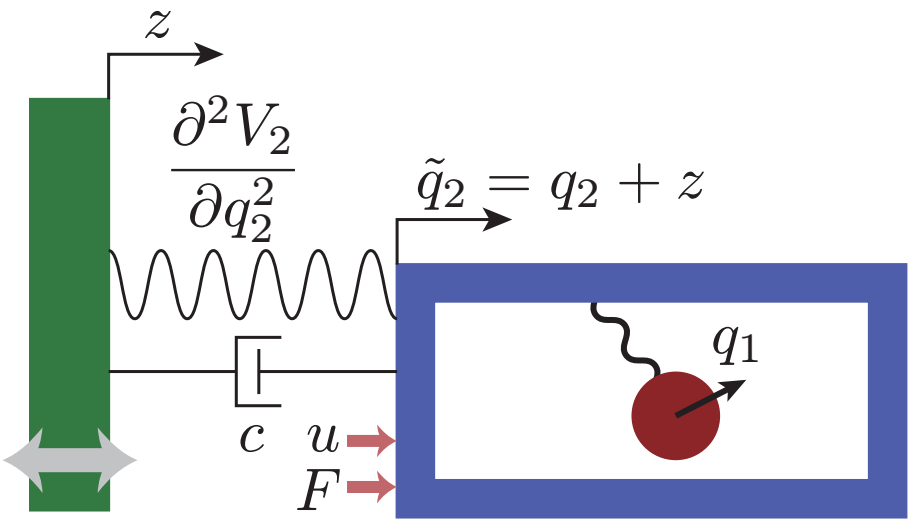

Figure 3.1: An example of a controlled object

The controlled object is under the velocity disturbance, which can be considered as the velocity of the base or ground, and the force disturbance simultaneously. Our strategy to cancel the excited vibration is using IDA-PBC to convert the controlled system into a desired system whose linearized structure includes a skyhook damper(see, e.g., [10, 15, 61]). By tuning the skyhook damper coefficient, the vibration suppression effect can be enhanced. We derive the guidelines for the parameter selection of the newly desired Hamiltonian system such that the controller can effectively suppress the vibration. Although the parameters of the controller are designed from the point of view of a linearized system, the global asymptotic stability of a nonlinear system is automatically guaranteed by using passivity-based control theory, which is an advantage of our method. Because the vibration of DVA is excited by the absolute motion of vibrating main mass, the absolute information of vibration can be obtained indirectly by utilizing the motion of DVA. With respect to the partial differential equations generated by the nonlinearity, we derive the conditions that can help us avoid a part of partial differential equations. And also we achieve the general solution of the rest of partial differential equations.

The rest of this paper is structured as follows: Section 2 presents the problem formulation and preliminaries. Section 3 defines the structure of the desired system and derives the constraints of the parameter design. Section 4 shows guidelines for the parameter selection. The effectiveness is confirmed through a numerical example in Section 5. Finally, provide some concluding remarks in Section 6.

3.2 Problem Formulation

Herein, we consider a general nonlinear 2 DOF mechanical system under velocity and force disturbances, which can be as shown in Fig. 3.1. The pH system described in local

coordinates is given in the following form:

$$\begin{aligned}
\dot{x} &= \begin{bmatrix}\dot{q}\\ \dot{p}\end{bmatrix} = (J-R)\frac{\partial H}{\partial x}^{\top} + \begin{bmatrix}\gamma\\ D\end{bmatrix}\omega + BF + \begin{bmatrix}0_{2\times 1}\\ G\end{bmatrix}u,\\
J &= \begin{bmatrix}O & I\\ -I & O\end{bmatrix},\ R = \begin{bmatrix}O & O\\ O & C\end{bmatrix},\\
C &= \begin{bmatrix}\mu & 0\\ 0 & c\end{bmatrix}, (\mu \geq 0, c \geq 0)\\
B &= (0\ 0\ 0\ 1)^{\top}, G = (1\ 0)^{\top},\\
D &= (0\ c)^{\top}, \gamma = (0, -1)^{\top}
\end{aligned} \tag{3.1}$$

where $q = (q_1, q_2)^{\top}$ is the relative displacement of the DVA, and the relative displacement of the vibrating main mass, $p = (p_1, p_2)^{\top}$, is the vector of generalized momenta, which is defined in the world coordinate. In addition, Hamiltonian $H(q, p)$ denotes the total energy of the system, $\omega(t) = \dot{z}$ is the velocity disturbance, $F(t)$ is the force disturbance, and $u(t)$ is the control input force. Here, J, R, μ, c, D, B, and G denote the skew-symmetric structure matrix, resistive structure matrix, damping coefficient of the displacement $\dot{q}_1$, damping coefficient of the displacement $\dot{q}_2$, velocity disturbance matrix, force disturbance matrix, and input matrix. The description of Hamiltonian function is given as follows:

$$\begin{aligned}
H(q,p) &= \frac{1}{2}p^{\top}M(q_1)^{-1}p + V_1(q_1) + V_2(q_2),\\
M(q_1) &= \begin{bmatrix}m_1(q_1) & m_2(q_1)\\ m_2(q_1) & m_3(q_1)\end{bmatrix},\\
p &= M(q_1)\left(\dot{q} - \gamma\omega\right),
\end{aligned} \tag{3.2}$$

where the positive-definite matrix $M(q_1)$ is the inertia matrix, $V_1(q_1) \geq 0$ is the potential energy of the DVA, and $V_2(q_2) \geq 0$ is the potential energy of the vibrating system. It is assumed that the second potential $V_2(q_2)$ is positive definite with respect to q_2 and satisfies $\partial V_2/\partial q_2 \neq 0$ $(q_2 \neq 0)$. Notice that there exists a mismatch between the coordinates of p and q, and therefore $p = M(q_1)\dot{q}$ is no longer satisfied.

Our control objective is to suppress the vibration of the main mass, i.e., the absolute displacement of main mass $\tilde{q}_2 \to 0$. With a normal IDA-PBC design procedure, we will obtain a controller based on the states q and p. However, p defined by (3.2) includes ω, and we aim to design a controller that only uses the relative displacements q and velocities $\dot{q}$.

Remark 3. Please note that the control input force u is set between the DVA q_1 and the main body $\tilde{q}_2$, while the difference from the study of [62, 60] is that they set the control input u at the same place as force disturbance F. This difference illustrates that their researches ignore the dynamics of actuator. Though their study utilize the dynamics of additional structure like other DVA studies, their main objective is to use it as a sensor, not to use it as DVA. An obvious example is that their proposed methods can suppress the vibration with very small mass of inner structure q_1, in other words, the vibration energy is suppressed by the force from outside (control input force). Thus, their additional structure do not have any functions that can absorb the vibration. Furthermore, the previously proposed technique requires numerical solutions of partial differential equations to obtain a new inertia matrix.

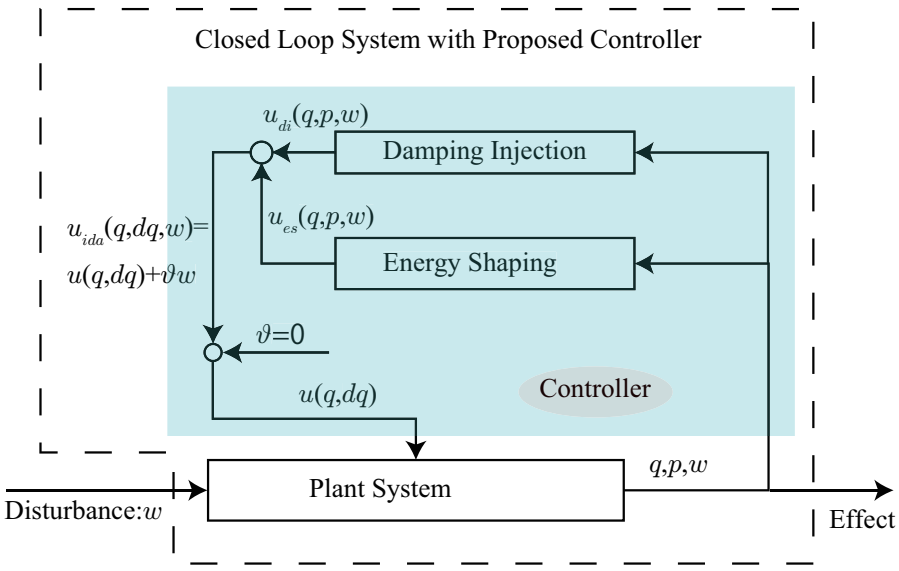

Figure 3.2: Control diagram of proposed method

3.3 Modified IDA-PBC

3.3.1 Overview

The solution to the control problem indicated in the preceding part is given in this section, which involves building an IDA-PBC-based controller. The control variables of the IDA-PBC basic controller are relative displacement q, absolute momenta p, and disturbance signal ω. A feedback rule that only requires the relative displacement, q, and the relative velocity, $\dot{q}$, is produced by rewriting momenta p into the form of $M(\dot{q}+\omega)$ and canceling the coefficient of ω. The following is a summary of our suggested controller's design process:

Step 1: The plant system's pH form is calculated, and it is rebuilt using relative coordinates.

Step 2: IDA-PBC is used to develop the feedback law.

Step 3: The feedback law is split into two parts: relative information and disturbance. The criteria for making the disturbance component zero have been discovered.

Step 4: To ensure suspension performance and strong stability, criteria for parameter selection for the controller are established.

Step 5: The feedback law's precise form is achieved.

In this section, we define the dynamics of desired system at first, and then obtain a matching condition between the controlled system and the desired system. The matching condition clarifies the degree of freedom in the controller design and the expression of feedback law with free parameters as well as equality and inequality constraints. One of the advantages of this study is that our methods focus on transforming the plant system into a desired system with ideal aseismatic properties, while most applications with IDA-PBC tend to control the position or velocity by designing a desired Hamiltonian function

with a new equilibrium point. We aim to obtain the ideal aseismatic properties through designing the mass, spring, and damper parameters of the desired system on the basis of priori knowledge for vibration suppression. The structure of desired system is designed as

$$\begin{aligned}\dot{x} = &(J_d(q_1) - R_d(q_1))\frac{\partial H_d}{\partial x}^\top \\ &+ \begin{bmatrix}\gamma \\ D_d(q_1,\dot{q})\end{bmatrix}\omega + \begin{bmatrix}0_{2\times 1} \\ D_{d\omega}(q_1,\dot{q})\end{bmatrix}\omega^2 + Bf,\end{aligned} \tag{3.3}$$

and the Hamiltonian of desired system is given as

$$\begin{aligned}&H_d(x) = \frac{1}{2}p^\top M_d(q_1)^{-1}p + V_d(q_1,q_2),\\ &q^* = \arg\min V_d(q) = 0,\\ &M_d(q_1) = \begin{bmatrix}m_{d1}(q_1) & m_{d2}(q_1)\\ m_{d2}(q_1) & m_{d3}(q_1)\end{bmatrix},\end{aligned}$$

where

$$\begin{aligned}&J_d(q_1) = \begin{bmatrix}O & M(q_1)^{-1}M_d(q_1)\\ -M_d(q_1)M(q_1)^{-1} & J_2(q_1)\end{bmatrix}\\ &J_2(q_1) = \begin{bmatrix}0 & j_e(q_1)\\ -j_e(q_1) & 0\end{bmatrix},\ R_d(q_1) = \begin{bmatrix}O & O\\ O & C_d(q_1)\end{bmatrix}\\ &C_d(q_1) = \begin{bmatrix}c_{d1}(q_1) & c_{d2}(q_1)\\ c_{d2}(q_1) & c_{d3}(q_1)\end{bmatrix}\\ &D_d(q_1,\dot{q}) = (d_1(q_1,\dot{q})\ d_2(q_1))^\top,\\ &D_{d\omega}(q_1) = (d_3(q_1)\ d_4(q_1))^\top.\end{aligned}$$

The matrix $C_d(q_1)$ is assumed to be smooth with respect to q_1. Note that the controlled system (3.1) includes a friction coefficient c alike the original IDA-PBC method in Section 2.1. Therefore, the new damping matrix C_d in this chapter is not limited to the form of (2.8). The original friction term will be enhanced by the proposed feedback so that a virtual skyhook damper is realized.

Remark 4. Note that the desired system with ideal aseismatic properties should be stable at origin, otherwise the vibration suppression of plant system cannot be achieved even the desired system has perfect aseismatic properties. Thus, we design the equilibrium point of the desired system be at origin, so that the plant system will be successfully stabilized at origin when the desired system is stabilized at the equilibrium point.

3.3.2 Conditions for Matching Dynamics

In this subsection, we derive the matching conditions and the expression of the feedback law with relative states q and $\dot{q}$. By equating the right-hand sides of (3.1) and (3.3), we obtain the matching equation

$$\begin{aligned}&G^\perp(x)\left[-\frac{\partial H}{\partial q} - C\frac{\partial H}{\partial p} + D\omega\right] =\\ &\quad G^\perp(x)\left[-M_d M^{-1}\frac{\partial H_d}{\partial q} + (J_2 - C_d)\frac{\partial H_d}{\partial p} + D_d\omega + D_{d\omega}\omega^2\right],\end{aligned} \tag{3.4}$$

and the control input

$$\begin{aligned} u = \left(G^\top G\right)^{-1} G^\top \Big(& \frac{\partial H}{\partial q} + C\frac{\partial H}{\partial p} + D\omega \\ & - M_d M^{-1}\frac{\partial H_d}{\partial q} + \left(J_2 - C_d\right)\frac{\partial H_d}{\partial p} \\ & + D_d\omega + D_{d\omega}\omega^2 \Big). \end{aligned} \tag{3.5}$$

Note that the equation (3.4) is a set of partial differential equations for kinetic and potential energies, and the feedback law. The matching condition for the momenta p leads to the partial differential equations for the kinetic energy, and the remainder derives the partial differential equations of the potential energy, which is independent of the term p.

We define

$$\begin{aligned} S(q_1) = M^{-1}(q_1) &= \begin{bmatrix} s_1(q_1) & s_2(q_1) \\ s_2(q_1) & s_3(q_1) \end{bmatrix}, \\ S_d(q_1) = M_d^{-1}(q_1) &= \begin{bmatrix} s_{d1}(q_1) & s_{d2}(q_1) \\ s_{d2}(q_1) & s_{d3}(q_1) \end{bmatrix}, \end{aligned} \tag{3.6}$$

for simplicity of the calculations. By extracting the second-order term of p in the equation (5.2), we determine that one of the following equality constraints needs to be satisfied:

$$m_{d2}(q_1)m_3(q_1) - m_{d3}(q_1)m_2(q_1) = 0, \tag{3.7}$$

$$s'_{d1} = s'_{d2} = s'_{d3} = 0, \tag{3.8}$$

where $*'$ indicates the derivative with respect to q_1. The controller designer should choose one of the conditions, (3.7) or (3.8). Clearly, choosing (3.8) will avoid further complications caused by a nonlinearity, and thus the desired inertia matrix is selected as follows:

$$M_d = \begin{bmatrix} m_{d1} & m_{d2} \\ m_{d2} & m_{d3} \end{bmatrix}.$$

This desired inertia matrix setting can satisfy the condition (3.7). By extracting the first-order term of p in the equation (5.2), we obtain the following:

$$c_{d3}(q_1) = c\left[s_3(q_1)m_{d3} + s_2(q_1)m_{d2}\right], \tag{3.9}$$

$$c_{d2}(q_1) = c\left[s_3(q_1)m_{d2} + s_2(q_1)m_{d1}\right] - j_e(q_1), \tag{3.10}$$

and from the terms of ω and ω^2 we have

$$d_2 = c, \quad d_4 = 0.$$

The partial differential equation with respect to the potential energy is obtained as

$$\begin{aligned} & a(q_1)\frac{\partial V_d}{\partial q_2} = \frac{\partial V_2}{\partial q_2} - b(q_1)\frac{\partial V_d}{\partial q_1}, \\ & a(q_1) = m_{d2}s_2(q_1) + m_{d3}s_3(q_1), \\ & b(q_1) = m_{d2}s_1(q_1) + m_{d3}s_2(q_1). \end{aligned} \tag{3.11}$$

We achieve the general solution of (3.11) as

$$\begin{aligned} V_d(q) &= V_{d1}(q) + P(q_2 - \xi(q_1)), \\ V_{d1}(q) &= \left(\int_0^{q_1} \frac{1}{b(s)} \frac{\partial V_2}{\partial q_2}\Big|_{q_2 = q_{20} + \xi(s)} ds \right) \Big|_{q_{20} = q_2 - \xi(q_1)}, \\ \xi(s) &= \int_0^s \frac{a(q_1)}{b(q_1)} dq_1. \end{aligned} \tag{3.12}$$

Assumption 5. $V_d(q)$ is a positive definite smooth function and proper on the space of q.

A function such that inverse images of any compact set is also compact is said to be proper. A proper and positive definite function on a Euclidean space is always radially unbounded.

Remark 6. At the state where $b(q_1) = 0$, the value of $V_d(q)$ may diverge. However, by restricting the state space the positive definiteness and properness in the new space are often satisfied. Please see the example in Section 5. In the rest of paper, the term "global" will be used for the globality in the restricted state space.

With respect to the feedback law $u = \alpha_{\text{raw}}(q, p, \omega)$, notice that the feedback law should be a function of q and $\dot{q}$ only, and thus we decompose the feedback law as follows:

$$\alpha_{\text{raw}}\left(q, M(q_1)(\dot{q} - a\omega), \omega\right) = \alpha(q, \dot{q}) + \alpha_{\text{rest}}(q, \dot{q}, \omega)\omega,$$

where the term of $\alpha_{\text{rest}}(\cdot)$ should be zero. By rewriting it as

$$\alpha_{\text{rest}}(q, \dot{q}, \omega) = \alpha_1(q, \dot{q}) + \alpha_2(q, \dot{q})\omega,$$

and resolving $\alpha_i = 0$ $(i = 1, 2)$ with respect to $d_1(q_1, \dot{q})$ and $d_3(q_1)$ and applying (3.8), the following is given:

$$\begin{aligned} d_1(q_1, \dot{q}) =& c_{d1}(q_1)\left[m_2(q_1)s_{d1} + m_3(q_1)s_{d2}\right] \\ & - \left[j_e(q_1) - c_{d2}(q_1)\right] \\ & \cdot \left[m_3(q_1)s_{d3} + m_2(q_1)s_{d2}\right] \\ & - \Big[(m_1(q_1)m_2(q_1)\dot{q}_1 + m_2(q_1)^2\dot{q}_2)s_1' \\ & + ((m_2(q_1)^2 + m_1(q_1)m_3(q_1))\dot{q}_1 \\ & + 2m_2(q_1)m_3(q_1)\dot{q}_2)s_2' \\ & + (m_2(q_1)m_3(q_1)\dot{q}_1 + m_3(q_1)^2\dot{q}_2)s_3'\Big], \end{aligned} \tag{3.13}$$

$$\begin{aligned} d_3(q_1) =& -\frac{1}{2}\Big[m_2(q_1)^2 s_1' \\ & + 2m_2(q_1)m_3(q_1)s_2' + m_3(q_1)^2 s_3'\Big]. \end{aligned} \tag{3.14}$$

With these equality constraints, we obtain the following feedback law:

$$\begin{aligned} u = \alpha(q, \dot{q}) =& \mu\dot{q}_1 - \left[c_{d1}(q_1), 2c_{d2}(q_1)\right] S_d\tilde{p} \\ & + \frac{1}{2}\tilde{p}^\top S'\tilde{p} + \frac{\partial V_1}{\partial q_1} - \frac{\partial V_d}{\partial q} S(q_1)(m_{d1}, m_{d2})^\top, \end{aligned} \tag{3.15}$$

where $\tilde{p} = M(q_1)\dot{q}$, which is defined in the local coordinates.

Note that all the partial differential equations that occur in the parameters derivations are easy to calculate and do not depend on the numerical solutions.

3.3.3 Stability Analysis with Zero Disturbances

The asymptotic stability of the origin of the closed-loop system with the null disturbances is guaranteed under several conditions.

Proposition 7. *With the designed control input u, the origin of the system (3.1) with zero disturbances ($\omega = 0, F = 0$) is globally asymptotically stable if the following constraints and the Assumption 1 are satisfied:*

$$\begin{aligned} &m_{d1}m_{d3} - m_{d2}^2 > 0, \quad m_{d1} > 0 \\ &c_{d1}(q_1) > 0, \\ &c\left[s_3(q_1)m_{d3} + s_2(q_1)m_{d2}\right] c_{d1}(q_1) - c_{d2}(q_1)^2 > 0, \end{aligned} \tag{3.16}$$

Proof. We consider the desired Hamiltonian function H_d as a Lyapunov candidate function, which is described as follows:

$$H_d(q,p) = \frac{1}{2}\left(p^\top M_d^{-1} p + V_d\right), \tag{3.17}$$

Since V_d is positive definite, H_d is positive definite when M_d is positive definite. $M_d > 0$ is equivalent to

$$\begin{cases} m_{d1} > 0, \\ \det M_d > 0, \end{cases} \tag{3.18}$$

which can be satisfied by $r_1 \geq \beta$. The time derivation of the desired Hamiltonian function H_d is given as follows:

$$\begin{aligned} \dot{H}_d &= -\frac{\partial H_d}{\partial x} R_d \frac{\partial H_d}{\partial x}^\top \\ &= -\frac{\partial H_d}{\partial p} C_d \frac{\partial H_d}{\partial p}^\top \\ &= -p^\top M_d^{-1} C_d M_d^{-1} p \end{aligned} \tag{3.19}$$

Here, $\dot{H}_d \leq 0$ holds when M_d and C_d are positive definite. In addition, C_d is positive-definite when

$$\begin{cases} c_{d1}(q_1) > 0, \\ c\left[s_3(q_1)m_{d3} + s_2(q_1)m_{d2}\right] c_{d1}(q_1) - c_{d2}(q_1)^2 > 0, \end{cases} \tag{3.20}$$

are satisfied.

It can be concluded that if (3.16) is satisfied, $H_d(x)$ is positive definite and $\dot{H}_d$ is negative semi-definite as (3.19), and consequently H_d is monotonous decreasing. Therefore, all the positive trajectory are included in compact set, i.e., $x(t) \in \{x \mid H_d(x) \leq H_d(0)\}$ $(t > 0)$, which means $\ddot{H}_d(x(t)) = -2p^\top M_d^{-1} C_d(q_1) M_d^{-1} \dot{p} - p^\top M_d^{-1} (\partial C_d(q_1)/\partial q_1) M_d^{-1} p \cdot \dot{q}_1$ is bounded. From Barbalat's Lemma, one can conclude that $\dot{H}_d \to 0$ $(t \to \infty)$, i.e., $p \to 0$ $(t \to \infty)$. Since the system is zero-state observable for the velocity output, i.e., $q \equiv 0$ if $\dot{q} = M^{-1}p \equiv 0$. From the invariance principle, the system is global asymptotically stable. □

Remark 8. For a nonlinear system with disturbances, the input-to-stability (ISS) [63] should be considered. Although asymptotically stable linear systems are always ISS, we cannot conclude ISS property from GAS property for nonlinear systems by considering the Hamiltonian as ISS Lyapunov function, since the Hamiltonian is not a strong Lyapunov function; that is, the time derivative of the Hamiltonian is negative semi-definite. In [31], Aoki et al. have shown the ISS property for a specified case, but a construction of ISS Lyapunov function for general pH system is expected. Therefore, one of our future work is to construct an ISS Lyapunov function for general nonlinear pH system under disturbances.

Our objective is to design the parameters of the desired system such that it has an ideal aseismatic property, whereas the design procedure is under the matching conditions (3.9), (3.10), (3.12), (3.13), and stability conditions (3.16). Here, we select m_{d1}, m_{d2}, m_{d3}, $c_{d2}(q_1)$, $d_1(q_1, p)$, and $P(\cdot)$ as free parameters, and the other parameters $c_{d1}(q_1)$, $c_{d3}(q_1)$, $j_e(q_1)$, and $V_d(q)$ with the control law u will then be derived after we design the free parameters. The guidelines on how to design the free parameters are introduced in the next section.

3.4 Guidelines for Parameter Selection

3.4.1 Linear Approximation

To clarify the relation between each parameter and vibration suppression performance, the energy interpretation of the desired system should be clearly shown, whereas the practical meaning of parameters in the given matrix is uncertain because of the nonlinear term. Hence, we first derive the parameter selection guidelines for the linearly approximated system, which determines the low-order terms of the free parameters.

Through a quadratic approximation of H, the Hamiltonian of the linearized controlled system is given as follows:

$$H_L(p,q) = \frac{1}{2}p^\top S_0 p + \frac{1}{2}(k_1 q_1^2 + k_2 q_2^2),$$

where

$$S_0 = \begin{bmatrix} s_{10} & s_{20} \\ s_{20} & s_{30} \end{bmatrix} = S(0) \left(= M_0^{-1} = \begin{bmatrix} m_{10} & m_{20} \\ m_{20} & m_{30} \end{bmatrix}^{-1} \right)$$
$$k_1 = \frac{\partial^2 V_1}{\partial q_1^2}(0), \quad k_2 = \frac{\partial^2 V_2}{\partial q_2^2}(0).$$

We have the following dynamic of the linearized controlled object system:

$$\begin{aligned} \dot{x} = &\begin{bmatrix} 0 & I \\ -I & -C \end{bmatrix} \begin{pmatrix} \mathrm{diag}(k_1, k_2) q \\ S_0 p \end{pmatrix} \\ &+ \begin{pmatrix} \gamma \\ -C\gamma \end{pmatrix} \omega + B_1 F + B_2 u. \end{aligned} \tag{3.21}$$

Similarly, we have the quadratic approximation of the desired Hamiltonian H_d:

$$H_{dL}(p,q) = \frac{1}{2}p^\top S_d p + V_{d0}(q),$$

where

$$V_{d0}(q) = \frac{1}{2}\left(\frac{k_2 a_0}{b_0^2}q_1^2 + \frac{2k_2}{b_0}q_1 q_{20} + k_P q_{20}^2\right),$$
$$a_0 = a(0), \qquad b_0 = b(0), \qquad q_{20} = q_2 - (a_0/b_0)q_1,$$
$$k_P = \frac{\partial^2 P(q_{20})}{\partial q_{20}^2}(0).$$

The linearized desired system is described as follows:

$$\dot{x} = (J_{d0} - R_{d0})\begin{pmatrix} K_d q \\ S_{d0} p \end{pmatrix} + D_{w0}\omega + B_1 F, \tag{3.22}$$

where

$$J_{d0} = \begin{bmatrix} O & M_0^{-1}M_d \\ -M_d M_0^{-1} & J_{20} \end{bmatrix}, \; J_{20} = \begin{bmatrix} 0 & j_{e0} \\ -j_{e0} & 0 \end{bmatrix},$$
$$j_{e0} = j_e(0), \; D_{w0} = (0 \;\; -1 \;\; d_{10} \;\; c)^\top, \; d_{10} = d_1(0,0),$$
$$R_{d0} = \begin{bmatrix} O & O \\ O & C_{d0} \end{bmatrix},$$
$$C_{d0} = \begin{bmatrix} c_{d10} & c_{d20} \\ c_{d20} & c_{d30} \end{bmatrix} = \begin{bmatrix} c_{d1}(0) & c_{d2}(0) \\ c_{d2}(0) & c_{d3}(0) \end{bmatrix},$$
$$K_d q = (\partial V_{d0}/\partial q)^\top,$$
$$K_d = \begin{bmatrix} a_0(a_0 k_P - k_2)/b_0^2 & -(a_0 k_P - k_2)/b_0 \\ -(a_0 k_P - k_2)/b_0 & k_P \end{bmatrix}.$$

3.4.2 Coordinate Transformation

Considering that a diagonalized inertia matrix can simplify the analysis of a desired linearized system structure, we transform the state coordinates into the following:

$$\hat{q} = L^{-1}q, \quad \hat{p} = L^\top p, \quad L = \begin{bmatrix} r_0 & -r_0 \\ 0 & 1 \end{bmatrix}, \tag{3.23}$$

where

$$\frac{m_{20}}{m_{10}} = \frac{m_{d20}}{m_{d10}} = r_0 > 0, \tag{3.24}$$

is a newly defined equality constraint. We then have the following:

$$\hat{p} = L^\top M_0 L(\dot{\hat{q}} - L^{-1}L^\top \gamma\omega) = \hat{M}(\dot{\hat{q}} - \hat{\gamma}\omega),$$

where

$$\hat{M} = L^\top M_0 L = \mathrm{diag}(\hat{m}_1, \hat{m}_2),$$
$$\hat{m}_1 = m_{10}r_0^2, \quad \hat{m}_2 = m_{30} - m_{10}r_0^2,$$
$$\hat{\gamma} = L^{-1}L^\top\gamma = (-1 \;\; -1)^\top.$$

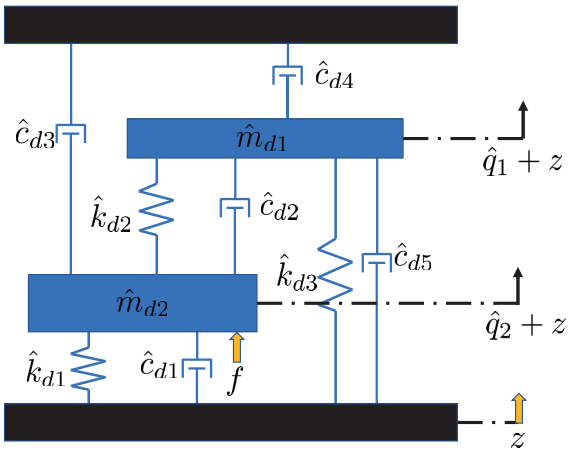

Figure 3.3: Desired linearized system

Note that the coordinates of the controlled object q_2 are fixed under this coordinate transformation. The inertia matrix of the desired linearized system in the new coordinates is also diagonalized in the same way:

$$\begin{aligned}\hat{M}_d &= L^\top M_{d0} L = \mathrm{diag}(\hat{m}_{d1}, \hat{m}_{d2}) \\ &= \mathrm{diag}(m_{d10} r_0^2, m_{d30} - m_{d10} r_0^2).\end{aligned}$$

The desired linearized system in a port-Hamilton form is also transformed into the following:

$$\begin{pmatrix}\dot{\hat{q}} \\ \dot{\hat{p}}\end{pmatrix} = (\hat{J}_d - \hat{R}_d) \begin{pmatrix}\hat{K}_d \hat{q} \\ \hat{S}_d \hat{p}\end{pmatrix} + \hat{D}_d \omega + \hat{B}_1 F, \tag{3.25}$$

where

$$\begin{aligned}&\hat{J}_d = \begin{bmatrix} O & \hat{M}^{-1}\hat{M}_d \\ -\hat{M}_d\hat{M}^{-1} & \hat{J}_2 \end{bmatrix},\ \hat{J}_2 = \begin{bmatrix} 0 & r_0 j_{e0} \\ -r_0 j_{e0} & 0 \end{bmatrix}, \\ &\hat{S}_d = \hat{M}_d^{-1},\ \hat{K}_d = L^\top K_d L,\ \hat{R}_d = \begin{bmatrix} O & O \\ O & \hat{C}_d \end{bmatrix}, \\ &\hat{C}_d = L^T C_{d0} L \\ &\qquad = \begin{bmatrix} r_0^2 c_{d10} & r_0 c_{d20} - r_0^2 c_{d10} \\ r_0 c_{d20} - r_0^2 c_{d10} & r_0^2 c_{d10} - 2 r_0 c_{d20} + c_{d30} \end{bmatrix}, \\ &\hat{D}_d = \mathrm{diag.}(L^{-1}, L^T) D_{w0} = (-1,\ -1,\ r_0 d_{10},\ c - r_0 d_{10})^\top, \\ &\hat{B}_1 = \mathrm{diag.}(L^{-1}, L^T) B_1 = B_1.\end{aligned}$$

Consequently, the desired linearized system (3.25) can be roughly regarded as the system shown in Fig. 3.3, which is a desired main mass $\hat{m}_{d2}$ connected with a DVA-like device

$\hat{m}_{d1}$ and multiple springs and dampers, where

$$\begin{aligned}
&\hat{c}_{d1} = c - r_0 d_{10}, \quad \hat{c}_{d2} = r_0^2 c_{d10} - r_0 c_{d20}, \\
&\hat{c}_{d3} = c_{d30} + r_0 d_{10} - r_0 c_{d20} - c, \quad \hat{c}_{d4} = r_0 c_{d20} - r_0 d_{10}, \\
&\hat{c}_{d5} = r_0 d_{10}.
\end{aligned}$$

We aim to suppress the vibrations excited by disturbances f and z by adjusting the spring, mass, and damper terms of the desired system. How to adjust these terms to gain a desired system with a good vibration suppression performance and analyze the sensitivity from the design of the free parameters used to the control performance is described in the next section.

3.4.3 Parameter Design

For the sake of convenience of the parameter design presentation, we define the mass ratios as follows:

$$r_1 = \frac{m_{d1}}{m_{10}} = \frac{m_{d2}}{m_{20}}, \tag{3.26}$$

$$r_2 = \frac{\hat{m}_{d2}}{\hat{m}_2} = \frac{m_{d3} - m_{d1} r_0^2}{m_{30} - m_{10} r_0^2} = \frac{m_{d3} - m_{10} r_1 r_0^2}{m_{30} - m_{10} r_0^2}, \tag{3.27}$$

where r_1 and r_2 are positive to maintain the positive definiteness of M_d. Under the definitions in (3.26) and (3.27), the matching conditions are rewritten as follows:

$$c_{d10} = \frac{r_1(2c_{d20} - d_{10} r_2)}{r_0(r_1 - r_2)} \tag{3.28}$$

$$c_{d20} = -j_{e0} \tag{3.29}$$

$$c_{d30} = c r_2 \tag{3.30}$$

$$\hat{k}_{d1} = \frac{r_1 k_P - k_2}{r_1 - r_2}, \ \hat{k}_{d2} = \frac{r_1(r_2 k_P - k_2)}{(r_1 - r_2)^2} \tag{3.31}$$

$$\hat{k}_{d3} = -(1 - r_2/r_1)\hat{k}_{d2}. \tag{3.32}$$

Here, we select d_{10}, c_{d20}, r_1, r_2, and k_P as free parameters for designing the desired linearized system. The linearized control input is expressed as follows:

$$\begin{aligned}
u =& \mu \dot{q}_1 + \frac{(2c_{d20} - d_{10} r_2)}{r_0(r_2 - r_1)} \dot{q}_1 - d_{10} \dot{q}_2 + k_1 q_1 \\
&- \frac{r_1 r_2 (r_2 k_P - k_2)}{r_0^2 (r_1 - r_2)^2} q_1 \\
&+ \left(\frac{r_2(k_2 - r_1 k_P)}{r_0(r_2 - r_1)} - \frac{k_2}{r_0} \right) q_2.
\end{aligned} \tag{3.33}$$

The inequality constraint (3.20) can be rewritten as follows:

$$\begin{aligned}
|C_{d0}| = & \frac{c r_1 r_2^2 \left[r_0(r_2 - r_1) d_{10} + c r_1 \right]}{r_0^2 (r_2 - r_1)^2} \\
& - \left(c_{d20} + \frac{c r_1 r_2}{r_0(r_2 - r_1)} \right)^2 > 0.
\end{aligned} \tag{3.34}$$

From the perspective of skyhook systems ([10]), it is natural to set a large value of the skyhook damper coefficient $\hat{c}_{d3}$ to enhance the vibration suppression/isolation effects. Observe that the high-frequency gain from the ground disturbance z to the absolute displacement of the main mass is determined by $\hat{c}_{d1}$ and $\hat{c}_{d5}$. Because $\hat{c}_{d1} + \hat{c}_{d5}$ is a constant c, we let

$$0 \leq r_0 d_{10} \leq c, \tag{3.35}$$

and thus $\hat{c}_{d1} \geq 0$ and $\hat{c}_{d5} \geq 0$ are held. The obvious way to enlarge the value of $\hat{c}_{d3}$ is increasing the values of r_2 and $-r_0 c_{d20}$. A small dissipation matrix is unexpected for the sake of the energy dissipation, and thus we propose the following:

$$c_{d20} = -\frac{c r_1 r_2}{r_0 (r_2 - r_1)}, \tag{3.36}$$

and c_{d10} then becomes

$$c_{d10} = \frac{r_1 r_2 \left[2 c r_1 + r_0 \left(r_2 - r_1\right) d_{10}\right]}{r_0^2 \left(r_2 - r_1\right)^2}, \tag{3.37}$$

which maximizes $|C_{d0}|$ for fixed values of r_1 and r_2. Note that (3.37) is positive as long as $|C_{d0}| > 0$. Hence, under (3.36) and (3.34), $C_{d0} > 0$ is satisfied.

With (3.36), $|C_{d0}|$ becomes

$$|C_{d0}| = \frac{r_2^2}{4 r_0^2} \cdot \left\{ \left(\frac{2c}{(r_2/r_1 - 1)} + d_{10} r_0 \right)^2 - r_0^2 d_{10}^2 \right\}.$$

We know that a positive $(r_2/r_1 - 1)$ makes $|C_{d0}|$ positive, and $r_1 \approx r_2$ enlarges $|C_{d0}|$, whereas the feedback coefficients will go toward infinity as $r_1 \to r_2$. Thus, we recommend that we can set r_1 to hold $2c/(r_2/r_1 - 1) \approx r_0 d_{10}$, i.e., $r_2/r_1 \approx 2c/(r_0 d_{10}) + 1$. The potential energy of desired system V_{d0} is positive when

$$\frac{k_2}{r_2} \leq k_P \tag{3.38}$$

is satisfied. Because the low-frequency gain from the force disturbance f to the absolute displacement of main mass is fixed at $1/k_2$, we focus herein on the design of the high-frequency gain. The design of the resonance frequency should be considered when selecting the potential energy parameter k_P.

To summarize the previous discussion, the following are recommended for a parameter selection in a linear case:

1. Large r_2.
2. $r_2/r_1 \approx 2c/(r_0 d_{10}) + 1$.
3. Positive $c - r_0 d_{10}$.
4. Positive $c_{d20} = -c r_1 r_2 / \{r_0 (r_2 - r_1)\}$.

The parameter d_{10} value will influence the vibration from z to relative displacements $\hat{q}_1$ and $\hat{q}_2$, but the vibration suppression performance will be mainly determined by the value of skyhook damper $\hat{c}_{d3}$.

Consequently, the parameter for our nonlinear DVA controller should be designed through the following steps:

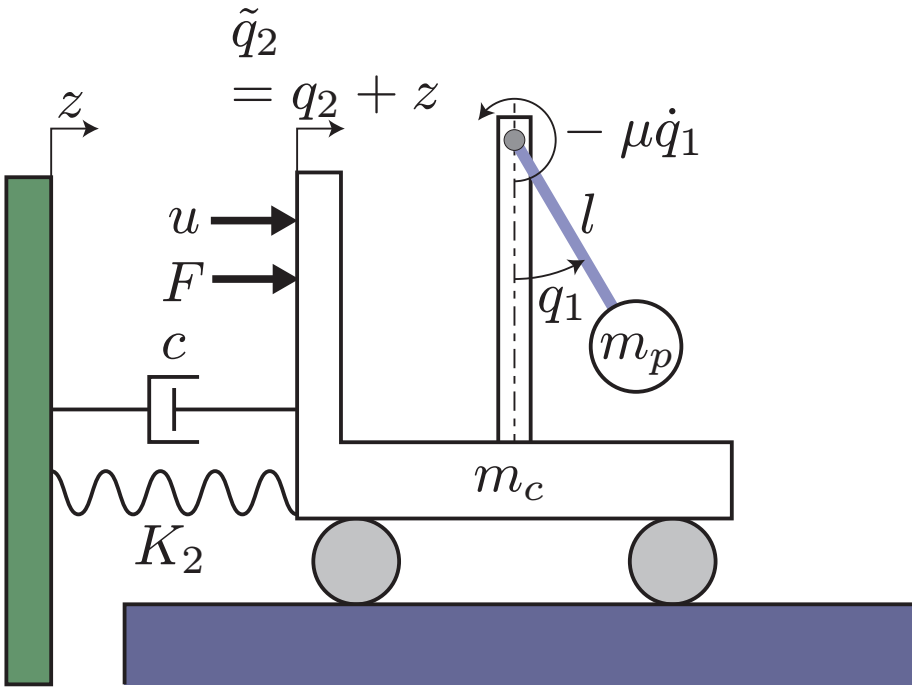

Figure 3.4: Cart and pendulum system.

1. Select a sufficiently large value of r_2, and choose r_1 such that $r_2/r_1 \approx 2c/(r_0 d_{10}) + 1$. The value of M_d is derived using (3.26) and (3.27). The value of C_{d0} is determined through (3.37), (3.36), and (3.30).
2. The values of d_{10} and k_P are adequately selected such that $c - r_0 d_{10}$ and V_{d0} are positive.
3. Design a positive function $P[\cdot]$.
4. Set $c_{d3}(q_1)$ as (3.9). Choose the high-order terms of $c_{d1}(q_1)$ and $c_{d2}(q_1)$.
5. Check the condition (3.16). If the condition is not satisfied, return to step 1.
6. Calculate $j_e(q_1)$ and $V_d(q)$ using (3.10) and (3.12), respectively.
7. Obtain the control input by substituting the parameters into (3.15).

Note that the global asymptotical stability of the nonlinear system is always guaranteed with this parameter selection procedure, although the parameters are designed by considering a linearized system.

3.5 Simulation Result

In this section, we illustrate the vibration suppression effect of the proposed feedback law by providing a numerical example. We consider a cart-pendulum system, which is one of the benchmark models of a 2DOF system. The model is shown in Fig. 3.4, where q_1, $\tilde{q}_2$, z, F, and u denote the swing angle of a pendulum, displacement of a cart in

Table 3.1: Parameters of the cart pendulum system

Parameters	Symbol	Unit	Value
pendulum mass	m_p	Kg	10
cart mass	m_c	Kg	10
length of mass less bar	l	m	1
viscosity dumper coefficient	c	N/(m/s)	10
rotational friction coefficient	μ	N/(m^2/s)	2
elastic coefficient	k_2	N/m	10

Table 3.2: Free parameters of the proposed controller

Parameters	Value
r_1	3
r_2	10
k_P	1
d_{10}	10

world coordinates, a disturbance from the basement, a force disturbance on a cart, and an input force, respectively. The system is tested by the disturbances $z = \sin(rt)$ and $F = 10\cos(rt)$. We set frequency r as $10, 100$, and 1000 to see the vibration suppression performance under different disturbance frequencies. The potential energy of the plant system is

$$V = V_1(q_1) + V_2(q_2) = m_p g l(1 - \cos q_1) + \frac{1}{2} k q_2^2. \tag{3.39}$$

The parameters of the controlled object are set as indicated in Table 3.1. For the sake of embodying the nonlinear property of the discussed model, the initial state values of the controlled system are set as $q_1 = \pi/3, \tilde{q}_2 = 0, \dot{q}_1 = 0$, and $\dot{\tilde{q}}_2 = 0$.

According to the guidelines of the parameter selection summarized in Section 3.4.3, we first design the free parameter as shown in Table 3.2. Regarding the potential energy of the desired system, there exists a domain with respect to q_1 , which is determined as

$$q_1 \in Q_L = \left(-\frac{r_1 (m_c + m_p)}{r_2 m_c + r_1 m_p}, \frac{r_1 (m_c + m_p)}{r_2 m_c + r_1 m_p} \right). \tag{3.40}$$

The positive function P is set as $P = k_p(q_2 - \xi(q_1))^2$. Then we obtain the desired potential energy function $V_d(q)$ from (3.12). In order to facilitate the understanding of the integral expression in the positive definite and proper performance, the 3D surface figures are shown in Fig. 3.5. We observe that the potential energy function $V_d(q)$ is positive definite and proper on the space of $Q_L \times \mathbb{R}$. Furthermore, $V_d(q)$ increases infinitely when q_1 closes to the domain limit, which means that there exists a virtual huge force pushing back the system to the origin when the system displacement becomes large. Hence, the restricted space is positively invariant for finite disturbances. The high-order terms of $c_{d1}(q_1)$ and

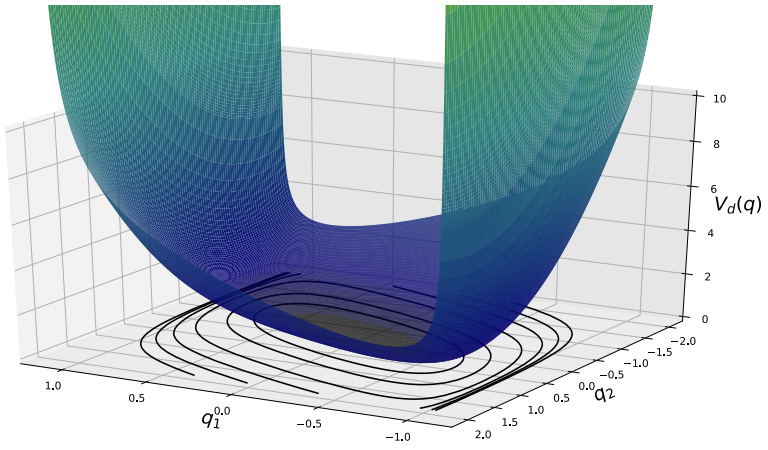

Figure 3.5: V_d surface.

$c_{d2}(q_1)$ are designed as follows:

$$c_{d1}(q_1) = \begin{cases} c_{d10} & (c_{d10} > \tilde{c}_{d1}) \\ \tilde{c}_{d1}(q_1) & (\text{otherwise}) \end{cases}$$
$$c_{d2}(q_1) = c_{d20}$$

where

$$\tilde{c}_{d1}(q_1) = \frac{d_{10} + [j_e(q_1) - c_{d2}]\,[m_3(q_1)s_{d3} + m_2(q_1)s_{d2}]}{m_2(q_1)s_{d1} + m_3(q_1)s_{d2}},$$

which is derived from (3.13). The positivity of $|C_d(q_1)|$ will be guaranteed by the above definition.

To verify the performance of the proposed method, we conduct simulations for the open loop system, the closed loop system using the proposed feedback law, and the closed loop system using on-off groundhook damper controller ([64]). The on-off ground hook control law can be described as

$$u = \begin{cases} -c_{on}\dot{\tilde{q}}_2, & \dot{\tilde{q}}_2\dot{q}_1 \geq 0 \\ 0, & \dot{\tilde{q}}_2\dot{q}_1 < 0. \end{cases} \tag{3.41}$$

Note that the utilization of on-off groundhook controller requires the measurement of $\dot{\tilde{q}}_2$ — absolute velocity of the cart —, while the proposed controller only requires the relative information. For comparison, we choose the groundhook damper coefficient c_{on} and the skyhook damper term $\hat{c}_{d3}$ of the desired system as the same value, i.e., $c_{on} = \hat{c}_{d3} = 142.8571$.

Fig. 3.6, 3.7, and 3.8 show the times histories of cart displacement for open loop system, system with proposed controller, and system with on-off ground hook controller in the case

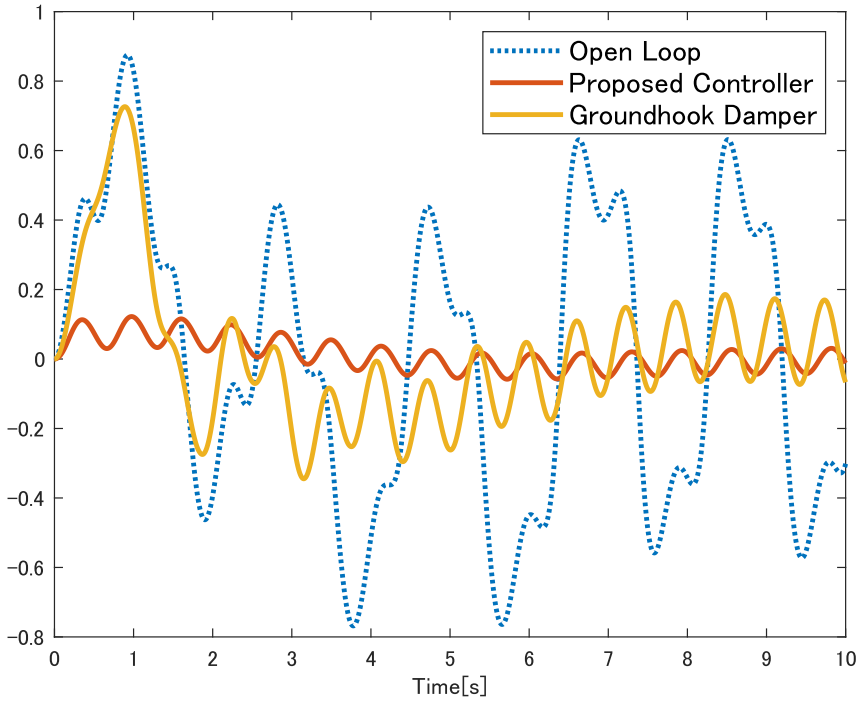

Figure 3.6: The response comparison of the absolute displacement of the cart under frequency $r = 10$.

of the disturbance frequencies $r = 10, 100, 1000$, respectively. We can observe that there is a vibration peak during the first second, which is caused by the initial up swing of the pendulum. The groundhook damper controller obtains a good vibration performance under low frequency $r = 10$. It works worse when the system is tested under high frequency. By contrast, the cart displacement performance under the proposed method is better than that of the groundhook damper controller and open loop system. From the above figures, we can conclude that the proposed controller can improve the vibration suppression performance with only relative displacement and velocity information.

3.6 Conclusion

We presented a new nonlinear active DVA control system, in which the information of the controller is not based on the world-coordinate information. The proposed method can control the vibrations that are excited by a force disturbance and velocity disturbance simultaneously. The control law uses only the relative displacement and velocity of the vibration system, which can be easily measured by sensors. We revealed the equality and inequality constraints for matching the plant system with the desired system. The numerical solutions of the partial differential equations are not required with our proposed method. The main idea of the controller design is to convert a nonlinear DVA system into a desired system with multiple virtual springs and dampers. We also derived selection guidelines for the parameters of the desired system. The global asymptotical stability is

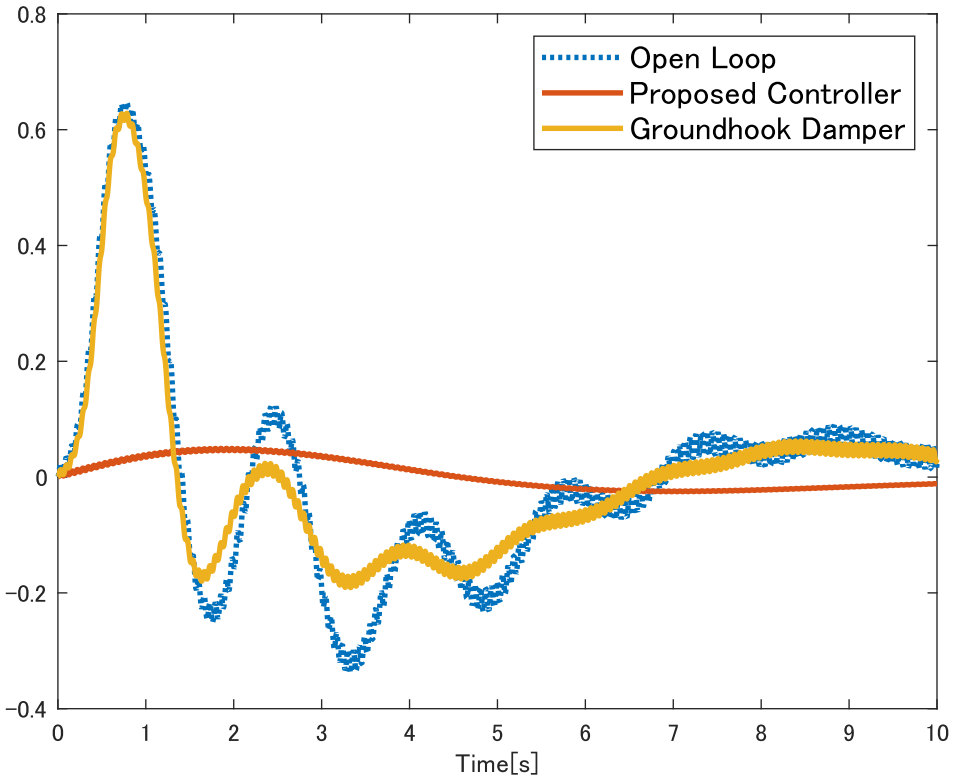

Figure 3.7: The response comparison of the absolute displacement of the cart under frequency $r = 100$.

guaranteed automatically through passivity-based control theory, although the parameter design is based on a linearization. The effectiveness of our controller was confirmed through simulations for a cart-pendulum system. Our future study will be to find guidelines for the choice of potential energy parameter k_P under consideration of the vibration modes.

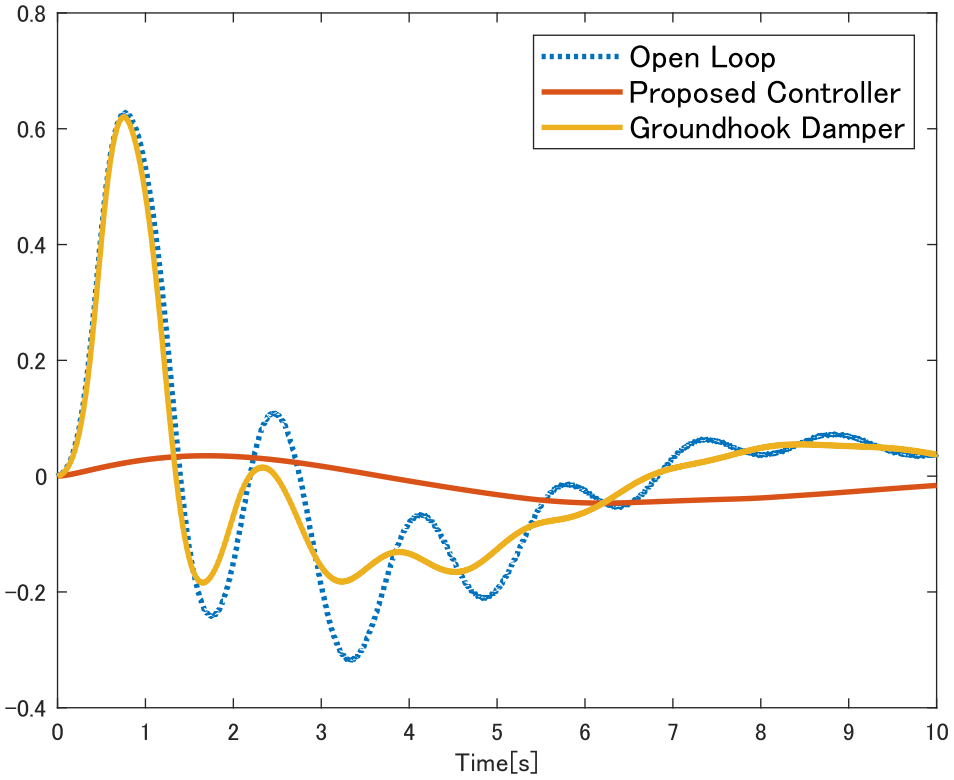

Figure 3.8: The response comparison of the absolute displacement of the cart under frequency $r = 1000$.

Chapter 4

ISS Analysis for Nonlinear Systems with Multiple Disturbances

4.1 Introduction

In the decades after [65] first established the concept of input to state stability (ISS), it has been widely used in the nonlinear control field. Two basic approaches to system stability were fused to form the concept of ISS: the state space method, often known as Lyapunov, and the operator approach. The fundamental characteristic of ISS is that if the inputs are consistently tiny, the state must also be small. The main material and latest efforts of ISS were introduced in the survey article [66]. Constructing an ISS Lyapunov function is one of the most commonly used methods for determining whether the controlled system is ISS. Furthermore, by creating ISS Lyapunov functions, an essential approach known as the ISS small gain theorem [67, 68, 69, 70] may readily assure connectivity of numerous ISS systems. As a result, when considering the ISS attribute of a controlled system, creating ISS Lyapunov functions is frequently significant [71, 72, 73, 74].

Interconnection and Damping Assignment Passivity-Based Control (IDA-PBC) ([25]) has, on the other hand, been widely used in mechanical systems as a potent energy shaping control approach for nonlinear systems. Aside from parameter uncertainty resilience, the system's global asymptotic stability (GAS) under IDA-PBC without disturbance is always assured since the Hamiltonian function may be naturally built as a Lyapunov function. When examining a nonlinear mechanical system with external matched or unmatched disturbances, however, IDA-PBC could not guarantee the ISS property by treating the Hamiltonian as an ISS Lyapunov function, because the Hamiltonian is always set to semi-positive definite.

Several approaches that use IDA-PBC to reject disturbance or reduce vibration to solve this issue have been documented in the literature. The ISS Lyapunov function may be built in a specific way based on the characteristics of the considered system, such as the one described by [31], but a design method for the generic port Hamiltonian (pH) system is expected. [75] proposed an ISS Lyapunov function with respect to a pH system with PI controller. A class of nonlinear pH system with disturbance and a nonlinear disturbance observer are studied by [76], and the authors construct an ISS Lyapunov function for the

augmented system consists with pH system and disturbance estimation error system is constructed. Despite the fact that many authors have done investigations [77, 78, 79, 80], the design of a general pH system has yet to be fully explored.

We will create an ISS Lyapunov function for a class of nonlinear pH systems under a force and velocity disturbance without addressing any plant system operations in this chapter. With this study result, we can not only simplify asymptotic stability analysis of nonlinear pH systems, but we can also integrate the study findings with the ISS small gain theorem to explore system stability in a broader context.

The remainder of the paper is listed below. In Section 2, we introduce our problem formulation and preliminaries. In Section 3, we state our main research result. In Section 4, we verify our result through a simple numerical example.

4.2 Preliminaries and problem formulation

4.2.1 Preliminaries

Before stating our construction of ISS Lyapunov function, we firstly need to recall a preliminary theorem.

Theorem 9. *Considering a system*

$$\dot{x} = f(x, u, t), \tag{4.1}$$

where f: $\mathbb{R}^n \times \mathbb{R}^m \times [0, \infty) \to \mathbb{R}^n$ is locally Lipschitz in x and u and piecewise continuous in t, if there exist a function $V_S(x,t)$:$\mathbb{R}^n \to [0, \infty)$ satisfying

$$\begin{aligned} V_m(|x|) \leqslant V_S(x) \leqslant V_M(|x|), \\ \tfrac{\partial V_S}{\partial x} f(x, u, t) \leqslant -\alpha(|x|) + \beta(|u|), \end{aligned}$$

where $\alpha(|x|)$ is a class K_∞ function and $\beta(|u|)$ is a class K function, then we say system (4.1) is input-to-state stable (ISS).

4.2.2 Motivation and problem formulation

First, we consider n degree of freedom mechanical systems without disturbance modeled in pH form as

$$\begin{aligned} \dot{x} = \begin{pmatrix} \dot{q} \\ \dot{p} \end{pmatrix} &= (J - R_0)\frac{\partial H}{\partial x}^\top + \begin{pmatrix} 0 \\ G(q) \end{pmatrix} u, \\ y &= G(q)^\top \frac{\partial H}{\partial p}^\top, \end{aligned} \tag{4.2}$$

with

$$J = \begin{bmatrix} 0 & I_n \\ -I_n & 0 \end{bmatrix}, \quad R_0 = \begin{bmatrix} 0 & 0 \\ 0 & R(q) \end{bmatrix},$$

where $x = (q, p)$ is the state, $q, p \in \mathbb{R}^n$ are the generalized positions and momenta, respectively, $u \in \mathbb{R}^m, (m \leq n)$denotes control input, $R \geq 0$ is a disspation matrix, $G \in$

$\mathbb{R}^{n\times m}$ is a full rank matrix. The Hamiltonian function $H \in \mathbb{R}$ is the total energy of the system, which is given as

$$H(q,p) = \frac{1}{2}p^\top M^{-1}(q)p + V(q), \tag{4.3}$$

where the positive definite matrix $M(q) \in \mathbb{R}^{n\times n}$ is the inertia matrix and $V(q)$ is the positive-definite potential energy. We assume that the Hamiltonian function $H(x)$ has a minimum point at $x = 0$. According to the passivity of the Hamiltonian system, it is easy to show that the system with the feedback law

$$u = -C_s y \tag{4.4}$$

is asymptotic stability at the point $x = 0$ when $H(x)$ is positive definite and the system is zero state detecable.

By contrast, if there exists a force disturbance d on the same channel of input u, and a velocity disturbance that can expressed as

$$p = M(q)(\dot{q} + aw), \tag{4.5}$$

where $a \in \mathbb{R}^{n\times m}$, and $w \in \mathbb{R}^m, m < n$ is the velocity disturbance, the system (4.2) becomes

$$\begin{aligned} \dot{x} &= (J - R_0)\begin{pmatrix}\partial H/\partial q \\ \partial H/\partial p\end{pmatrix} + \begin{pmatrix}0 \\ G(q)\end{pmatrix}(u+d) + \begin{pmatrix}-a \\ R(q)a\end{pmatrix} w \\ y &= G(q)^\top \frac{\partial H}{\partial p}^\top, \\ u &= -C_s y. \end{aligned} \tag{4.6}$$

For controlling such a disturbed mechanical system, the input to state stability (ISS) property should be ensured. For linear systems, GAS always imply ISS, however, this property does not hold when we consider nonlinear systems. Although the Hamiltonian function can be used as Lyapunov function for proving GAS, it is not able to become an ISS Lyapunov function. Thus, we need to construct an ISS Lyapunov function for the system (4.6).

4.2.3 Assumptions

For the systems we discussed in this chapter, the following preliminary assumptions are needed.

Assumption 10. Since the potential energy $V(q)$ is a positive definite function, it can be decomposed as

$$V(q) = \frac{1}{2}v^\top(q)v(q,) \tag{4.7}$$

where $v(q)$ is diffeomorphic. Here we assume that the matrix

$$\bar{K}(q) = K(q)^\top + K(q)$$

is positive definite, where

$$K(q) = \frac{\partial v(q)}{\partial q}.$$

Note that $(\partial V(q)/\partial q)^\top = K(q)v(q)$ holds with this assumption.

Assumption 11. We assume that $R(q)$ and $M^{-1}(q)$ are both bounded, i.e.,

$$0 \leqslant R_m(|q|) \leqslant R(q) \leqslant R_M(|q|), \tag{4.8}$$
$$0 \leqslant M_m^{-1}(|q|) \leqslant M^{-1}(q) \leqslant M_M^{-1}(|q|). \tag{4.9}$$

4.3 Main result

The construction issue for system (4.6) is investigated in two parts. Firstly, we construct the ISS Lyapunov function for the system with $w = 0$. The construction of this part is based on the general system under the aforementioned assumptions, which are easy to be satisfied in practice. Secondly, we construct the ISS Lyapunov function for the system with $d = 0$. The construction of the second part is based on the system with another assumption, which will be introduced in Section 4.3.2 later. It seems easy to prove that if the system $\Sigma_1 : \dot{x} = f(x) + g(x)d$ and the system $\Sigma_2 : \dot{x} = f(x) + h(x)w$ are both ISS, the combined system $\Sigma_3 : \dot{x} = f(x) + g(x)d + h(x)w$ is ISS with a simple condition. Unfortunately, the ISS Lyapunov function for the system Σ_3 is not able to be constructed by adding the ISS Lyapunov function for the system Σ_1 and the one for the system Σ_2 together. Since the total energy of the system Σ_3 is different from the one of Σ_1 and Σ_2, the property for ISS Lyapunov function will not hold when the discussed system is changed. Herein, we use the following assumption:

Assumption 12. If the system $\Sigma_1 : \dot{x} = f(x)+g(x)d$ and the system $\Sigma_2 : \dot{x} = f(x)+h(x)w$ are both ISS, the combined system $\Sigma_3 : \dot{x} = f(x) + g(x)d + h(x)w$ is ISS as well.

The condition derivation for the above assumption is our future work.

4.3.1 ISS for the system with force disturbance

Consider a general port-Hamilton mechanical system with force disturbance:

$$\dot{x} = \begin{pmatrix} \dot{q} \\ \dot{p} \end{pmatrix} = \begin{pmatrix} O & I \\ -I & -R(q) \end{pmatrix} \begin{pmatrix} \frac{\partial H}{\partial q} \\ \frac{\partial H}{\partial p} \end{pmatrix} + \begin{pmatrix} 0 \\ G(x) \end{pmatrix} d. \tag{4.10}$$

The Hamiltonian is described as

$$H = \frac{1}{2} p^\top M^{-1}(q) p + V(q). \tag{4.11}$$

We consider the ISS Lyapunov function candidate

$$\tilde{H} = \frac{1}{2} [p + D]^\top M^{-1} [p + D] + V(q) - \frac{1}{2} D^\top M^{-1} D, \tag{4.12}$$

where

$$D = \mu \left(q^\top q + 1 \right)^{-\frac{1}{2}} M(q) q, \tag{4.13}$$
$$V(q) - \frac{1}{2} D^\top M^{-1}(q) D > 0, \tag{4.14}$$

and μ is a small positive constant. Then the ISS Lyapunov function candidate $\tilde{H}$ can be rewritten as

$$\tilde{H} = H + \mu \Xi(q) p, \quad \mu > 0, \tag{4.15}$$

where

$$\Xi(q) = \frac{1}{\sqrt{q^\top q + 1}} v(q)^\top. \tag{4.16}$$

The time derivative of Ξ is

$$\begin{aligned} \frac{d}{dt}\Xi &= \frac{d}{dt}\left(\frac{1}{\sqrt{q^\top q + 1}} v(q)\right)^\top \\ &= \dot{q}^\top \Theta(q)^\top, \end{aligned} \tag{4.17}$$

where

$$\Theta = \frac{(-qq^\top + (q^\top q + 1)I)}{(q^\top q + 1)^{\frac{3}{2}}} v(q) + \frac{1}{\sqrt{q^\top q + 1}} K(q). \tag{4.18}$$

Assumption 13. We assume that $\Theta(q)$ is bounded, i.e.,

$$\Theta_m \leqslant \Theta(q) \leqslant \Theta_M \tag{4.19}$$

Theorem 14. *Suppose that those assumptions are satisfied, then the nonlinear system (4.10) is ISS with respect to the force disturbance d at the point $x = 0$.*

Proof. The time derivative of ISS Lyapunov function candidate $\tilde{H}$ is calculated as

$$\begin{aligned} \dot{\tilde{H}} =& \dot{H} + \mu\Xi(q)\dot{p} + \mu\dot{q}^\top\Theta^\top p \\ =& -\left(\frac{\partial H}{\partial p}\right)^\top R(q)\frac{\partial H}{\partial p} + \left(\frac{\partial H}{\partial p}\right)^\top G(x)d \\ &+ \mu\Xi(q)\left(-\frac{\partial H}{\partial q} - R(q)\frac{\partial H}{\partial p} + G(x)d\right) + \mu\left(\frac{\partial H}{\partial p}\right)^\top \Theta^\top p \\ =& -p^\top M^{-1}R(q)M^{-1}p + p^\top M^{-1}G(x)d \\ &+ \mu\Xi(q)\left(-\frac{1}{2}\frac{\partial p^\top M^{-1}(q)p}{\partial q} - \frac{\partial V(q)}{\partial q} - R(q)M^{-1}p + G(x)d\right) \\ &+ \mu p^\top M^{-1}\Theta^\top p \\ =& -\frac{1}{2}p^\top M^{-1}RM^{-1}p + \frac{1}{2}[G(x)d]^\top R^{-1}G(x)d \\ &- \frac{1}{2}\left[pM^{-1} - R^{-1}G(x)d\right]^\top R\left[pM^{-1} - R(q)^{-1}G(x)d\right] \\ &+ \mu\frac{1}{\sqrt{q^\top q + 1}} v(q)^\top\left(-\frac{1}{2}\frac{\partial p^\top M^{-1}p}{\partial q}\right. \\ &\left.-R(q)M^{-1}p - Kv(q) + G(x)d\right) + \mu p^\top M^{-1}\Theta^\top p \end{aligned}$$

Since the third term is negative definite, we obtain the inequality as below through dividing

K into $K_1 + K_2 + K_3$,

$$\begin{aligned}\dot{\hat{H}} \leqslant & -\frac{1}{2}p^\top M^{-1}R(q)M^{-1}p + \frac{1}{2}[G(x)d]^\top R^{-1}G(x)d \\ & + \mu\frac{1}{\sqrt{q^\top q+1}}\left(-\frac{1}{2}v(q)^\top\frac{\partial p^\top M^{-1}(q)p}{\partial q}\right. \\ & - v(q)^\top R(q)M^{-1}p - v(q)^\top\left(K_1+K_2+K_3\right)v(q) \\ & \left. + v(q)^\top G(x)d\right) + \mu p^\top M^{-1}\Theta^\top p,\end{aligned}$$

Here we use K_1 and K_3 to complete the square on $v(q)^\top R(q)M^{-1}p$ and $v(q)^\top G(x)d$, then we obtain

$$\begin{aligned}\dot{\hat{H}} \leqslant & -\frac{1}{2}p^\top M^{-1}R(q)M^{-1}p + \frac{1}{2}[G(x)d]^\top R^{-1}G(x)d \\ & + \mu\frac{1}{\sqrt{q^\top q+1}}\left\{-\frac{1}{2}v(q)^\top\frac{\partial p^\top M^{-1}(q)p}{\partial q}\right. \\ & - \frac{1}{2}v(q)^\top\left(K_1+2K_2+K_3\right)v(q) + E + F + U \\ & \left. + \frac{1}{2}\left[G(x)d\right]^\top K_3^{-1}G(x)d\right\} + \mu p^\top M^{-1}\Theta^\top p,\end{aligned}$$

where

$$\begin{aligned}E &= -\frac{1}{2}\left[v(q)+K_1^{-1}R(q)M^{-1}p\right]^\top K_1\left[v(q)+K_1^{-1}R(q)M^{-1}p\right], \\ F &= \frac{1}{2}\left[R(q)M^{-1}p\right]^\top K_1^{-1}R(q)M^{-1}p, \\ U &= -\frac{1}{2}\left[v(q)-K_3^{-1}G(x)d\right]^\top K_3\left[v(q)-K_3^{-1}G(x)d\right], \\ K &= K_1+K_2+K_3.\end{aligned}$$

For the negative definite term E and U, we have

$$\begin{aligned}\dot{\hat{H}} \leqslant & -\frac{1}{2}p^\top M^{-1}R(q)M^{-1}p + \frac{1}{2}[G(x)d]^\top R^{-1}G(x)d \\ & + \mu\frac{1}{\sqrt{q^\top q+1}}\left\{-\frac{1}{2}v(q)^\top\frac{\partial p^\top M^{-1}(q)p}{\partial q}\right. \\ & - \frac{1}{2}v(q)^\top\left(K_1+2K_2+K_3\right)v(q) + F \\ & \left. + \frac{1}{2}\left[G(x)d\right]^\top K_3^{-1}G(x)d\right\} + \mu p^\top M^{-1}\Theta^\top p\end{aligned}$$

By contracting the second order terms on p, the above inequality can be rewritten as

$$\begin{aligned}\dot{\tilde{H}} \leqslant & p^\top \left[-\frac{1}{2}M^{-1}RM^{-1} + \mu\left(L + \phi - S\right)\right] p \\ & - \frac{\mu}{2\sqrt{q^\top q + 1}} v(q)^\top \left(K_1 + 2K_2 + K_3\right) v(q) \\ & + \frac{1}{2}[G(x)d]^\top R^{-1} G(x)d \\ & + \frac{\mu}{2\sqrt{q^\top q + 1}} \left\{\frac{1}{2}\left[G(x)d\right]^\top K_3^{-1} G(x)d\right\},\end{aligned} \tag{4.20}$$

where

$$\begin{aligned}L(q) &= M^{-1}\Theta^\top, \\ \Phi(q) &= \frac{1}{2\sqrt{q^\top q + 1}} M^{-1}RK_1^{-1}RM^{-1}, \\ \tilde{S}(q)_{ij} &= v(q)^\top \frac{\partial M_{ij}(q)^{-1}}{\partial q} \\ S(q) &= \frac{1}{2\sqrt{q^\top q + 1}}\tilde{S}.\end{aligned} \tag{4.21}$$

Since L, Φ, and S are bounded due to assumptions 1-3, it is obvious that there exists a sufficiently small μ satisfying

$$-\frac{1}{2}M^{-1}RM^{-1} + \mu\left(L + \phi - S\right) < 0. \tag{4.22}$$

Therefore, we obtain the class-K^∞ functions

$$\begin{aligned}\alpha(|x|) = & \lambda_{min}\left(-\frac{1}{2}M^{-1}RM^{-1} + \mu\left(L + \phi - S\right)\right)|p|^2 \\ & + \frac{\mu}{2\sqrt{q^\top q + 1}}\lambda_{min}\left(K_1 + 2K_2 + K_3\right)|v(q)|^2,\end{aligned} \tag{4.23}$$

$$\begin{aligned}\beta(|d|) = & \frac{1}{2}\lambda_{max}\Bigg(\left(G(x)^\top R^{-1} G(x)\right) \\ & + \frac{\mu}{2\sqrt{q^\top q + 1}} G(x)^\top K_3^{-1} G(x)\Bigg)|d|^2,\end{aligned} \tag{4.24}$$

satisfying

$$\dot{\tilde{H}} \leq -\alpha(|x|) + \beta(|d|).$$

Therefore, $\tilde{H}$ becomes an ISS Lyapunov function, and so the ISS property for the system (4.10) has been shown. □

4.3.2 ISS for the system with velocity disturbance

If we consider a case that only q is measurable, a class of Hamiltonian system can be linear in the unmeasurable state p through a coordinate transformation $(q, P) = (q, T^\top(q)p)$. This property is fully determined by the inertia matrix $M(q)$; and the system is called

"Partially Linearizable via Coordinate Changes" (PLvCC). As introduced in ([81, 82, 83]), linear property of P simplify the observation and control problems. Here we focus on a large subset of PLvCC mechanical systems, which is developed by [83]. The following assumption, which is uniquely determined by inertia matrix $M(q)$, is needed in this subsection.

Assumption 15. We assume that there exist a full rank matrix $T \in \mathbb{R}^{n\times n}$ that is determined from

$$M^{-1}(q) = T(q)T^{\top}(q),$$

where T satisfies

$$\sum_{j=1}^{n} [T_i, T_j]\, T_j^{\top} = -\left[\sum_{j=1}^{n} [T_i, T_j]\, T_j^{\top}\right]^{\top}, \quad i = 1, 2, ..., n, \tag{4.25}$$

with a standard Lie bracket $[T_i, T_j] = \frac{\partial T_j}{\partial q} T_i - \frac{\partial T_i}{\partial q} T_j$, and we say that $M(q) \in S_T \subseteq S_{PLvCC}$.

Ignoring the force disturbance d, the dynamics (4.6) with $M \in S_T$ in the coordinates (q, P), where $P = T^{\top} p$, becomes

$$\begin{aligned} \dot{q} =& TP - a(q)w \\ \dot{P} =& -T^{\top}(q)\left[K(q)v(q) + G(q)C_s G^{\top} TP + R(q)(TP - aw)\right], \end{aligned} \tag{4.26}$$

where the Hamiltonian function is expressed as

$$H(q, P) = \frac{1}{2} P^{\top} P + V(q). \tag{4.27}$$

Herein, we construct an ISS Lyapunov function for the disturbed system (4.26).

We consider the ISS Lyapunov function candidate

$$\tilde{H} = H + \mu \Xi(q) P, \tag{4.28}$$

where

$$\Xi(q) = v(q)^{\top} \left(T(q)^{\top}\right)^{-1}. \tag{4.29}$$

The time derivative of $\Xi(q)^{\top}$ can be expressed as

$$\frac{d}{dt}\Xi^{\top} = \Theta(q)\dot{q}, \tag{4.30}$$

where

$$\Theta(q) = \frac{\partial T(q)^{-1} v(q)}{\partial q} = \frac{\partial T(q)^{-1}}{\partial q} v(q) + T(q)^{-1} K(q).$$

Note that the symbols Θ and Ξ, which is used in this part, are different from the symbols used in the previous subsection.

Theorem 16. *Suppose that those assumptions are satisfied, then the nonlinear system (4.26) is ISS with respect to the velocity disturbance w.*

Proof. The time derivative of ISS Lyapunov function candidate $\tilde{H}$ is calculated as

$$\begin{aligned}
\dot{\tilde{H}} =& \dot{H} + \mu \cdot \left[\Xi \dot{P} + P^\top \Theta \dot{q}\right] \\
=& \dot{H} + \mu \cdot \left[-v(q)^\top \left(K(q)v(q) + GC_sG^\top TP + RTP - Raw\right) + P^\top \Theta \left(TP - aw\right)\right] \\
=& - P^\top T^\top GC_sG^\top TP - P^\top T^\top RTP \\
&+ P^\top T^\top Raw - v(q)^\top K^\top aw \\
&+ \mu \cdot \left[-v(q)^\top Kv(q) - v(q)^\top GC_sG^\top TP - v(q)^\top RTP + v(q)^\top Raw \right. \\
&\left. + P^\top \Theta \left(TP - aw\right)\right] \\
=& - \begin{bmatrix} P^\top & v(q)^\top \end{bmatrix} X \begin{bmatrix} P \\ v(q) \end{bmatrix} + \begin{bmatrix} P^\top & v(q)^\top \end{bmatrix} Yaw,
\end{aligned}$$

where

$$X = \begin{bmatrix} T^\top GC_sG^\top T + T^\top RT - \mu\Theta T & (\mu/2)T^\top GC_sG^\top - (\mu/2)\mu T^\top R \\ (\mu/2)T^\top GC_sG^\top - (\mu/2)\mu T^\top R & \mu K \end{bmatrix}, \tag{4.31}$$

$$Y = \begin{bmatrix} T^\top R - \mu\Theta \\ -K^\top + \mu R \end{bmatrix}. \tag{4.32}$$

We decompose X as

$$X = L - \mu Q, \tag{4.33}$$

where

$$\begin{aligned}
L &= \begin{bmatrix} T^\top GC_sG^\top T + T^\top RT & 0 \\ 0 & 0 \end{bmatrix}, \\
Q &= \begin{bmatrix} \Theta T & -(1/2)T^\top GC_sG^\top + (1/2)\mu T^\top R \\ -(1/2)T^\top GC_sG^\top + (1/2)\mu T^\top R & -K \end{bmatrix}.
\end{aligned}$$

Since L is positive semi-definite, it is possible to decompose it as $L = B^\top B$. Due to Finsler's lemma [84, 85, 86], the following two statements are equivalent:

$$B^\top B - \mu Q > 0, \tag{4.34}$$

$$B^{\perp\top} Q B^\perp < 0, \tag{4.35}$$

where

$$B = \begin{bmatrix} T^\top GC_sG^\top T^{1/2} & T^\top RT^{1/2} \\ 0 & 0 \end{bmatrix}.$$

Since the inequality (4.35) can be satisfied by $K > 0$, the positive definiteness of X is ensured by $K > 0$. Consequently, for the state $x = (P, v(q))^\top$ and the input $r = aw$, we obtain the following inequality:

$$\begin{aligned}
\dot{\tilde{H}} &= -x^\top Xx + x^\top Yr \\
&= -\frac{1}{2}x^\top Xx - \frac{1}{2}\left[x - X^{-1}Yr\right]^\top X \left[x - X^{-1}Yr\right] + \frac{1}{2}r^\top Y^\top X^{-1}Yr \\
&\leq -\frac{1}{2}x^\top Xx + \frac{1}{2}r^\top Y^\top X^{-1}Yr \\
&\leq -\frac{1}{2}\lambda_{min}(X)|x|^2 + \frac{1}{2}\lambda_{max}(Y^\top X^{-1}Y)|r|^2,
\end{aligned}$$

which satisfy the condition of ISS Lyapunov function. Therefore, $\tilde{H}$ becomes an ISS Lyapunov function, and so the ISS property has been shown. □

4.4 Conclusion

This paper proposed constructing an ISS Lyapunov function for a class of nonlinear mechanical Hamilton systems with a force disturbance and a velocity disturbance. We divided the discussed system into a system with a force disturbance and a system with a feedback input and a velocity disturbance. Then we constructed the ISS Lyapunov function for those two systems, respectively. The construction is based on several assumptions for the system parameters, while those assumptions are easy to be satisfied in practical application. There is a problem that the constructed ISS Lyapunov functions are for the divided systems, and the relation between the ISS property of divided systems and the one of the total system needs to be analyzed theoretically, which is our future work.

Chapter 5

Active Nonlinear Suspension Systems Design

5.1 Introduction

Passive suspension systems are widely recognized for adopting passive ways to provide vibration isolation and absorption, such as changing the strength of springs and dampers or adding dynamic vibration absorbers [32]. Active suspension systems, on the other hand, use actuators, sensors, controllers, and extra energy sources to suppress road-excited vibrations and can achieve superior vibration suppression performance than passive suspension systems. A suspension system's performance is usually assessed in terms of ride comfort, road holding ability, rattling space size, and dynamic tire force, according to [9]. Among these needs, handling the trade-off between ride comfort and vehicle road holding ability is a crucial challenge in creating the controller for an active suspension system.

The skyhook (SH) control approach, which successfully reduces the resonant peak of a sprung mass (vehicle body) to increase ride comfort, has been widely investigated and utilized in automobile applications ([10, 12, 61]). Some SH control-based active suspension systems that use the information of an unsprung mass and road profiles have been developed to extend the vibration isolation effect to 5,Hz (4–8,Hz), which is considered the most sensitive vibration frequency range of the human viscera and vertebral system according to International Standardization Organization 2631, and to improve the vibration isolation effect [87, 88]. These proposed solutions, on the other hand, not only complicate the control rules, but also necessitate the installation of sensors to monitor the suspension state in detail. Furthermore, the vibration of the sprung mass is commonly set as the control aim of an SH controller; hence, using an SH controller without adaptation will decrease the vehicle's road handling performance. To overcome this problem, different control strategies have been developed, including modified SH approaches [89, 90, 91] and active force control [92, 93].

Although the aforementioned approaches can provide a significant vibration reduction impact, they need precise monitoring of all states. In actuality, certain measured states involve disruptions owing to sensor and actuator dynamics errors.

Robust suspension controllers based on a linear-quadratic-Gaussian methodology [16, 94, 95, 96], H_∞ control technique [22, 23], adaptive fuzzy control [52], iterative learning control [97], and saturated adaptive robust control strategy ([24]) have been proposed to improve vehicle performance in the presence of system uncertainties. However, there

are few researches on the cost of sensors. In prior investigations, when a system was subjected to an external displacement vibration, the controllers used world coordinate information, ignoring the fact that information collected from low-cost sensors is typically based on relative coordinates. Using a disturbance observer approach, obtaining the absolute displacement and velocity of a vibration may necessitate costly sensors or multiple calculations. To conclude, a novel active suspension controller based solely on relative information must be developed in order to use a low-cost sensor.

Another drawback of the aforementioned research is that the active suspension system control design is based on linear models, which simplifies the controller design calculation process. These approaches cannot be directly applied to nonlinear instances in general; nonetheless, most components, such as springs and dampers, have nonlinearities in practice. [98, 99] created a number of controllers based on nonlinear suspension models, including nonlinear stiffening springs and piece-wise linear dampers. Ensuring the global asymptotic stability (GAS) of a nonlinear system is one of the challenges of applying the linear state feedback rule to nonlinear systems. The asymptotic stability of nonlinear controlled systems is ensured by the dissipative features of Euler—Lagrange (or Hamiltonian) systems [100, 101, 102]. The GAS of closed-loop systems is no longer guaranteed with a linear state feedback, which is developed based on linear approximations, because the feedback destroys the structures of Hamiltonian systems. For the regulation of nonlinear systems, approaches that retain the structures of Hamiltonian systems are necessary. Alternatively, the GAS requires certain Hamilton—Jacobi partial differential equations, which might be difficult to solve [103, 104, 105].

As a result, while building an active suspension system, two key challenges need be addressed. The first is its suitability for use in nonlinear situations. The suspension controller, on the other hand, solely utilizes relevant information. Because this technique may be readily applied to nonlinear systems and retains the structure of generalized Hamiltonian systems, IDA-PBC methods [106] are used to construct the controller. Many design techniques, including as derivation of the feedback law, assurance of the GAS, disturbance attenuation, and robustness against parameter uncertainties, have been well acknowledged for nonlinear physical systems employing an IDA-PBC for equilibrium stabilization issues [107]. Sandoval et al.[108], for example, suggested an IDA-PBC-based controller for a class of mechanical systems with dynamic friction that are underactuated. Researchers showed how to use a nonlinear observer to adjust for friction, and how to attain asymptotic stability with a few criteria. For underactuated mechanical systems with matched disturbances, Romero et al. presented the robustification of IDA-PBC. An external regulator (such as a nonlinear proportional, integral, or derivative controller) was added to IDA-PBC to protect the closed loop's equilibrium from being altered. As described in [109, 110], there have been a slew of additional recent research regarding IDA-PBC disturbance rejection. Aoki et al. [31] concentrated on changing a plant system into physically separate systems with optimal anti-vibration qualities, rather than managing the displacement or speed as in prior investigations. Despite the fact that the vibration was successfully controlled in [31], the proposed system was a linear model with an external control force, thus the movement of the actuators had no bearing on the one of the target system. Furthermore, the effects of nonlinear springs and dampers on vibration suppression were not studied, and the control purpose was distinct from that of the suspension design. As a result, applying [31] to suspension design is problematic.

We develop a novel IDA-PBC design for a quarter car nonlinear active suspension

system, noting that an IDA-PBC design has seldom been employed in nonlinear active suspension systems with model uncertainties. We developed the main concept of [31] and converted the plant system into a desired system with multiple SHs and ground dampers. IDA-PBC may be used to implement the primary notion of SH control as an energy shaping tool. We use the features of the energy shaping approach to adjust the sprung and unsprung masses in addition to the damping term, in order to increase the vibration suppression effect. In [111], a preliminary study of this research is described, in which a linear suspension system with no model uncertainty is employed and assessed. Although a pilot investigation suggested that IDA-PBC may be used in nonlinear suspension systems, the complete controller was built and calculated using a linear suspension model. In contrast to [111], we used a nonlinear suspension system with model uncertainty in this study. Furthermore, the approach given in this chapter is more advanced than the previous one, allowing for greater flexibility in parameter design while also maintaining strong stability against parameter uncertainty in terms of mass., springs, and dampers. The main contributions of this study are summarized as follows:

- We develop a feedback rule based solely on the relative displacement and velocity of the suspension system, whereas most previous research has relied on absolute data. It is calculated by obtaining the suspension system's pH form from the dynamics of the suspension system and rewriting it using relative coordinates. A low-cost sensor may be employed in practice with our unique controller.

- There is a proposal for an IDA-PBC-based controller design for an active suspension system with a nonlinear spring, a nonlinear damper, and mass uncertainty. Our approaches focus on changing the nonlinear suspension system into a desired linear system with perfect aseismatic features, unlike other IDA-PBC implementations, which tend to regulate the position or velocity.

- We design a virtual vehicle body, an unsprung mass, and damper coefficients in addition to a standard controller utilizing the SH control approach.

- We establish the requirements that guarantee the suspension system's GAS in the absence of model errors or disturbances, as well as parameter selection suggestions that can assure robust stability in the face of parameter uncertainties in the mass, springs, and dampers. Variations in passenger numbers and vehicle body loads, as well as aging suspension parts and measurement mistakes, can all contribute to these inaccuracies.

The following is how the rest of the paper is organized: The basic notion of the IDA-PBC standard is provided in Section 2. The problem statements and control goals are briefly introduced in Section 3. In Section 4, we look at how to utilize IDA-PBC to construct a control rule that simply takes into account relative displacement and velocity. In Section 5, we give advice for choosing the control law's parameters to achieve stable stability and suspension performance. Section 6 discusses the performance evaluation of the proposed controller using numerical simulations. Section 7 concludes with a few closing words.

5.2 Standard IDA-PBC Formulation

The IDA-PBC approach is a strong controller design methodology for solving the stabilization problem, and the dynamics with a pH form are commonly described as follows:

$$\dot{x} = \begin{bmatrix} \dot{q} \\ \dot{p} \end{bmatrix} = \begin{bmatrix} 0_{n\times n} & I_n \\ -I_n & 0_{n\times n} \end{bmatrix} \frac{\partial H}{\partial x}^\top + \begin{bmatrix} 0_{n\times m} \\ G(q) \end{bmatrix} u, \tag{5.1}$$

where $q, p \in \mathbb{R}^n$ are the generalized position and momentum, respectively, $u \in \mathbb{R}^m$ is the control input, and $G(q) \in \mathbb{R}^{n\times m}$, with rank$(G)= m$. The controlled system is underactuated when $m < n$. The Hamiltonian function, H, is defined as follows:

$$H(q, p) = \frac{1}{2} p^\top M^{-1}(q) p + V(q),$$

where $M \in \mathbb{R}^{n\times n}$ is a positive-definite inertia matrix and $V \in \mathbb{R}$ is the potential energy. The goal of the control is to create a static state feedback loop that will stabilize the controlled system. The IDA-PBC design technique is divided into two steps: energy shaping and damping injection.

$$u = u_{es} + u_{di}.$$

Figure 5.1 shows an example of a simple pendulum to outline the mechanism. It is assumed that the support part of the pendulum is connected to the external environment by a frictionless pin joint, and torque can be input to the pendulum from the pin joint. Consider controlling the simple pendulum to an inverted state from the viewpoint of energy. When there is no control input, the simple pendulum vibrates vertically and downward. This can be explained by the fact that the vertical downward direction is the minimum energy state of the simple pendulum system. IDA-PBC initially controls the minimum energy state of the system to be an inverted state by Energy Shaping. As a result, it becomes a natural state in a sense that the simple pendulum makes a simple vibration around the vertically upward direction.

On top of that, a damping effect called Damping Injection is added, and the system converges to the minimum energy state. In other words, the simple pendulum is controlled to the inverted state. In this case, the damping effect is the negative feedback of the angular velocity of the pendulum, which physically corresponds to the damper and friction. In addition, the angular velocity of the pendulum corresponds to the passive output of this system, and since stabilization is achieved by negative feedback, it is called passivity-based control (PBC).

Energy shaping step The fundamental idea is to match the controlled system with a desired system using a new connectivity matrix and energy function while keeping the whole system's pH form in a closed loop. This is described as follows:

$$\dot{x} = \begin{bmatrix} 0_{n\times n} & I_n \\ -I_n & 0_{n\times n} \end{bmatrix} \frac{\partial H}{\partial x}^\top + \begin{bmatrix} 0_{n\times m} \\ G(q) \end{bmatrix} u_{es} = \begin{bmatrix} 0_{n\times n} & M^{-1}(q) M_d(q) \\ -M_d(q) M^{-1}(q) & J_2(q, p) \end{bmatrix} \frac{\partial H_d}{\partial x}^\top, \tag{5.2}$$

with the new Hamiltonian function,

$$H_d(q, p) = \frac{1}{2} p^\top M_d^{-1}(q) p + V_d(q),$$

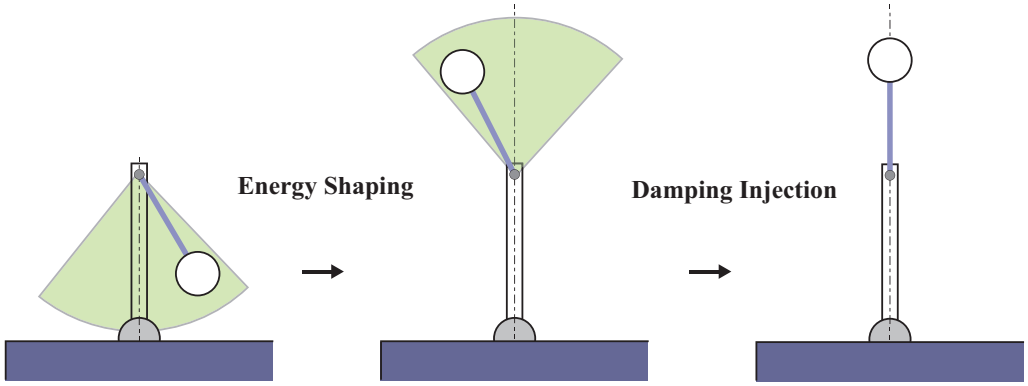

Figure 5.1: Illustration of IDA-PBC with an example of single pendulum

where the desired mass matrix, $M_d \in \mathbb{R}^{n\times n}$, is positive definite, and the desired potential energy, $V_d \in \mathbb{R}$, verifies

$$q^\star = \text{argmin} H_d(q) = \text{argmin} V_d(q). \tag{5.3}$$

The matrix, $J_2 \in \mathbb{R}^{n\times n}$, is available to a designer and fulfills the skew-symmetry condition, $J_2(q,p) = -J_2^\top(q,p)$. For holding (5.3), two conditions need to be satisfied.

1. Necessary extremum assignment: $\nabla_q H_d(q^\star) = 0$.
2. Sufficient minimum assignment: $\nabla_q^2 H_d(q^\star) > 0$, which indicates that the Hessian of the function at the equilibrium point is positive.

If M_d, V_d, and J_2 are provided, we can derive the following:

$$\begin{aligned} u_{es} =& \left(G^\top G\right)^{-1} G^\top \left(\nabla_q H - M_d M^{-1} \nabla_q H_d + J_2 M_d^{-1} p\right) \\ =& G^+ \left(\nabla_q H - M_d M^{-1} \nabla_q H_d + J_2 M_d^{-1} p\right), \end{aligned}$$

from the matching equation (5.2).

Damping injection step The second step is to design a damping injection controller u_{di}, which can be expressed as follows:

$$u_{di} = -R_d G^\top \nabla_p H_d,$$

where R_d is a positive-definite matrix. With the damping injection controller, u_{di}, asymptotic stabilization of the desired equilibrium is ensured.

Therefore, the pH system in (5.1) can be transformed into the desired pH system, which is described as

$$\dot{x} = \begin{bmatrix} 0_{n\times n} & M^{-1}(q) M_d(q) \\ -M_d(q) M^{-1}(q) & J_2(q,p) - C_d(q) \end{bmatrix} \frac{\partial H_d}{\partial x}^\top, \tag{5.4}$$

using the control law, $u = u_{es} + u_{di}$, where

$$C_d(q) = G(q) R_d G^\top(q) > 0, \tag{5.5}$$

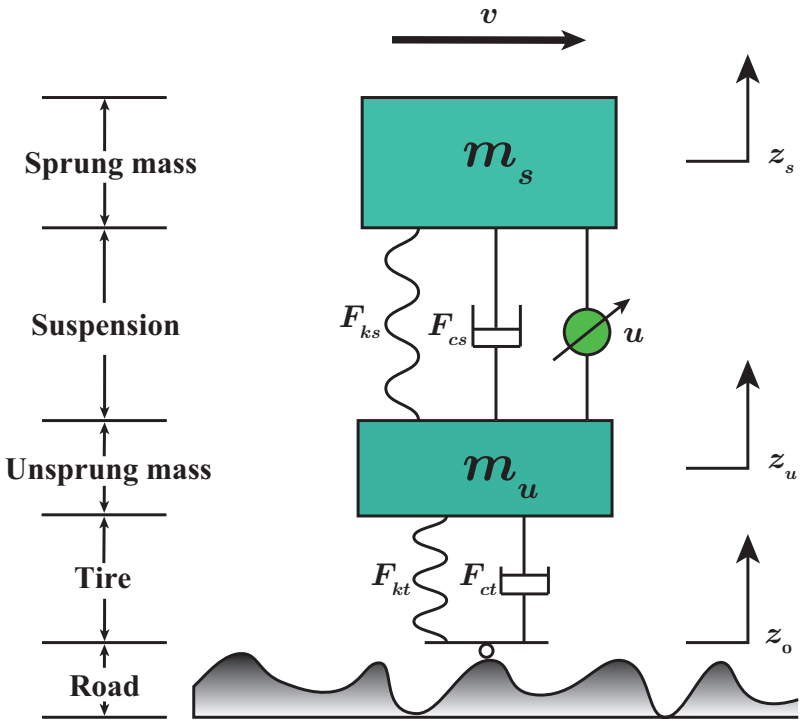

Figure 5.2: Nonlinear quarter car suspension model with controller.

is the dissipation matrix if and only if the following matching equation holds:

$$G^{\perp}(x)\left[\begin{bmatrix}0_{n\times n} & I_n\\ -I_n & 0_{n\times n}\end{bmatrix}\frac{\partial H}{\partial x}^{\top}-\begin{bmatrix}0_{n\times n} & M^{-1}(q)M_d(q)\\ -M_d(q)M^{-1}(q) & J_2(q,p)-C_d(q)\end{bmatrix}\frac{\partial H_d}{\partial x}^{\top}\right]=0. \quad (5.6)$$

The primary disadvantage of IDA-PBC is that it requires the use of (5.6) to solve nonlinear partial differential equations. Because a closed-form solution of the matching equation is hard to discover in most cases, it is required to assess whether the desired goal dynamics can be achieved.

5.3 Problem Statements

5.3.1 Nonlinear Active Suspension Model with Uncertain Parameters

We explore a quarter car nonlinear active suspension model, as illustrated in Fig. 5.2. The dynamics of this model may be represented by the following equations, which are based on Newton's second law:

$$\begin{aligned} m_s\ddot{z}_s =& -F_{cs}(\dot{z}_s,\dot{z}_u)-F_{ks}(z_s,z_u)+u,\\ m_u\ddot{z}_u =& F_{cs}(\dot{z}_s,\dot{z}_u)+F_{ks}(z_s,z_u)-F_{ct}(\dot{z}_u,\dot{z}_0)-F_{kt}(z_u,z_0)-u, \end{aligned} \quad (5.7)$$

where m_s denotes the quarter car body mass, m_u is the unsprung mass (e.g., tire and wheel), and z_s and z_u are the vertical displacements of the sprung and unsprung masses, respectively, z_0 is the road displacement input and u is the actuator input force. The

nonlinear suspension spring force, F_{ks}, and the nonlinear suspension damper force, F_{cs}, are defined as

$$F_{ks}(z_s, z_u) = k_s(q_1)q_1, \tag{5.8}$$
$$F_{cs}(\dot{z}_s, \dot{z}_u) = c_s(\dot{q}_1)\dot{q}_1, \tag{5.9}$$

and the tire elastic force, F_{kt}, and the tire damper force, F_{ct}, are expressed as

$$F_{kt}(z_u, z_0) = k_t q_2, \tag{5.10}$$
$$F_{ct}(\dot{z}_u, \dot{z}_0) = c_t \dot{q}_2, \tag{5.11}$$

where $q_1 = z_s - z_u$, $q_2 = z_u - z_0$, k_t is the tire stiffness, k_s is the stiffness of the spring between the tire and the chassis, and c_s and c_t are the damping coefficients of the suspension and tire, respectively. Parameters m_s, m_u, c_s, c_t, k_s, and k_t are determined as uncertain parameters, and their nominal values are defined as $\tilde{m}_s, \tilde{m}_u, \tilde{c}_s, \tilde{c}_t, \tilde{k}_s$, and $\tilde{k}_t$. The uncertain parameters are assumed to be bounded as

$$\begin{aligned}
&m_{s\min} \le m_s \le m_{s\max},\\
&m_{u\min} \le m_u \le m_{u\max},\\
&c_{s\min} \le c_s \le c_{s\max},\\
&c_{t\min} \le c_t \le c_{t\max},\\
&k_{s\min} \le k_s \le k_{s\max},\\
&k_{t\min} \le k_t \le k_{t\max}.
\end{aligned} \tag{5.12}$$

The above bounded uncertainties may be caused by the variations in the passenger number and vehicle body load, aging of the suspension parts, or measurement errors.

5.3.2 Control Objectives

We consider the following aspects when designing the control law for the suspension systems:

1. Ride comfort: The ride comfort performance can be evaluated by the sprung mass acceleration, $\ddot{z}_s$.

2. Road holding ability: The dynamic loads of the tire should be limited to provide a firm, uninterrupted contact of the wheels to the road, i.e., the tire deflection should fulfill the inequality,

$$k_t q_2 < (m_s + m_u)\, g. \tag{5.13}$$

   As a result, the tire deflection, q_2, may be used to assess road holding capability.

3. Robust stability in the face of parameter variation: We use the following parameters to assess the influence of parameter uncertainties on stability:

$$\delta = \frac{u(m_s, m_u, c_s, c_t, k_s, k_t) - u(\tilde{m}_s, \tilde{m}_u, \tilde{c}_s, \tilde{c}_t, \tilde{k}_s, \tilde{k}_t)}{u(\tilde{m}_s, \tilde{m}_u, \tilde{c}_s, \tilde{c}_t, \tilde{k}_s, \tilde{k}_t)}.$$

As a result, the goal of this research is to use a feedback rule that solely uses relative information to reduce the sprung mass acceleration, $\ddot{z}_s$, and tire deflection, q_2, at the same time. The approach should ensure strong system stability in the face of parameter uncertainties in the mass, springs, and dampers, which can be produced by changes in the passenger number and vehicle body load, suspension part aging, or measurement mistakes. After the controller is developed, the parameter δ should converge to zero.

5.4 Suspension Design with IDA-PBC

The solution to the control problem indicated in the preceding part is given in this section, which involves building an IDA-PBC-based controller. The control diagram for the suggested technique is shown in Figure 5.3. The control variables of the IDA-PBC basic controller are relative displacement q, absolute momenta p, and disturbance signal ω. A feedback rule that only requires the relative displacement, q, and the relative velocity, $\dot{q}$, is produced by rewriting momenta p into the form of $M(\dot{q}+\omega)$ and canceling the coefficient of ω. The following is a summary of our suggested controller's design scheme:

Step 1: The plant system's pH form is calculated, and it is rebuilt using relative coordinates.

Step 2: IDA-PBC is used to develop the feedback law.

Step 3: The feedback law is split into two parts: relative information and disturbance. The criteria for making the disturbance component zero have been discovered.

Step 4: To ensure suspension performance and strong stability, criteria for parameter selection for the controller are established.

Step 5: The feedback law's precise form is achieved.

5.4.1 System modeling in pH form

We must restate the plant dynamics in the same way since the IDA-PBC approach demands the mentioned systems to be written in a pH form. Furthermore, because the state of displacement only employs relative values, the resultant feedback rule can only be described using relative state data. First, we define the target system's momentum vector as follows:

$$\tilde{p} = \begin{bmatrix} p_0 \\ p_s \\ p_u \end{bmatrix} = M \begin{bmatrix} \dot{z}_0 \\ \dot{z}_s \\ \dot{z}_u \end{bmatrix},$$

where $M = diag.\,(m_0, m_s, m_u)$ represents the inertia matrix, and m_0 denotes a temporary value of the ground mass for further explanation. The following is a formula for calculating the total energy of the plant system, including ground motion:

$$\tilde{H}\left(\tilde{x}\right) = \frac{1}{2}\left(pM^{-1}p^{\top} + 2\int k_s(\tau)\tau \mid_{\tau=z_s-z_u} + k_t\left(z_u - z_0\right)^2\right), \tag{5.14}$$

where the state vector, $\tilde{x}$, is defined as

$$\tilde{x} = \left(z_0, z_s, z_u, p_0, p_s, p_u\right)^{\top}.$$

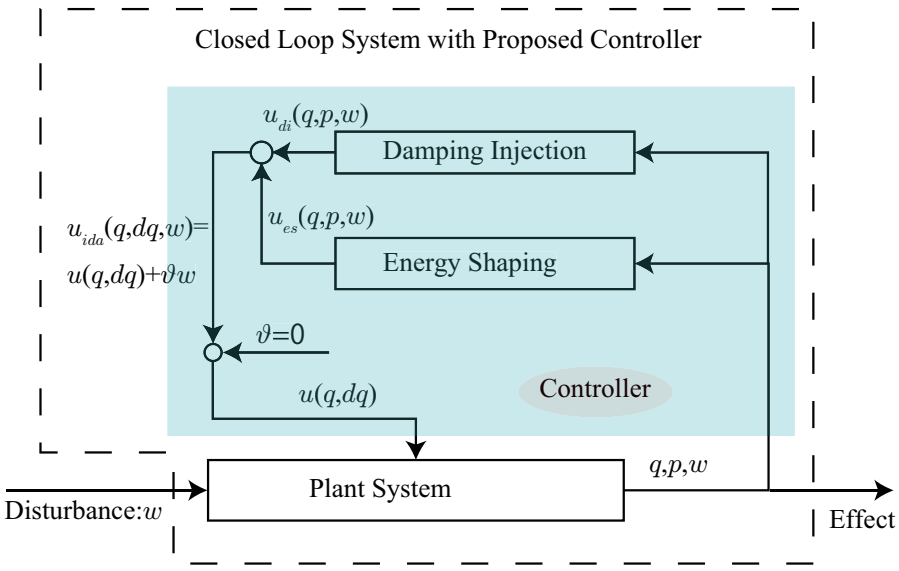

Figure 5.3: Control diagram of proposed method

Thus, the pH system including the ground motion is described as

$$\dot{\tilde{x}} = \begin{bmatrix} 0_{3\times3} & I \\ -I & -\tilde{C} \end{bmatrix} \frac{\partial \tilde{H}}{\partial \tilde{x}}^{\top} + \begin{bmatrix} 0_{3\times1} \\ \tilde{G} \end{bmatrix} u + eE, \tag{5.15}$$

where E is a virtual force acting on the ground, $\tilde{C}$ denotes the damping matrix, and

$$\tilde{C} = \begin{bmatrix} c_t & 0 & -c_t \\ 0 & c_s & -c_s \\ -c_t & -c_s & c_t + c_s \end{bmatrix}, \ \tilde{G} = \begin{bmatrix} 0 \\ 1 \\ -1 \end{bmatrix}, \ e = \begin{bmatrix} 0 \\ 0 \\ 1 \end{bmatrix}$$

Because we require a form that is independent of ground mass m_0, we remove the first and fourth row equations from (5.15) and replace $m_0\dot{z}_0$ with p_0 to get a pH subsystem that is free of ground dynamics:

$$\dot{\bar{x}} = \begin{bmatrix} 0_{2\times2} & I \\ -I & -\bar{C} \end{bmatrix} \frac{\partial \bar{H}}{\partial \bar{x}}^{\top} + \begin{bmatrix} 0_{2\times1} \\ \bar{G} \end{bmatrix} u + D\omega, \tag{5.16}$$

where

$$\begin{aligned} &\bar{x} = (z_s, z_u, p_s, p_u)^{\top}, \\ &\bar{H}(\bar{x}, z_0) = \frac{1}{2}\left(p\bar{M}^{-1}p^{\top} + 2\int k_s(\tau)\tau \,|_{\tau=z_s-z_u} + k_t (z_u - z_0)^2 \right), \\ &\bar{M} = \begin{bmatrix} m_s & 0 \\ 0 & m_u \end{bmatrix}, \ \bar{C} = \begin{bmatrix} c_s & -c_s \\ -c_s & c_t + c_s \end{bmatrix}, \ \bar{G} = \begin{bmatrix} 1 \\ -1 \end{bmatrix}, \bar{D} = (0\ 0\ 0\ c_t)^{\top}. \end{aligned}$$

In (5.16), we regard z_0 and $\dot{z}_0$ as independent external disturbance signals. Because one of our goals is to use just relative displacement and velocity, it will be easier to develop the

control rule if the system's configuration is characterized by relative displacement. The state vector is modified as follows: $x = (q, p)^\top$, where

$$q = \begin{bmatrix} q_1 \\ q_2 \end{bmatrix}, \quad p = \begin{bmatrix} p_1 \\ p_2 \end{bmatrix} = M \begin{bmatrix} \dot{q}_1 \\ \dot{q}_2 + w \end{bmatrix}, \quad w = \dot{z}_0, \quad M = \begin{bmatrix} m_s & m_s \\ m_s & m_s + m_u \end{bmatrix}.$$

Thus, the pH subsystem can be redescribed as

$$\dot{x} = \begin{bmatrix} \dot{q} \\ \dot{p} \end{bmatrix} = (J - R)\frac{\partial H}{\partial x}^\top + Dw + \begin{bmatrix} 0_{2\times 1} \\ G \end{bmatrix} u, \tag{5.17}$$

where

$$\begin{aligned} &H(q,p) = \frac{1}{2}p^\top M^{-1} p + V,\ V = \frac{1}{2}\left(2\int k_s(q_1)q_1 + k_t q_2^2\right), \\ &J = \begin{bmatrix} O & I \\ -I & O \end{bmatrix},\ R = \begin{bmatrix} O & O \\ O & C \end{bmatrix},\ C = \begin{bmatrix} c_s(\dot{q}_1) & 0 \\ 0 & c_t \end{bmatrix}, \\ &G = (1\ 0)^\top,\ D = (0\ \ -1\ 0\ c_t)^\top. \end{aligned}$$

In contrast to the original IDA-PBC technique outlined in Section 2, the controlled system in (5.17) contains the damping matrix, C. As a result, in this work, the required damping matrix, C_d, is not confined to the form (5.5). The suggested feedback enhances the initial damping term, resulting in the implementation of a virtual SH damper.

5.4.2 Construction of desired system

Our approaches focus on changing a nonlinear suspension system into a desirable linear system with optimal aseismatic features, which is one of the study's benefits. Most IDA-PBC applications, on the other hand, tend to regulate the position or velocity by creating a desired Hamiltonian function with a new equilibrium point. As illustrated in Fig. 5.4, we suggest a method for constructing a desired system with numerous virtual springs and dampers.

Energy shaping As illustrated in Section 5.2, the main concept of IDA-PBC is to design a desired system with a new interconnection matrix and a new energy function, which can satisfy the following energy shaping equation:

$$J\frac{\partial H}{\partial x}^\top + \begin{bmatrix} 0_{2\times 1} \\ G \end{bmatrix} u_{es} = \begin{bmatrix} 0_{n\times n} & M^{-1}(q)M_d(q) \\ -M_d(q)M^{-1}(q) & J_2(q,p) \end{bmatrix} \frac{\partial H_d}{\partial x}^\top, \tag{5.18}$$

where $J_2 = \begin{bmatrix} 0 & j_e \\ -j_e & 0 \end{bmatrix}$. Because the desired system's inertia matrix has the same structure as the plant system's and the mass parameters are configurable, we can readily examine the motion of the desired mass. The below is a technical definition:

$$M_d = \begin{bmatrix} m_{ds} & m_{ds} \\ m_{ds} & m_{du} + m_{ds} \end{bmatrix}.$$

The mass ratios are defined as follows for the sake of parameter design:

$$r_1 = \frac{m_{ds}}{m_s}, \quad r_2 = \frac{m_{du}}{m_u}. \tag{5.19}$$

During the modeling of the desired system, we discovered that by making the potential energy structure equivalent to that of the plant, i.e. $V_d = \frac{1}{2}\left(k_{d1}q_1^2 + k_{d2}q_2^2\right)$, and preventing the mass ratios to have the same values, i.e., $r_1 \neq r_2$, the given M_d and V_d cannot hold the matching equation in (5.18). As a result, we add a linked term to the required potential energy in the following way:

$$V_d(q) = \frac{1}{2}\left(k_{d1}q_2^2 + k_{d2}q_1^2 + k_{d3}(q_1+q_2)^2\right) = \frac{1}{2}q^\top K_d q,$$
$$K_d = \begin{bmatrix} k_{d2}+k_{d3} & k_{d3} \\ k_{d3} & k_{d1}+k_{d3} \end{bmatrix},$$

finally, the control input for energy shaping may be stated as

$$\begin{aligned} u_{es}(q,p) =& G^+\left(\nabla_q H - M_d M^{-1}\nabla_q H_d + J_2 M_d^{-1} p\right) \\ =& k_s(q_1)q_1 - r_1(k_{d2}+k_{d3})q_1 - r_1 k_{d3} q_2 - \frac{j_e}{m_u r_2}(p_1 - p_2). \end{aligned} \tag{5.20}$$

Damping injection The dissipation matrix and disturbance coefficients of the desired system are now shown. The dampers are placed to the same position as the springs to modify the motion, which includes the spring terms, k_{di}. We also add two SH dampers, m_{ds} and m_{du}, to the required masses. As a result, we match the controlled system with the intended system, whose structure is given in Fig. 5.4. The desired system with an artificial structure matrix is constructed as follows:

$$\dot{x} = \begin{bmatrix} \dot{q} \\ \dot{p} \end{bmatrix} = (J_d - R_d)\frac{\partial H_d}{\partial x}^\top + D_d\omega, \tag{5.21}$$

where

$$H_d(q,p) = \frac{1}{2}\left(p^\top M_d^{-1} p + V_d(q)\right),$$

denotes the total energy of the desired system, and

$$M_d = \begin{bmatrix} m_{ds} & m_{ds} \\ m_{ds} & m_{ds}+m_{du} \end{bmatrix}, J_d = \begin{bmatrix} O & M^{-1}M_d \\ -M_d M^{-1} & J_2 \end{bmatrix}, J_2 = \begin{bmatrix} 0 & j_e \\ -j_e & 0 \end{bmatrix},$$
$$R_d = \begin{bmatrix} O & O \\ O & C_d \end{bmatrix}, C_d = \begin{bmatrix} c_{d2}+c_{d4}+c_{d5} & c_{d4}+c_{d5} \\ c_{d4}+c_{d5} & c_{d1}+c_{d3}+c_{d4}+c_{d5} \end{bmatrix},$$
$$D_d = (0 \;\; -1 \;\; c_{d5} \;\; c_{d1}+c_{d5})^\top.$$

The artificial skew-symmetric structure matrix, positive semi-definite damping matrix, potential energy, and inertia matrix in the desired Hamiltonian are denoted by J_d, R_d, $V_d(q)$, and M_d, respectively. Thereafter, the damping injection force is calculated by matching the dynamics, which includes the dissipation matrices and disturbance coefficients, as follows:

$$-R\frac{\partial H}{\partial x}^\top + Dw + \begin{bmatrix} 0_{2\times 1} \\ G \end{bmatrix} u_{di} = -R_d\frac{\partial H_d}{\partial x}^\top + D_d\omega. \tag{5.22}$$

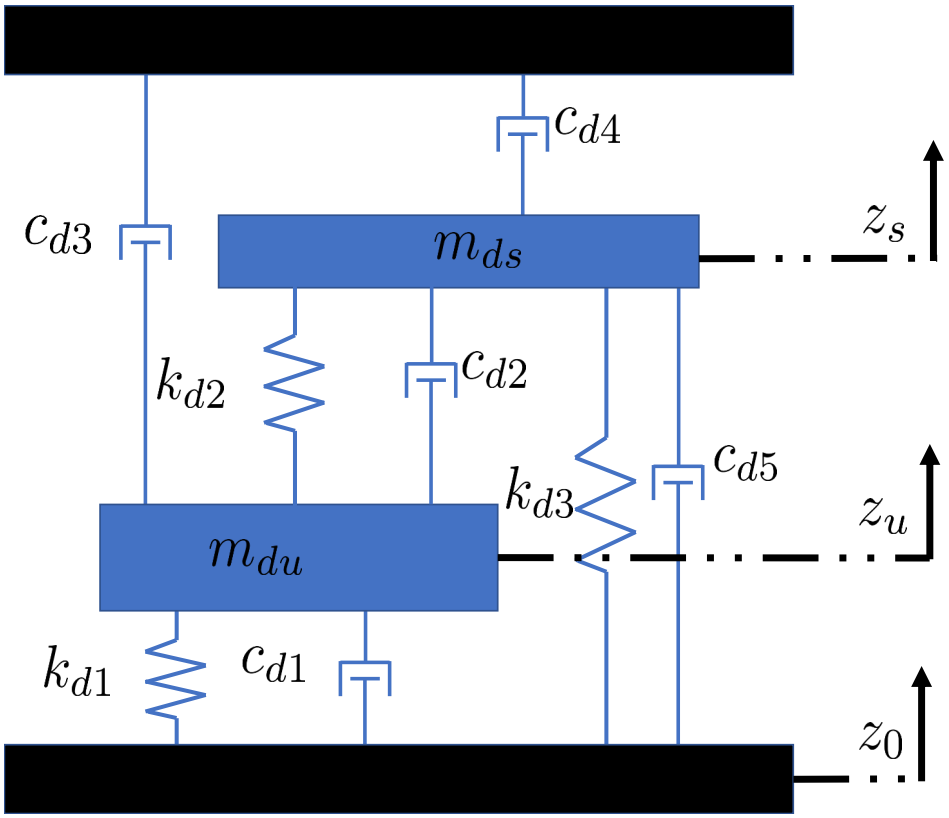

Figure 5.4: Desired system with several virtual springs and dampers.

From the above equation, the damping injection force is obtained as

$$\begin{aligned} u_{di}(p,\omega) = c_s\frac{m_u+m_s}{m_s m_u}p_1 - c_s\frac{1}{m_u}p_2 - \frac{(c_{d2}+c_{d4}+c_5)m_u r_2 + c_{d2}m_s r_1}{m_s m_u r_1 r_2}p_1 \\ + \frac{c_{d2}}{m_u r_2}p_2 + c_{d5}\omega, \end{aligned} \tag{5.23}$$

and the total control input, $u = u_{es} + u_{di}$, is expressed as

$$\begin{aligned} u(q,p,\omega) = k_s(q_1)q_1 - r_1(k_{d2}+k_{d3})q_1 - r_1 k_{d3}q_2 - \frac{j_e}{m_u r_2}(p_1-p_2) \\ + c_s\frac{m_u+m_s}{m_s m_u}p_1 - c_s\frac{1}{m_u}p_2 - \frac{(c_{d2}+c_{d4}+c_5)m_u r_2 + c_{d2}m_s r_1}{m_s m_u r_1 r_2}p_1 \\ + \frac{c_{d2}}{m_u r_2}p_2 + c_{d5}\omega. \end{aligned} \tag{5.24}$$

5.4.3 Conditions for matching dynamics

Another benefit of this research is that the suggested control rule is based on relative displacement and relative velocity, both of which are easily monitored by low-cost sensors. As a result, we'll show you how to get the feedback legislation in terms of relative information.

By matching the dynamics of the desired system with those of the controlled system, the following equation for the feedback law with equality and inequality constraints of the parameters of the desired system may be derived:

$$(J_d - R_d)\frac{\partial H_d}{\partial x}^{\top} = (J-R)\frac{\partial H}{\partial x}^{\top} + B_2 u + (D - D_d)w. \tag{5.25}$$

By removing the coefficients of q_1, q_2, p_1, p_2, and ω, the matching equation may be reduced into the following equations.

$$\begin{aligned} &(r_1 - r_2)k_{d2} + r_1 k_{d3} = 0 \\ &r_2 k_{d1} + r_1 k_{d3} = k_t \\ &\frac{c_t}{m_u} = -\frac{(j_e + c_{d5} + c_{d4})m_u r_2 + (j_e - c_{d1} - c_{d3})m_s r_1}{m_s m_u r_1 r_2} \\ &-\frac{c_t}{m_u} = \frac{j_e - c_{d1} - c_{d3}}{m_u r_2} \\ &c_t = c_{d1} + c_{d5} \end{aligned}$$

Herein, we select c_{d2}, c_{d4}, c_{d5}, k_{d2}, r_1, and r_2 as temporary free parameters, and the other parameters are obtained from the following equations:

$$\begin{aligned} &r_1 k_{d3} = (r_2 - r_1)k_{d2} \\ &k_{d1} = \frac{k_t + (r_1 - r_2)k_{d2}}{r_2} \\ &j_e = -c_{d4} - c_{d5} \\ &c_{d1} = c_t - c_{d5}, \\ &c_{d3} = (r_2 - 1)c_t - c_{d4} \end{aligned}$$

By substituting the previous equations and $p = M(\dot{q} - a\omega)$ into u, we obtain the following:

$$\begin{aligned} u(q,\dot{q},\omega) = k_s q_1 - r_2 k_{d2} q_1 + (r_1 - r_2) k_{d2} q_2 + c_s \dot{q}_1 - \frac{c_{d2} + c_{d4} + c_{d5}}{r_1} \dot{q}_1 \\ + \frac{r_2(-c_{d2} - c_{d4} - c_{d5}) + r_1(c_{d2} - c_{d4} - c_{d5})}{r_1 r_2} \dot{q}_2 + \theta\omega, \end{aligned} \tag{5.26}$$

where

$$\theta = \frac{(r_1 c_{d5} - c_{d5} - c_{d4} - c_{d2}) r_2 + r_1(c_{d2} - c_{d4} - c_{d5})}{r_1 r_2}. \tag{5.27}$$

If θ is zero, we can express the feedback law in terms of the relative displacement and velocity. Thus, by solving θ to zero for c_{d2}, we obtain the following additional condition:

$$c_{d2} = \frac{(r_1 r_2 - r_1 - r_2) c_{d5} - (r_1 + r_2) c_{d4}}{r_2 - r_1} \tag{5.28}$$

With these equality constraints, we obtain the following feedback law:

$$u(q,\dot{q}) = (k_s - r_2 k_{d2}) q_1 + (r_1 - r_2) k_{d2} q_2 + c_s \dot{q}_1 - \frac{(r_2 - 2) c_{d5} - 2 c_{d4}}{r_2 - r_1} \dot{q}_1 - c_{d5} \dot{q}_2. \tag{5.29}$$

Remark 17. It is difficult to solve and create the required potential matrix and dissipation matrix if the potential matrix and dissipation matrix are nonlinear. Because the nonlinearity of the desired potential matrix and the dissipation matrix must often cover the nonlinearity of the original system. Our suspension system (k_s and c_s) has nonlinearity in the actuated coordinates (q_1 and p_1), but linear parameters in the underactuated coordinates (q_2 and p_2). Only the parameters on the underactuated coordinates are included in the matching equations produced by the underactuated attribute. As a result, the required suspension model may be built linearly.

5.4.4 Stability analysis with zero disturbances

As advantages of using IDA-PBC is that the controller can achieve asymptotic stability by considering the desired Hamiltonian function as a Lyapunov function.

Theorem 18. *The origin of the system in (5.17) with zero disturbances ($z_0 = 0$) is globally asymptotic stable if the following constraints are satisfied:*

$$\begin{aligned} & r_1 > r_2 > 0 \\ & k_{d2} > 0. \\ & c_{d4} + c_{d5} = \frac{c_t r_1 r_2}{r_1 - r_2}, \\ & c_{d5} < 0 \\ & r_2 < \frac{2 r_1 c_t + r_1 c_{d4}}{r_1 c_t + c_{d4}}. \end{aligned} \tag{5.30}$$

Proof. We consider the desired Hamiltonian function, H_d, as a Lyapunov candidate function, which is described as follows:

$$H_d(q,p) = \frac{1}{2}\left(p^\top M_d^{-1} p + q^\top K_d q\right), \tag{5.31}$$

For the positive definiteness of H_d, M_d and K_d should be positive definite, i.e.,

$$\begin{cases} m_{ds} = r_1 m_s > 0, \\ \det M_d = r_1 r_2 m_s m_u > 0 \end{cases} \tag{5.32}$$

$$\begin{cases} k_{d2} + k_{d3} = \frac{r_2 k_{d2}}{r_1} > 0, \\ \det K_d = \frac{k_t k_{d2}}{r_1} > 0 \end{cases} \tag{5.33}$$

We observe that the constraint in (5.32) can be satisfied by $r_1 > 0$ and $r_2 > 0$. With $r_1 > 0$ and $k_{d2} > 0$, (5.33) is ensured.

The time derivation of the desired Hamiltonian function, H_d, is expressed as follows:

$$\begin{aligned} \dot{H}_d &= -\frac{\partial H_d}{\partial x} R_d \frac{\partial H_d}{\partial x}^\top \\ &= -\frac{\partial H_d}{\partial p} C_d \frac{\partial H_d}{\partial p}^\top \\ &= -p^\top M_d^{-1} C_d M_d^{-1} p \end{aligned} \tag{5.34}$$

Here, $\dot{H}_d \leq 0$ holds when M_d and C_d are positive definite. In addition, C_d is positive definite when

$$c_{d2} + c_{d4} + c_{d5} > 0, \tag{5.35}$$

$$\det C_d = r_2 c_t \frac{r_1 r_2 c_{d5} - r_1 (c_{d4} + c_{d5})}{r_2 - r_1} - (c_{d4} + c_{d5})^2 > 0 \tag{5.36}$$

are satisfied. Herein, if we set

$$c_{d4} + c_{d5} = \frac{c_t r_1 r_2}{r_1 - r_2}, \tag{5.37}$$

(5.36) can be rewritten as $\frac{r_1 r_2^2 c_t c_{d5}}{r_2 - r_1} > 0$, which can be ensured by

$$r_1 > r_2 > 0, \ c_{d5} < 0 \tag{5.38}$$

or

$$r_2 > r_1 > 0, \ c_{d5} > 0. \tag{5.39}$$

According to the SH theorem [10], a large positive value of the SH damper term, c_{d4}, enhances the vibration suppression effect on the sprung mass, m_{ds}. However, a large positive c_{d4} leads to a negative c_{d5} when $r_2 > r_1 > 0$ holds. Thus, we select (5.38) to satisfy (5.36). With the conditions in (5.28), (5.37), and (5.38), the constraint in (5.35) is equivalent to

$$r_2 < \frac{2 r_1 c_t + r_1 c_{d4}}{r_1 c_t + c_{d4}} \tag{5.40}$$

for a fixed r_1 and c_{d4}.

It can be concluded that if (5.30) is satisfied, $H_d(x)$ is positive definite and $\dot{H}_d$ is negative semi-definite as (5.34). Since C_d is positive definite, from Barbalat's lemma

$\partial H_d/\partial p = M_d^{-1}p \to 0$ $(t \to \infty)$, i.e., $\dot{q} = M^{-1}p \to 0$ $(t \to \infty)$. Note that the desired system is linear, and hence, the uniform-continuity condition for Barbalat's lemma is fulfilled. Because $V_d(q)$ is quadratic and positive definite with respect to q, the system is zero-state observable for the velocity output, i.e., $q \equiv 0$ if $\dot{q} \equiv 0$. From the invariance principle, the system is globally asymptotically stable. Because our desired system is constructed as a linear system, the global property is natural.

We can also design the desired system as a nonlinear system, i.e., making K_d and C_d as functions with respect to state x. We assume that the new potential function, $V_d(q)$, derived from the nonlinear K_d is radially unbounded and satisfies $\partial V_d/\partial q \neq 0$ $(q \neq 0)$. Under these assumptions, the zero-state observability is also satisfied, and therefore, the GAS property can be shown. □

Remark 19. We can establish that the system is input-to-state stable (ISS) [63] since the desired system, which is identical to a closed-loop system, is linear and coefficient D_d is a constant vector. Our findings may be used to situations involving nonlinear desirable systems. The input-to-stability should be addressed for a nonlinear system with disturbances. Although asymptotically stable linear systems are often ISS, treating the Hamiltonian as an ISS Lyapunov function does not allow us to deduce the ISS feature from the GAS property for nonlinear systems. Because the Hamiltonian is always semi-positive definite, this is the case. In [31], Aoki et al. demonstrated the ISS feature for a specific scenario; nonetheless, building of the ISS Lyapunov function is expected for a universal PH system. As a result, one of our future research projects will focus on developing an ISS Lyapunov function for generic nonlinear pH systems with disturbances.

When creating the parameters for the intended system, we must keep in mind that all parameters must adhere to the equality requirements, which are described as follows:

$$\begin{aligned}
k_{d3} &= \left(\frac{r_2}{r_1} - 1\right) k_{d2} \\
k_{d1} &= \frac{k_t + (r_1 - r_2)k_{d2}}{r_2} \\
j_e &= -c_{d4} - c_{d5} \\
c_{d1} &= c_t - c_{d5}, \\
c_{d2} &= \frac{(r_1 r_2 - r_1 - r_2)c_{d5} - (r_1 + r_2)c_{d4}}{r_2 - r_1} \\
c_{d3} &= (r_2 - 1)c_t - c_{d4} \\
c_{d5} &= \frac{c_t r_1 r_2}{r_1 - r_2} - c_{d4},
\end{aligned} \tag{5.41}$$

as well as the inequality constraints,

$$\begin{aligned}
&r_1 > r_2 > 0 \\
&k_{d2} > 0 \\
&c_{d5} < 0 \\
&r_2 < \frac{2r_1 c_t + r_1 c_{d4}}{r_1 c_t + c_{d4}}.
\end{aligned}$$

The proposed system has 11 parameters that must be developed using the seven equality constraints in (5.41). Thus, we select r_1, r_2, k_{d2}, c_{d4} as free parameters, and determine the

other parameters from the equality constraints in (5.41). Finally, we have the following feedback law:

$$\begin{aligned} u = {} & (k_s - r_2 k_{d2}) q_1 + (r_1 - r_2) k_{d2} q_2 \\ & + c_s \dot{q}_1 + \frac{r_1 r_2 (r_2 - 2) c_t + r_2 (r_2 - r_1) c_{d4}}{(r_1 - r_2)^2} \dot{q}_1 - \left(\frac{c_t r_1 r_2}{r_1 - r_2} - c_{d4} \right) \dot{q}_2, \end{aligned} \tag{5.42}$$

which converts the system in (5.17) into the desired system in (5.21) with equality constraints (5.41). Moreover, if (5.30) holds, the origin of the controlled system with zero disturbances is the GAS.

5.5 Guidelines for Parameter Selection

5.5.1 Robust Stability Against Parameter Uncertainty

Despite the fact that we have demonstrated the GAS of the controlled system with minimal disturbance, one of our major contributions is to assure robust stability in the face of parameter uncertainties in the mass, springs, and dampers. Variations in the number of passengers and the vehicle body weight, as well as the age of suspension elements and measurement mistakes, can all contribute to these inaccuracies.

The following parameters are used to assess robust stability against parameter uncertainties:

$$\delta = \frac{u(m_s, m_u, c_s, c_t, k_s, k_t) - u(\tilde{m}_s, \tilde{m}_u, \tilde{c}_s, \tilde{c}_t, \tilde{k}_s, \tilde{k}_t)}{u(\tilde{m}_s, \tilde{m}_u, \tilde{c}_s, \tilde{c}_t, \tilde{k}_s, \tilde{k}_t)}. \tag{5.43}$$

Noticeably, the control input, u, (5.42) is independent of M and k_t, i.e.,

$$u(M) = u(\tilde{M}, \tilde{k}_t).$$

The suggested controller is robust against mass parameter and tire stiffness parameter uncertainties in particular, and robustness against mass parameter uncertainties is the most crucial indicator when building a robust suspension system. The controller may be broken down into:

$$u(q, \dot{q}) = u_1(\dot{q}_1) + u_2(\dot{q}_2) + u_3(q_1) + u_4(q_2),$$

where

$$\begin{aligned} u_1 &= c_s \dot{q}_1 + \frac{r_1 r_2 (r_2 - 2) c_t + r_2 (r_2 - r_1) c_{d4}}{(r_1 - r_2)^2} \dot{q}_1 \\ u_2 &= - \left(\frac{c_t r_1 r_2}{r_1 - r_2} - c_{d4} \right) \dot{q}_2 \\ u_3 &= (k_s - r_2 k_{d2}) q_1 \\ u_4 &= (r_1 - r_2)\, k_{d2} q_2. \end{aligned}$$

The nonlinear coefficients $k_s(q_1)$ and $c_s(\dot{q}_1)$ are assumed to be limited in this paper. As a result, robust stability may be attained by calculating the sensitivity of the controller

to the uncertainty of the parameters. The following is how we define sensitivity, which should be near to zero:

$$e_1 = \frac{u_1(c_s, c_t) - u_1(\tilde{c}_s, \tilde{c}_t)}{u_1(c_s, c_t)} \approx 0, \tag{5.44}$$

$$e_2 = \frac{u_2(c_t) - u_2(\tilde{c}_t)}{u_2(c_t)} \approx 0, \tag{5.45}$$

$$e_3 = \frac{u_3(k_s) - u_3(\tilde{k}_s)}{u_3(k_s)} \approx 0. \tag{5.46}$$

The sufficient conditions of (5.44) are

$$\frac{r_1 - r_2}{r_1|r_2 - 2|} c_{d4} \gg c_t, \tag{5.47}$$

$$\frac{r_2}{r_1 - r_2} c_{d4} \gg c_s(\dot{q}_1). \tag{5.48}$$

The sufficient condition of (5.45) is

$$\frac{r_1 - r_2}{r_1 r_2} c_{d4} \gg c_t. \tag{5.49}$$

The sufficient condition of (5.46) is

$$r_2 k_{d2} \gg k_s(q_1). \tag{5.50}$$

For instance, when $k_s(q_1) = 10\sin(q_1)$, $c_s(\dot{q}_1) = 10\sin(\dot{q}_1)$, and $c_t = 1$, by setting $r_1 = 10.1, r_2 = 0.1, c_{d4} = 10^4, k_{d2} = 10^3$, one can satisfy the conditions in (5.47),(5.48),(5.49),and (5.50).

Remark 20. When the nonlinear coefficients $k_s(q_1)$ and $c_s(\dot{q}_1)$ are unbounded, additional requirement for robust stability in the global sense must be considered. We define the error between the controller with nominal parameters and the one with unknown parameters as $u_e = \delta_1(q_1) + \delta_2(\dot{q}_1)$ for a controller with uncertain parameters $\tilde{k}_s(q_1)$ and $\tilde{c}_s(\dot{q}_1)$. The errors produced by the uncertainty of $k_s(q_1)$ and $c_s(\dot{q}_1)$ are $\delta_1(q_1)$ and $\delta_2(\dot{q}_1)$, respectively. Robust stability is ensured when the time derivation of the Lyapunov function, H_d, satisfies

$$\dot{H}_d = -p^\top M_d^{-1} C_d M_d^{-1} p + p^\top M_d^{-1} G u_e < 0. \tag{5.51}$$

5.5.2 Suspension Performance

Because the free parameters are r_1, r_2, k_{d2}, and c_{d4}, we can design the damper terms of the suspension system like other conventional controllers using the SH control strategy. Moreover, we can design the values of the spring, k_{d2}, virtual vehicle body mass m_{ds}, and virtual unsprung mass m_{du} to improve the suspension performance.

As previously mentioned, our aim is to decrease the sprung mass acceleration, $\ddot{z}_s$, and the tire deflection, q_2, simultaneously. Considering the empirical knowledge of the SH system [10], we expect that large c_{d4} and m_{ds} will enhance the vibration suppression/isolation effects with respect to the sprung mass, m_{ds}. For the tire deflection, q_2, a large c_{d1} should be selected. We rewrite c_{d1} in (5.41) as

$$c_{d1} = \left(1 - \frac{r_1 r_2}{r_1 - r_2}\right) c_t + c_{d4}, \tag{5.52}$$

Table 5.1: Parameters of suspension system

Parameters	Symbol	Unit	Value
Sprung mass	m_s	Kg	500
Unsprung mass	m_u	Kg	50
Spring stiffness	k_s	N/m	30,000
Suspension damping coefficient	c_s	Ns/m	2,000
Tire damping coefficient	c_t	Ns/m	200
Tire stiffness	k_t	N/m	300,000

and we observe that selecting $0 < r_2 < 1$ and a large r_1, c_{d4} lead to a large c_{d1}.

As a result, the criteria for selecting the appropriate system's parameters are $0 < r_2 < 1$ and a big r_1, as well as c_{d4}. The other parameters are chosen by the equality criteria, and the aforementioned parameter configuration automatically satisfies the inequality constraints that assure the intended system's asymptotical stability.

Remark 21. Setting a big r_1 and a small r_2, from the perspective of the desired system, makes the virtual vehicle body and virtual unsprung mass (usually the tire structure) heavy and light, respectively. A hefty body is well recognized for suppressing vibration, whereas a small unsprung mass is well known for following the undulations of roadways. In general, controlling a hefty body necessitates a considerable lateral force, which may surpass the tire capacity. Our feedback law, on the other hand, only examines the vertical direction, therefore the intended system's horizontal performance will remain unchanged.

5.6 Simulation Verification

In this part, we show how we used simulations to verify the suspension effect of the feedback rule. Table 5.1 lists the parameters of the controlled suspension system. The nonlinear spring force and damper force have the following mathematical expressions:

$$F_{cs} = c_s \left(\dot{q}_1 + \dot{q}_1^3 \right) \tag{5.53}$$

$$F_{ks} = k_s \left(\dot{q}_2 + \dot{q}_2^3 \right) \tag{5.54}$$

In the case of an isolated bump, the vertical road displacement input, $z_0(t)$, is described as

$$z_0(t) = \begin{cases} \frac{A}{2}(1 - \cos(\frac{2\pi v}{L}t)), & 0 \le t \le \frac{L}{v} \\ 0, & t > \frac{L}{v}, \end{cases}$$

where A denotes the bump height, L is the bump length, and v is the velocity of the passing vehicle. We let $A = 0.08$,[m], $L = 5$ [m], and $v = 12.5$ [m/s]. The disturbance signal of the controlled suspension system in (5.17) is the derivation of z_0, i.e.,

$$\omega(t) = \begin{cases} \frac{\pi A v}{L} \sin(\frac{2\pi v}{L}t), & 0 \le t \le \frac{L}{v} \\ 0, & t > \frac{L}{v}. \end{cases}$$

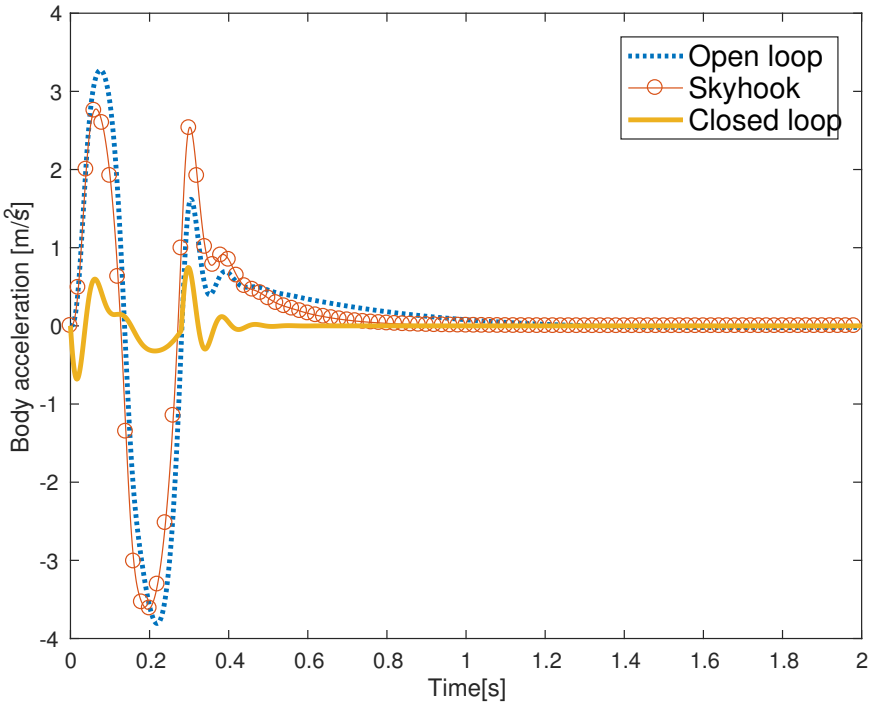

Figure 5.5: Comparison of body accelerations

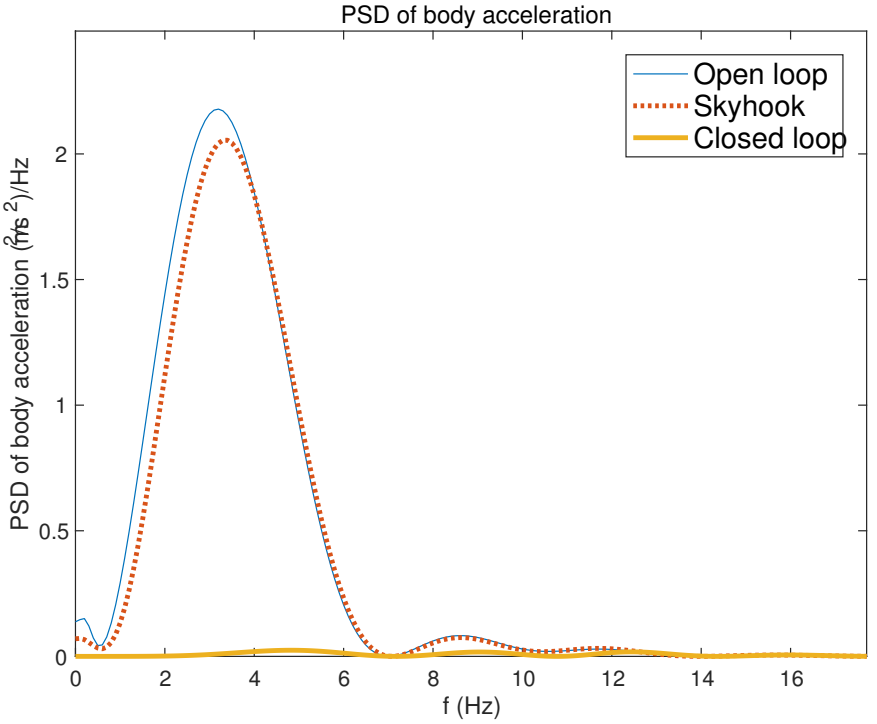

Figure 5.6: Comparison of power spectral density (PSD) of body accelerations

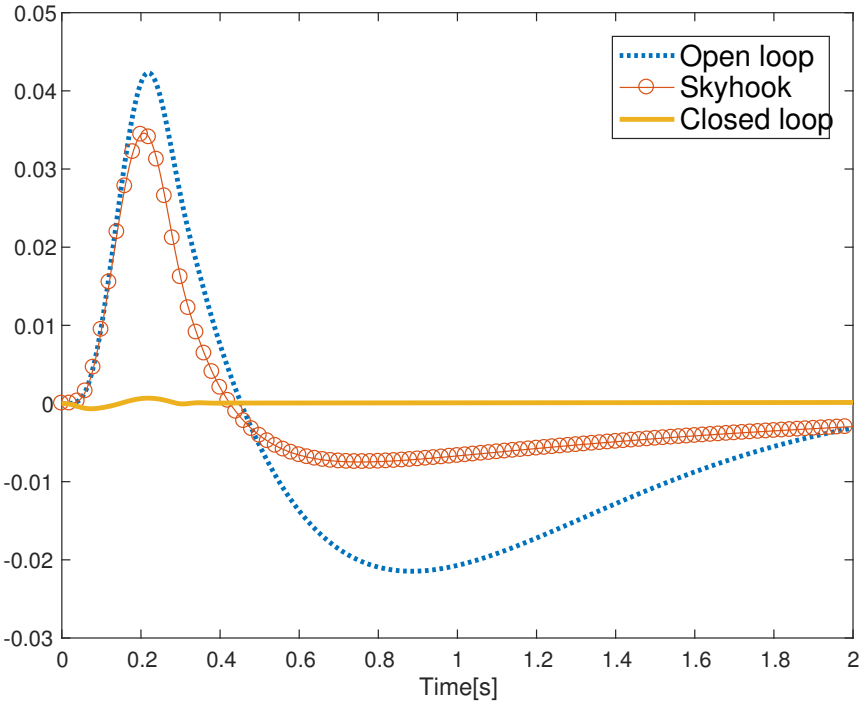

Figure 5.7: Comparison of body displacements

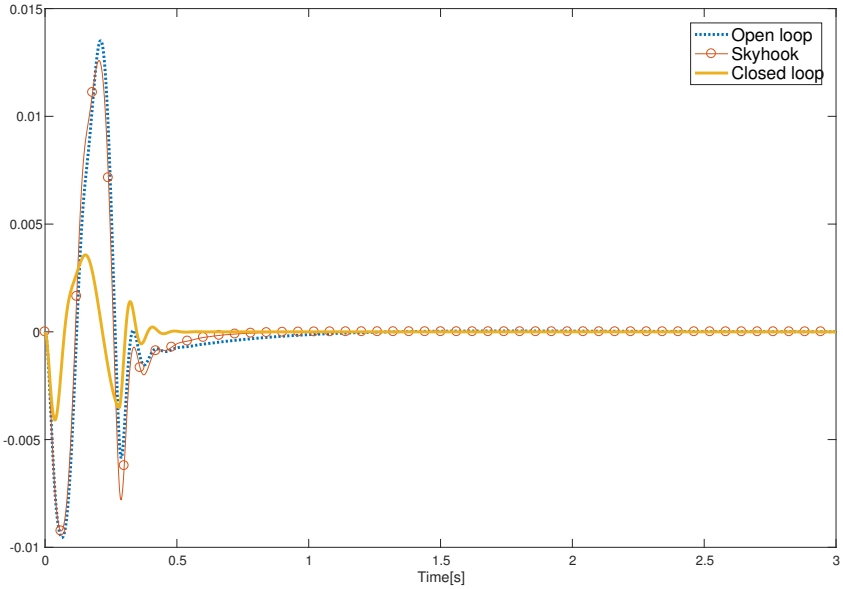

Figure 5.8: Comparison of tire deflections

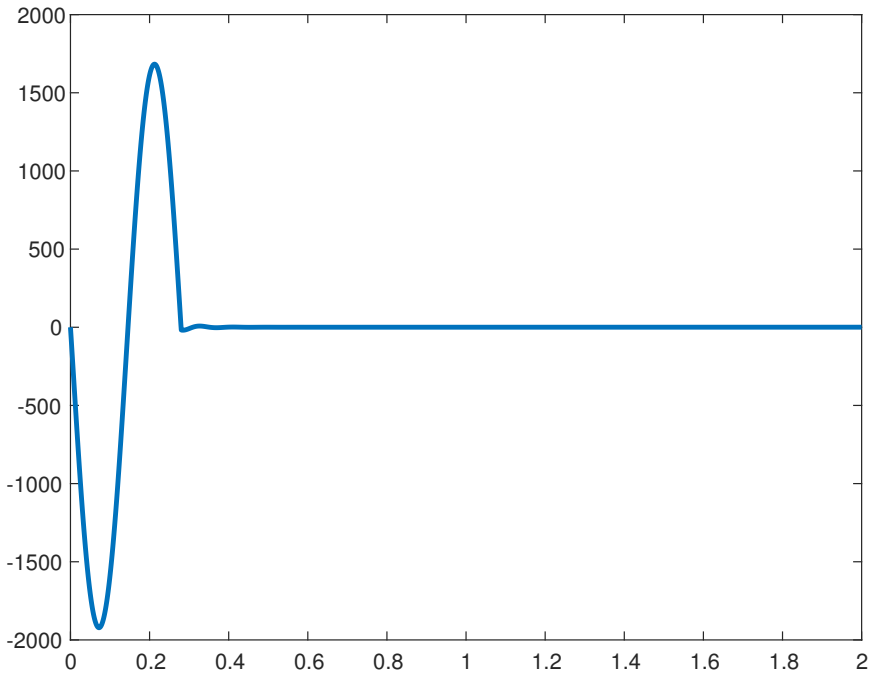

Figure 5.9: Control force

The simulation results of the active suspension with the proposed controller were compared with those of a passive suspension and an active suspension with the SH damper controller. The SH damper control law can be described as

$$u = -c_{sh}\dot{z}_u.$$

To compare the two controllers, we set the SH damper coefficients of the conventional and suggested controllers to the identical values. We select $c_{d4} = c_{sh} = 2000$, and $r_1 = 100$, $r_2 = 0.1$, and $k_{d2} = 20$. The matching equations are used to calculate the additional parameters of the desired system. When compared to the open-loop and SH damper systems, the major aims of our study—-sprung mass acceleration and tire deflection—-were significantly improved.

The time response comparison of the vertical acceleration of the sprung mass under varied control inputs is shown in Figure 5.5. The temporal response of the vertical displacement of the sprung mass under varied control inputs is shown in Figure 5.7. It is clear that the SH control input improves the body displacement performance over the passive system. The body acceleration under the SH control input, on the other hand, is ineffective. We can see from Figure 5.6, which shows the power spectral density (PSD) of the sprung mass acceleration, that in the frequency range of 4–8 Hz, the performance under the SH control is the same as the passive one. The suggested solution, on the other hand, outperforms the SH control and passive systems in terms of body acceleration. The root-means-square (RMS) of the acceleration under a bumpy road disturbance is compared in Table 5.2. The time response comparisons of tire deflections under various control inputs are shown in Figure 5.8. The active control force of the suggested controller is shown

Table 5.2: RMS of body accelerations

Controller	$\ddot{z}_s$	Changes
Passive	1.0126	-
Skyhook damper	0.9468	6.5 %
IDA-PBC	0.1891	81.3 %

in Figure 5.9, and we can see that it is less than 2500 N, which is the usual evaluation value of a control force [99]. Using simply relative displacement and velocity information, the suggested controller can increase ride comfort and road holding performance, as seen in the figures above. Furthermore, because the maximum force is less than the control force's standard evaluation value, the magnitude of the control force corresponds to a real situation [99].

5.7 Conclusion

We present a novel IDA-PBC design for a quarter car nonlinear active suspension system in this chapter. First, we use relative coordinates to obtain the pH form for the quarter car nonlinear active suspension system. We get the requirements that ensure the feedback only utilizes the relative displacement and velocity after calculating the feedback law using IDA-PBC. Following that, parameter selection instructions for the controller are offered in order to achieve suspension performance and strong stability. We may easily set the parameters according to the rules, ensuring GAS and control performance. Finally, we run many simulations to test the suspension's performance. The maximum force is less than 2500 N, which is the usual control force assessment value [99]. The focus of our future research will be in two directions. One way is to create an ISS Lyapunov function for a nonlinear pH system that is subject to perturbations. The second goal is to apply our technology to either a half- or full-suspension system.

Chapter 6

Conclusion

In this dessertation, vibration controllers based on relative information for nonlinear mechanical systems are proposed. The key idea of the controllers is based on the passivity properties of the mechanical systems and skyhook strategies. Interconnection and damping assignment passivity-based control (IDA-PBC) method is applied in most result, due to its theoretical advantages on energy shaping and stabilization of nonlinear systems.

We solved the vibration suppression problem of the general pH system in Chapter 2 by constructing the IDA-PBC controller. Any floating nonlinear mechanical structure with spring and damper can be used to represent the system under consideration. The matching condition between the controlled system and the desired system has been demonstrated. We demonstrate a control law with various free parameters and limitations. Only relative information, which is easily measured, is used by the controller. In comparison to earlier work, we offer a novel parameter design technique for more generalized nonlinear controlled devices. The inertia matrix of the intended closed-loop system is determined using differential equations. The IDA-PBC approach theoretically guarantees the stability of the nonlinear closed-loop system. We have presented a parameter selection strategy that is both efficient and effective in providing a decent vibration suppression effect. The suggested control law achieved a virtual skyhook damper utilizing just relative information under the specified parameter selection.

In Chapter 3, we presented a new nonlinear active DVA control system, in which the information of the controller is not based on the world-coordinate information. The proposed method can control the vibrations that are excited by a force disturbance and velocity disturbance simultaneously. The control law uses only the relative displacement and velocity of the vibration system, which can be easily measured by sensors. We revealed the equality and inequality constraints for matching the plant system with the desired system. The numerical solutions of the partial differential equations are not required with our proposed method. The main idea of the controller design is to convert a nonlinear DVA system into a desired system with multiple virtual springs and dampers. We also derived selection guidelines for the parameters of the desired system. The global asymptotical stability is guaranteed automatically through passivity-based control theory, although the parameter design is based on a linearization. The effectiveness of our controller was confirmed through simulations for a cart-pendulum system.

We built ISS Lyapunov functions for a type of nonlinear mechanical Hamilton systems with a force and velocity disturbance in Chapter 4. The system under consideration was split into two parts: one with a force disturbance and the other with a feedback

input and a velocity disturbance. Then, for each of those two systems, we built the ISS Lyapunov function. The construction is based on a number of assumptions regarding the system parameters, all of which are easily met in practice. The created ISS Lyapunov functions have an issue in that they are for split systems, and the relationship between the ISS property of divided systems and the one of the entire system has to be studied theoretically, which is our future study.

A novel IDA-PBC design for a quarter car nonlinear active suspension system was suggested in Chapter 5. First, we use relative coordinates to obtain the pH form for the quarter car nonlinear active suspension system. We get the requirements that ensure the feedback only utilizes the relative displacement and velocity after calculating the feedback law using IDA-PBC. Following that, parameter selection instructions for the controller are offered in order to achieve suspension performance and strong stability. We may easily set the parameters according to the rules, ensuring GAS and control performance. Finally, we run many simulations to test the suspension's performance. It will be instructive to see how our strategy works with a half- or full-suspension system.

Acknowledgements

I would like to express my gratitude to all those who helped me during the writing of this thesis.

First and foremost I am extremely grateful to my supervisors, Prof. Yuh Yamashita for his invaluable advice, continuous support, and patience during my PhD study. His immense knowledge and plentiful experience have encouraged me in all the time of my academic research and daily life. I would also like to thank Associate Professor Koichi Kobayashi for his technical support on my study. I would like to thank all the members in the Dynamical Systems and Control Laboratory. It is their kind help and support that have made my study and life in the Hokkaido University a wonderful time. Finally, I would like to express my gratitude to my parents and my wife. Without their tremendous understanding and encouragement in the past few years, it would be impossible for me to complete my study.

References

[1] M. L. Corradini, G. Ippoliti, and G. Orlando, "Fully sensorless robust control of variable-speed wind turbines for efficiency maximization," *Automatica*, vol. 49, no. 10, pp. 3023–3031, 2013.

[2] ——, "Sensorless efficient fault-tolerant control of wind turbines with geared generator," *Automatica*, vol. 62, pp. 161–167, 2015.

[3] J. Wang, S.-X. Tang, and M. Krstic, "Adaptive output-feedback control of torsional vibration in off-shore rotary oil drilling systems," *Automatica*, vol. 111, p. 108640, 2020.

[4] S. Miani, M. Zilletti, P. Gardonio, F. Blanchini, and P. Colaneri, "Switching and sweeping vibration absorbers: Theory and experimental validation," *Automatica*, vol. 93, pp. 290–301, 2018.

[5] U. H. Shah and K.-S. Hong, "Active vibration control of a flexible rod moving in water: Application to nuclear refueling machines," *Automatica*, vol. 93, pp. 231–243, 2018.

[6] T. Zeng, J. Brooks, and P. Barooah, "Simultaneous identification of linear building dynamic model and disturbance using sparsity-promoting optimization," *Automatica*, vol. 129, p. 109631, 2021.

[7] K. Deng, S. Goyal, P. Barooah, and P. G. Mehta, "Structure-preserving model reduction of nonlinear building thermal models," *Automatica*, vol. 50, no. 4, pp. 1188–1195, 2014.

[8] P.-J. Meyer, A. Girard, and E. Witrant, "Robust controlled invariance for monotone systems: Application to ventilation regulation in buildings," *Automatica*, vol. 70, pp. 14–20, 2016.

[9] D. Hrovat, "Survey of advanced suspension developments and related optimal control applications," *Automatica*, vol. 33, no. 10, pp. 1781–1817, 1997.

[10] D. Karnrop, M. J. Crosby, and R. A. Harwood, "Vibration control using semi-active force generators," *Transactions of the ASME, Journal of Engineering for Industry*, vol. 96, no. 2, pp. 619–626, 1974.

[11] J. Alanoly and S. Sanker, "Semi-active force generators for shock isolation," *Journal of Sound and Vibration*, vol. 126, no. 1, pp. 145–156, 1988.

[12] D. Sammier, O. Sename, and L. Dugard, "Skyhook and H_∞ control of semi-active suspensions: Some practical aspects," *International Journal of Vehicle Mechanics and Mobility*, vol. 39, no. 4, pp. 279–308, 2003.

[13] J. Emura, S. Kakizaki, F. Yamaoka, and M. Nakamura, "Development of the semi-active suspension system based on the sky-hook damper theory," in *SAE Technical Paper*. SAE International, 1994.

[14] D. Hrovat, "Applications of optimal control to advanced automotive suspension design," *Transactions of the ASME, Journal of Dynamics, Measurement, and Control*, vol. 115, no. 2B, pp. 328–342, 1993.

[15] S. Nagarajaiah, M. A. Riley, and A. Reinhorn, "Control of sliding-isolated bridge with absolute acceleration feedback," *Journal of Engineering Mechanics*, vol. 119, no. 11, pp. 2317–2332, 1993.

[16] D. Noh, N. Jo, and J. Seo, "Nonlinear observer design by dynamic observer error linearization," *IEEE Transactions on Automatic Control*, vol. 49, no. 10, pp. 1746–1753, 2004.

[17] A. G. Ulsoy, D. Hrovat, and T. Tseng, "Stability robustness of LQ and LQG active suspensions," *Journal of Dynamic Systems, Measurement, and Control*, vol. 116, no. 1, pp. 123–131, 1991.

[18] Z. Li, D. Marelli, M. Fu, Q. Cai, and W. Meng, "Linear quadratic gaussian stackelberg game under asymmetric information patterns," *Automatica*, vol. 125, p. 109406, 2021.

[19] D. Li, F. Qian, and P. Fu, "Optimal nominal dual control for discrete-time linear-quadratic gaussian problems with unknown parameters," *Automatica*, vol. 44, no. 1, pp. 119–127, 2008.

[20] J. Xu, G. Gu, Y. Tang, and F. Qian, "Channel modeling and lqg control in the presence of random delays and packet drops," *Automatica*, vol. 135, p. 109967, 2022.

[21] H. Yu, J. Shang, and T. Chen, "Stochastic event-based lqg control: An analysis on strict consistency," *Automatica*, vol. 138, p. 110157, 2022.

[22] H. Li, X. Jing, H.-K. Lam, and P. Shi, "Fuzzy sampled-data control for uncertain vehicle suspension systems," *IEEE Transactions on Cybernetics*, vol. 44, no. 7, pp. 1111 – 1126, 2014.

[23] A. Moran and M. Nagai, "Analysis and design of active suspensions by h∞ robust control theory," *JSME international journal. Series 3, Vibration, control engineering, engineering for industry*, vol. 35, pp. 427–437, 1992.

[24] W. Sun, Z. Zhao, and H. Gao, "Saturated adaptive robust control for active suspension systems," *IEEE Transactions on Industrial Electronics*, vol. 60, no. 9, pp. 3889–3896, 2013.

[25] R. Ortega, A. van der Schaft, B. Maschke, and G. Escobar, "Interconnection and damping assignment passivity-based control of port-controlled Hamiltonian systems," *Automatica*, vol. 38, no. 4, pp. 585–596, 2002.

[26] L. Rosier, "Homogeneous lyapunov function for homogeneous continuous vector field," *Systems & Control Letters*, vol. 19, no. 6, pp. 467–473, 1992.

[27] B. Maschke, R. Ortega, and A. J. Van Der Schaft, "Energy-based lyapunov functions for forced hamiltonian systems with dissipation," *IEEE Transactions on automatic control*, vol. 45, no. 8, pp. 1498–1502, 2000.

[28] R. Naldi and R. G. Sanfelice, "Passivity-based control for hybrid systems with applications to mechanical systems exhibiting impacts," *Automatica*, vol. 49, no. 5, pp. 1104–1116, 2013.

[29] M. Bürger, D. Zelazo, and F. Allgöwer, "Duality and network theory in passivity-based cooperative control," *Automatica*, vol. 50, no. 8, pp. 2051–2061, 2014.

[30] P. H. Heins, B. L. Jones, and A. S. Sharma, "Passivity-based output-feedback control of turbulent channel flow," *Automatica*, vol. 69, pp. 348–355, 2016.

[31] T. Aoki, Y. Yamashita, and D. Tsubakino, "Vibration suppression for mass-spring-damper systems with a tuned mass damper using interconnection and damping assignment passivity-based control," *International Journal of Robust and Nonlinear Control*, vol. 26, no. 2, pp. 235–251, 2016.

[32] O. J and D. H. JP., "The theory of the dynamic vibration absorber," *Transactions of the American Society of Mechanical Engineers, Applied Mechanics*, vol. 50, no. 7, pp. 9–22, 1928.

[33] S. Willy and F. Cantrijn, "Generalizations of noether's theorem in classical mechanics," *Society for Industrial and Applied Mathematics*, vol. 23, no. 4, pp. 467–494, 1981.

[34] I. Marvian and R. W. Spekkens, "Extending noether's theorem by quantifying the asymmetry of quantum states," *Nature communications*, vol. 5, no. 1, pp. 1–8, 2014.

[35] G. S. Frederico and D. F. Torres, "Fractional noether's theorem in the riesz–caputo sense," *Applied Mathematics and Computation*, vol. 217, no. 3, pp. 1023–1033, 2010.

[36] T. M. Atanacković, S. Konjik, S. Pilipović, and S. Simić, "Variational problems with fractional derivatives: invariance conditions and noether's theorem," *Nonlinear Analysis: Theory, Methods & Applications*, vol. 71, no. 5-6, pp. 1504–1517, 2009.

[37] J. Ormondroyd and J. Hartog, "The theory of the dynamic vibration absorber," in *Transactions of the American Society of Mechanical Engineers*, 1928, pp. 9–22.

[38] Y. Chang, J. Zhou, K. Wang, and D. Xu, "A quasi-zero-stiffness dynamic vibration absorber," *Journal of Sound and Vibration*, vol. 494, p. 115859, 2021.

[39] X. Huang, Z. Su, and H. Hua, "Application of a dynamic vibration absorber with negative stiffness for control of a marine shafting system," *Ocean Engineering*, vol. 155, pp. 131–143, 2018.

[40] Y. Hua, W. Wong, and L. Cheng, "Optimal design of a beam-based dynamic vibration absorber using fixed-points theory," *Journal of Sound and Vibration*, vol. 421, pp. 111–131, 2018.

[41] V. N. Dinh and B. Basu, "Passive control of floating offshore wind turbine nacelle and spar vibrations by multiple tuned mass dampers," *STRUCTURAL CONTROL AND HEALTH MONITORING*, vol. 22, no. 1, pp. 152–176, 2015.

[42] C. Li, "Optimum multiple tuned mass dampers for structures under the ground acceleration based on ddmf and admf," *Earthquake engineering & structural dynamics*, vol. 31, no. 4, pp. 897–919, 2002.

[43] M. Abé and Y. Fujino, "Dynamic characterization of multiple tuned mass dampers and some design formulas," *Earthquake engineering & structural dynamics*, vol. 23, no. 8, pp. 813–835, 1994.

[44] T. Igusa and K. Xu, "Vibration control using multiple tuned mass dampers," *Journal of sound and vibration*, vol. 175, no. 4, pp. 491–503, 1994.

[45] R. E. Roberson, "Synthesis of a nonlinear dynamic vibration absorber," *Journal of the Franklin Institute*, vol. 254, no. 3, pp. 205–220, 1952.

[46] B. G. Korenev and L. M. Reznikov, *Dynamic Vibration Absorbers: Theory and Technical Applications*. Willey, 1993.

[47] T. Pinkaew and Y. Fujino, "Effectiveness of semi-active tuned mass dampers under harmonic excitation," *Engineering Structures*, vol. 23, no. 1, pp. 850–856, 2001.

[48] D. Hrovat, "Survey of advanced suspension developments and related optimal control applications," *Automatica*, vol. 33, no. 10, pp. 1781–1817, 1993.

[49] ——, "Applications of optimal control to advanced automotive suspension design," *Transactions of the ASME, Journal of Dynamics, Measurement, and Control*, vol. 115, no. 2B, pp. 328–342, 1993.

[50] S. J. Dyke, B. F. Spencer, M. K. Sain, and J. D. Carlson, "Modeling and control of magnetorheological dampers for seismic response reduction," *Smart Materials and Structures*, vol. 33, no. 10, pp. 1781–1817, 1993.

[51] C.-W. Chen, K. Yeh, C.-H. Tsai, C.-Y. Chen, and D.-J. Wu, "Applying the linear matrix inequality for hybrid fuzzy/h-infinity control of active structural damping," in *IEEE International Conference on Automation Science and Engineering*, 2006, pp. 678 – 682.

[52] F.-H. Hsiao, C.-W. Chen, Y.-W. Liang, S.-D. Xu, and W.-L. Chiang, "T-s fuzzy controllers for nonlinear interconnected systems with multiple time delays," *IEEE Transactions on Circuits and Systems I: Regular Papers*, vol. 52, no. 9, pp. 1883 – 1893, 2005.

[53] A. M. Aly, "Vibration control of high-rise buildings for wind: a robust passive and active tuned mass damper," *Smart Structures and Systems*, vol. 13, no. 3, pp. 473 – 500, 2014.

[54] T. Nagase and T. Hisatoku, "Tuned pendulum mass damper installed in crystal tower," *The structural design of tall and special buildings*, vol. 1, no. 1, pp. 35–36, 1992.

[55] J. L. Almazán, J. C. De la Llera, J. Inaudi, D. López-García, and L. E. Izquierdo, "A bidirectional and homogeneous tuned mass damper: A new device for passive control of vibrations," *Engineering Structures*, vol. 29, no. 7, pp. 1548–1560, 2007.

[56] J.-C. Wu, M.-H. Shih, Yuh-YiLin, and Y.-C. Shen, "Design guidelines for tuned liquid column damper for structures responding to wind," *Engineering Structures*, vol. 27, no. 13, pp. 1893–1905, 2005.

[57] E. E. E. Behady and E. R. El-Zahar, "Vibration reduction and stability study of a dynamical system under multi-excitation forces via active absorber," *International Journal of Physical Sciences*, vol. 7, no. 48, pp. 6203–6209, 2012.

[58] S. Mohanty and S. K. Dwivedy, "Active nonlinear vibration absorber for a harmonically excited beam system," in *Proceedings of the First International Nonlinear Dynamics Conference (NODYCON)*, vol. 2, 2019, pp. 3–11.

[59] ——, "Nonlinear dynamics of piezoelectric-based active nonlinear vibration absorber using time delay acceleration feedback," *Nonlinear Dynamics*, vol. 98, pp. 1465–1490, 2019.

[60] S. Hao, Y. Yamashita, and K. Kobayashi, "Active vibration control of nonlinear 2dof mechanical systems via ida-pbc," *IEICE TRANSACTIONS on Fundamentals of Electronics, Communications and Computer Sciences*, vol. E103-A, no. 9, pp. 1078–1085, 2020.

[61] G. Priyandoko, M. Mailah, and H. Jamaluddin, "Vehicle active suspension system using skyhook adaptive neuro active force control," *Mechanical Systems and Signal Processing*, vol. 23, no. 3, pp. 855–868, 2009.

[62] T. Aoki, Y. Yamashita, and D. Tsubakino, "Vibration suppression for mass-spring-damper systems with a tuned mass damper using interconnection and damping assignment passivity-based control," *International Journal of Robust and Nonlinear Control*, vol. 26, no. 2, pp. 235–251, 2016.

[63] E. D. Sontag, "Smooth stabilization implies coprime factorization," *IEEE Transactions on Automatic Control*, vol. 34, no. 4, pp. 435–443, 1989.

[64] J.-H. Koo, M. Ahmadian, M. Setareh, and T. Murray, "In search of suitable control methods for semi-active tuned vibration absorbers," *Journal of Vibration and Control*, vol. 10, no. 2, pp. 163–174, 2004.

[65] E. Sontag, "Smooth stabilization implies coprime factorization," *IEEE Trans. Automat. Control*, vol. AC, no. 34, pp. 435–443, 1989.

[66] E. D. Sontag, "Input-to-state stability: Basic concepts and results," *Nonlinear and Optimal Control Theory*, pp. 163–220, 2007.

[67] A. T. Z.P. Jiang and L. Praly, "Small-gain theorem for iss systems and applications," *Mathematics of Control, Signals and Systems*, vol. 7, no. 34, pp. 95–120, 1994.

[68] A. R. Teel, "A nonlinear small gain theorem for the analysis of control systems with saturation," *IEEE Transactions on Automatic Control*, vol. 41, no. 9, pp. 1256–1270, 1996.

[69] Z.-P. Jiang, A. R., and L. Praly, "Small-gain theorem for iss systems and applications," *Mathematics of Control, Signals and Systems*, vol. 7, no. 34, pp. 95–120, 1994.

[70] S. Dashkovskiy, B. S. Rüffer, and F. R. Wirth, "An iss small gain theorem for general networks," *Mathematics of Control, Signals, and Systems*, vol. 19, no. 2, pp. 93–122, 2007.

[71] ——, "On the construction of iss lyapunov functions for networks of iss systems," in *Proceedings of the 17th Int. Symposium on Mathematical Theory of Networks and Systems, Kyoto, Japan.* Citeseer, 2006, pp. 77–82.

[72] S. N. Dashkovskiy, B. S. Rüffer, and F. R. Wirth, "Small gain theorems for large scale systems and construction of iss lyapunov functions," *SIAM Journal on Control and Optimization*, vol. 48, no. 6, pp. 4089–4118, 2010.

[73] S. Dashkovskiy, H. Ito, and F. Wirth, "On a small gain theorem for iss networks in dissipative lyapunov form," *European Journal of Control*, vol. 17, no. 4, pp. 357–365, 2011.

[74] C. Prieur and F. Mazenc, "Iss-lyapunov functions for time-varying hyperbolic systems of balance laws," *Mathematics of Control, Signals, and Systems*, vol. 24, no. 1, pp. 111–134, 2012.

[75] J. G. Romero, A. Donaire, and R. Ortega, "Robustifying energy shaping control of mechanical systems," in *2012 IEEE 51st IEEE Conference on Decision and Control (CDC)*, 2012, pp. 4424–4429.

[76] B. Fu, Q. Wang, and W. He, "Nonlinear disturbance observer-based control for a class of port-controlled Hamiltonian disturbed systems," *IEEE Access*, vol. 6, no. 2, pp. 50 299–50 305, 2018.

[77] P. Feketa and N. Bajcinca, "Average dwell-time for impulsive control systems possessing iss-lyapunov function with nonlinear rates," in *2019 18th European Control Conference (ECC).* IEEE, 2019, pp. 3686–3691.

[78] G. Zhang and A. Tanwani, "Iss lyapunov functions for cascade switched systems and sampled-data control," *Automatica*, vol. 105, pp. 216–227, 2019.

[79] F. Lopez-Ramirez, D. Efimov, A. Polyakov, and W. Perruquettil, "On implicit finite-time and fixed-time iss lyapunov functions," in *2018 IEEE Conference on Decision and Control (CDC).* IEEE, 2018, pp. 706–710.

[80] A. Mironchenko and F. Wirth, "Lyapunov characterization of input-to-state stability for semilinear control systems over banach spaces," *Systems & Control Letters*, vol. 119, pp. 64–70, 2018.

[81] D. Karagiannis, M. Sassano, and A. Astolfi, "Dynamic scaling and observer design with application to adaptive control," *Automatica*, vol. 45, no. 12, pp. 2883–2889, 2009.

[82] G. Besançon, "Global output feedback tracking control for a class of Lagrangian systems," *Automatica*, vol. 36, no. 12, pp. 1915–1921, 2000.

[83] A. Venkatraman, R. Ortega, I. Sarras, and A. van der Schaft, "Speed observation and position feedback stabilization of partially linearizable mechanical systems," *IEEE Transactions on Automatic Control*, vol. 55, no. 5, pp. 1059–1074, 2010.

[84] P. Finsler, "Über das vorkommen definiter und semidefiniter formen in scharen quadratischer formen." *Commentarii mathematici Helvetici*, vol. 9, pp. 188–192, 1936/37. [Online]. Available: http://eudml.org/doc/138679

[85] P. Polcz, T. Péni, B. Kulcsar, and G. Szederkényi, "Induced l2-gain computation for rational lpv systems using finsler' s lemma and minimal generators," *Systems & Control Letters*, vol. 142, p. 104738, 2020.

[86] D. S. Marinescu, M. Monea, M. Opincariu, and M. Stroe, "Note on hadwiger-finsler's inequalities," *J. Math. Inequal*, vol. 6, no. 1, pp. 57–64, 2012.

[87] K. Hudha, H. Jamaluddin, P. Samin, and R. Rahman, "Effects of control techniques and damper constraint on the performance of a semi-active magnetorheological damper," *International Journal of Vehicle Autonomous Systems*, vol. 3, no. 2-4, pp. 230–252, 2005.

[88] A. Mulla, S. Jalwadi, and U. Deepak, "Performance analysis of skyhook, groundhook and hybrid control strategies on semiactive suspension system," *International Journal of Current Engineering and Technology*, no. Special Issue-3, pp. 265–269, 2014.

[89] M. Ahmadian, X. Song, and S. C. Southward, "No-jerk skyhook control methods for semiactive suspensions," *Journal of Vibration and Acoustics–Transactions of the ASME*, vol. 126, no. 4, pp. 580–584, 2004.

[90] F. Besinger, D. Cebon, and D. Cole, "Force control of a semi-active damper," *Vehicle System Dynamics*, vol. 24, pp. 695–723, 1995.

[91] M. Novak and M. Valasek, "A new concept of semi-active control of trucks suspension," in *Proceedings of AVEC 96, International Symposium on Advanced Vehicle Control*, 1996, pp. 141–151.

[92] J. Hewit and J. Burdess, "Fast dynamic decoupled control for robotics using active force control," *Mechanism and Machine Theory*, vol. 16, no. 5, pp. 535–542, 1981.

[93] J. Hewit and K. Marouf, "Practical control enhancement via mechatronics design," *IEEE transactions on Industrial Electronics*, vol. 43, no. 1, pp. 16–22, 1996.

[94] J. K. Hedrick, R. Rajamani, and K. Yi, "Observer design for electronic suspension applications," *Vehicle System Dynamics*, vol. 23, no. 1, pp. 413–440, 1994.

[95] V. S. Deshpande, B. Mohan, P. Shendge, and S. Phadke, "Disturbance observer based sliding mode control of active suspension systems," *Journal of Sound and Vibration*, vol. 333, no. 11, pp. 2281–2296, 2014.

[96] D. Ning, S. Sun, F. Zhang, H. Du, W. Li, and B. Zhang, "Disturbance observer based takagi-sugeno fuzzy control for an active seat suspension," *Mechanical Systems and Signal Processing*, vol. 93, pp. 515–530, 2017.

[97] K. Fujimoto and T. Sugie, "Iterative learning control of hamiltonian systems: I/o based optimal control approach," *IEEE Transactions on Automatic Control*, vol. 48, no. 10, pp. 1756–1761, 2003.

[98] H. Pang, X. Zhang, J. Yang, and Y. Shang, "Adaptive backstepping-based control design for uncertain nonlinear active suspension system with input delay," *International Journal of Robust and Nonlinear Control*, vol. 29, no. 16, pp. 5781–5800, 2019.

[99] W. Sun, H. Pan, Y. Zhang, and H. Gao, "Multi-objective control for uncertain nonlinear active suspension systems," *Mechatronics*, vol. 24, no. 4, pp. 318–327, 2014.

[100] R. Lozano, B. Brogliato, O. Egeland, and B. Maschke, *Dissipative systems analysis and control: theory and applications*. Springer Science & Business Media, 2013.

[101] B. Brogliato, R. Lozano, B. Maschke, O. Egeland, *et al.*, "Dissipative systems analysis and control," *Theory and Applications*, vol. 2, 2007.

[102] G. Nicolis, "Dissipative systems," *Reports on Progress in Physics*, vol. 49, no. 8, p. 873, 1986.

[103] M. Bardi, I. C. Dolcetta, *et al.*, *Optimal control and viscosity solutions of Hamilton-Jacobi-Bellman equations*. Springer, 1997, vol. 12.

[104] J. A. Laval and L. Leclercq, "The hamilton–jacobi partial differential equation and the three representations of traffic flow," *Transportation Research Part B: Methodological*, vol. 52, pp. 17–30, 2013.

[105] P. Cannarsa and C. Sinestrari, *Semiconcave functions, Hamilton-Jacobi equations, and optimal control*. Springer Science & Business Media, 2004, vol. 58.

[106] R. Ortega, M. W. Spong, F. G?mez-Estern, and G. Blankenstein, "Stabilization of a class of underactuated mechanical systems via interconnection and damping assignment," *IEEE Transactions on Automatic Control*, vol. 47, no. 8, pp. 1218–1233, 2002.

[107] J. G. Romero, A. Donaire, R. Ortega, and P. Borja, "Global stabilisation of underactuated mechanical systems via PID passivity-based control," *Automatica*, vol. 96, pp. 178–185, 2018.

[108] J. Sandoval, R. Kelly, and V. Santibanez, "Interconnection and damping assignment passivity-based control of a class of underactuated mechanical systems with dynamic friction," *International Journal of Robust and Nonlinear Control*, vol. 21, no. 7, pp. 738–751, 2011.

[109] E. Franco, F. Rodriguez y Baenaa, and A. Astolfi, "Robust dynamic state feedback for underactuated systems with linearly parameterized disturbances," *International Journal of Robust and Nonlinear Control*, vol. 30, no. 10, pp. 4112–4128, 2020.

[110] E. Franco, "Adaptive ida-pbc for underactuated mechanical systems with constant disturbances," *International Journal of Adaptive Control and Signal Processing*, vol. 33, no. 1, pp. 1–15, 2019.

[111] S. Hao, Y. Yamashita, and K. Kobayashi, "Vibration suppression of hamiltonian systems with velocity and force disturbances using IDA-PBC," in *2nd IFAC Conference on Modelling, Identification and Control of Nonlinear Systems MICNON 2018*. Elsevier, 2018.

List of Publication of the Author

Journal Papers

1. Sheng Hao and Yuh Yamashita and Koichi Kobayashi,"Active vibration control of nonlinear 2DOF mechanical systems via IDA-PBC", IEICE Transactions on Fundamentals of Electronics, Communications and Computer Sciences, Vol.E103-A, No.9, pp.1078-1085, 2020.

2. Sheng Hao and Yuh Yamashita and Koichi Kobayashi,"Robust passivity-based control design for active nonlinear suspension system", International Journal of Robust and Nonlinear Control, Vol.32, No.1, pp.373-392, 2022.

Reviewed Conference Papers

1. Sheng Hao and Yuh Yamashita and Koichi Kobayashi,"Vibration suppression of Hamiltonian systems with velocity and force disturbances using IDA-PBC", in 2nd IFAC Conference on Modeling, Identification and Control of Nonlinear Systems MICNON, pp.285-290, Guadalajara, Jalisco, Mexico, 20-22 June 2018.

2. Sheng Hao and Yuh Yamashita and Koichi Kobayashi,"Active nonlinear tuned mass damper via IDA-PBC", in 2018 IEEE International Conference on Systems, Man, and Cybernetics (SMC), 2018, pp.4393-4398, Miyazaki, Japan 7-10 Oct. 2018.

3. Sheng Hao and Yuh Yamashita and Koichi Kobayashi,"Robust active vibration controller design for a class of underactuated nonlinear systems", in 2020 IEEE/SICE International Symposium on System Integration (SII), Honolulu, pp.465-470, HI, USA, 12-15 Jan. 2020.

4. Sheng Hao and Yuh Yamashita and Koichi Kobayashi,"Passivity-based nonlinear active suspension control utilizing relative information", in 21st IFAC World Congress 2020, pp.5586-5591, Berlin, Germany, 11-17 July. 2020.

5. Sheng Hao and Yuh Yamashita and Koichi Kobayashi,"Construction of ISS Lyapunov functions for Hamiltonian systems with multiple disturbances", in 3rd IFAC Conference on Modelling, Identification and Control of Nonlinear Systems MICNON, pp.281-286, Tokyo, Japan, 15-17 September 2021